Applications of Blind Interference Alignment in Dense Cellular Networks with Short Coherence Times

Ramin Bakhshi

Submitted to the
Institute of Graduate Studies and Research
in partial fulfillment of the requirements for the degree of

Doctor of Philosophy
in
Electrical and Electronic Engineering

Eastern Mediterranean University
December 2018
Gazimağusa, North Cyprus

Approval of the Institute of Graduate Studies and Research

<div align="right">

Assoc. Prof. Dr. Ali Hakan Ulusoy
Acting Director

</div>

I certify that this thesis satisfies all the requirements as a thesis for the degree of Doctor of Philosophy in Electrical and Electronic Engineering.

<div align="right">

Assoc. Prof. Dr. Hasan Demirel
Chair, Department of Electrical and
Electronic Engineering

</div>

We certify that we have read this thesis and that in our opinion it is fully adequate in scope and quality as a thesis for the degree of Doctor of Philosophy in Electrical and Electronic Engineering.

<div align="right">

Prof. Dr. Erhan A. İnce
Supervisor

</div>

<div align="right">

Examining Committee

</div>

1. Prof. Dr. Emre Aktaş

2. Prof. Dr. Aykut Hocanın

3. Prof. Dr. Erhan A. İnce

4. Prof. Dr. Erdal Panayırcı

5. Asst. Prof. Dr. Hassan Abou Rajab

ABSTRACT

Improving the efficiency of wireless communication systems has been the main concern of researchers within the last few decades. Much thought was put into the study of interference and its effect on cellular networks. Managing interference in cellular networks is a challenging task and embodies handling the interference between users of a single cell (intracell interference) and managing the interference between neighboring cells (intercell interfrence). Most efficient MIMO techniques are based on managing interference instead of avoiding it by employing orthogonal resource allocation schemes. These transmission schemes require the knowledge of the Channel State Information at the Transmitter (CSIT) to achieve the optimal Degrees of Freedom (DoF), also known as multiplexing gain. Providing an accurate CSIT in cellular environments requires precise synchronization and high-capacity backhaul links which use tremendous amounts of network resources.

To alleviate these aforementioned problems a new interference alignment method which does not require CSIT for MISO Broadcast Channel (BC) had been proposed. This new technique is known as the standard Blind Interference Alignment (s-BIA) and it can achieve the optimal DoF under MISO BC when CSIT is not available. BIA requires that the channel remains unchanged throughout the duration of the transmission. Therefore, coherence time or bandwidth is important when determining whether BIA can be adopted.

This thesis investigates the DoF and corresponding sum-rates of cellular networks in absence of CSIT and their achievability while using novel BIA schemes. The thesis

first proposes a new BIA scheme named hybrid-BIA that is designed for dense small-cell homogeneous cellular network with partial connectivity. Hybrid-BIA can align both the inter and intracell interferences by differentiating between users that can treat itercell interference optimally as noise and those who need to manage it. This method aims to reduce the supersymbol length (number of channel uses required by BIA) and overcome the DoF loss of the state-of-the-art hierarchical BIA (h-BIA) technique. The proposed scheme is evaluated under limited coherence time and its effectiveness for attaining good DoF over a small number of symbol extensions is shown. When compared against four different BIA schemes introduced in Chapter 3 (sync-BIA, ext-BIA, h-BIA and top-BIA) the proposed hybrid-BIA scheme was seen to have the shortest supersymbol length (9 symbol extensions for the setting explained in 4).

The thesis also proposes two other novel BIA-based schemes to manage the cross and co-tier interference in two-tier heterogeneous networks (HetNets) under which macrocell (MC) and femtocells (FC) co-exist. These schemes assume that MCs and FCs are working at the same time or in the same frequency band, MCs have access to the global CSIT and BIA is employed by each FC to manage intracell interference. Letting MBSs and FBSs operate in the same frequency band or time slot, HetNets can achieve higher DoF and sum-rates while at the same time they lower the load of the macrocell (when MUs are close to FCs they are served by FCs).

The first proposed HetNet scheme uses the knowledge of predetermined interference dimensions of the FUs set by BIA and CSIT at MBS to align the interference shed by MBS on the interference dimensions of FUs. In this work sum-rate and DoF of the first proposed HetNet scheme are derived and compared with the well known conventional

interference avoidance scheme (referred as the baseline scheme in thesis). Numerical results show that the sum-rate for proposed scheme is higher in comparison with the baseline scheme where the MBS applies zero-forcing precoder using a water filling power allocation strategy. This novel scheme can be extended to a general network via judicious selection and via orthogonalization.

The second proposed HetNet scheme presents a general framework to maximize the achievable DoF of FCs under limited coherence time MISO channels. DoF is optimized by using Pareto optimization and choosing the most beneficial FC configurations. For femtocells using s-BIA configuration denotes the number of users and antennas in each FC. Once the appropriate FC configurations are determined, interference from MBSs on all FUs are aligned on predetermined interference dimensions set by staggered antenna switching technique of s-BIA. For HetNet scheme #2 it was demonstrated that the maximum allowable coherence time could change the number of Pareto optimal solution vectors and the set of allowable $\{[K,M]\}$ configurations of each pair. It was pointed out that with multiple Pareto optimal solutions, the network planner could flexibly choose one of these Pareto optimal solutions based on available resources

Keywords: Blind interference alignment, supersymbol length, reconfigurable antenna, topological BIA, hierarchical BIA, hybrid BIA, Pareto optimal solutions.

ÖZ

Kablosuz iletişim sistemlerinin verimliliğini artırmak son birkaç yüzyılda araştırmacıları en çok ilgilendiren konu olmuştur. Parazit sinyallerinin hücresel şebekeler üzerindeki etkilerini anlamak için epey çalışılmıştır. Hücresel şebekelerdeki parazitin idaresi zorlayıcı bir görev olup bir hücredeki kullanıcılar arasındaki parazitin işlenmesini (hücre içi) ve komşu hücreler arasında bulunan parazitin (hücreler arası) işlenmesini içerir. Çoğu verimli MIMO teknikleri parazitden kaçınmak yerine dikey kaynak tahsis etme yöntemlerini kullanarak paraziti idare etmektedir. Bir diğer adıyla çoklama kazancı olarak da bilinen en optimal DoF değerlerini elde edebilmek için belirtilen iletim yöntemleri vericide kanal durum bilgisine ihtiyaç duymaktadır. Hücresel şebekeler içinde yanlışsız kanal durum bilgisini municiyle paylaşabilmek hassas senkronizasyon ve yüksek kapasiteli geri taşıma bağlantıları gerektirmektedir.

Belirtilen bu zorlukları hafifletebilmek için çok-girdili tek-çıktılı (MISO) yayımlama kanalları üzerinde çalışan ve kanal durum bilgisi gerektirmeyen yeni bir parazit hizalama yöntemi mevcuttur. Ayni zamanda standart Örtülü karışım yöntemi (s-BIA) olarak da bilinen bu yeni teknik kanal durum bilgisi olmadan da en optimal DoF değerlerini elde edebilmektedir. Standart örtülü karışım hizalama yöntemi iletişim esnasında kanalın değişmemesini gerektirmektedir. Bu nedenle, standart örtülü karışım hizalama yönteminin kullanılabilirliğini belirlerken evreuyumluluk zamanı veya bant genişliği önem arzetmektedir.

Bu tez kanal durum bilgisi olmayan durumlarda hücresel şebekelerdeki özgürlük derecelerini ve toplam hızları incelemekte ve bunların özgün örtülü karışım teknikleri

kullanırken uyarlanabilirliğini incelemektedir. Tez ilk olarak kısmi bağlantılı homojen hücresel sistemler için tasarlanmış ve melez-BIA olarak adlandırılan yeni bir örtülü karışım hizalama yöntemi sunmaktadır. Melez-BIA paraziti gürültü olarak kabul edebilecek kullanıcıları paraziti hizalaması gerekenlerden ayırt ederek hem hücreler arası hem de hücre içi paraziti hizalayabilmektedir. Bu yöntem super sembol uzunluğunu kısaltmayı hedeflerken ayni zamanda literatürdeki en gelişmiş yöntemlerden olan hiyerarşik örtülü karışım hizalama (h-BIA) yönteminin özgürlük derecesindeki kaybı telafi etmeye çalışmaktadır. Önerilen teknik sınırlı koherens zaman kısıtı altında değerlendirilmiş ve az sayıdaki sembol uzantı zamanı içinde iyi özgürlük dereceleri sağladığı gösterilmiştir. Bölüm üçte anlatılan dört diğer teknik ile (sync-BIA, ext-BIA, h-BIA ve top-BIA) kıyaslandığında önerilen melez-BIA yönteminin tümünden daha kısa supersembol uzunluğu olduğu görülmüştür.

Tezde ayrica makro ve femto hücrelerin birlikte çalıştığı çoktürel ağlardaki çarpraz ve ortak kanal girişimlerini yönetebilecek iki yeni BIA-tabanlı yöntem de önerilmektedir. Her iki yöntem de MC ve FC lerin ya ayni zamanda ya da ayni frekans bandında çalıştığını, MClerin evrensel CSITye erişebilir olduğunu ve hücre içi paraziti yönetebilmek için her FCde örtülü karışım hizalama kullanıldığını varsaymaktadırlar. Makro baz istasyonları ile femto baz istasyonlarının ayni frekans bandı veya zaman aralığında çalışmalarına izin veren evrensel şebekeler özgürlük derecelerini ve toplam-hızlarını artırırken ayni zamanda makto hücrenin yükünü hafifletebilmektedirler (Makro kullanıcılar femto hücreye yakın iken femto hücreler tarafından servis edilmektedir).

Önerilen ilk çoktürel şebeke (HetNet) yöntemi makro baz istasyonundan femto kullanıcıların girişim boyutlarına dökülen paraziti hizalamak için BIA tarafından

önceden belirlenen femto kullanıcı girişim boyutları bilgisini ve vericideki kanal durum bilgisini kullanmaktadır. Tezde önerilen birinci çoktürel şebeke yöntemi için toplam-hız ve özgürlük derecesi hesaplandıktan sonra temel yöntem olarak da bilinen klasik girişim yöntemi ile karşılaştırılmıştır. Sayısal sonuçlar önerilen yöntemin toplam-hızının makro baz istasyonunda ZF önkodlayıcı ve su doldurma yolu ile güç tahsis eden bir strateji kullanan temel klasik yönteme göre daha yüksek olduğunu göstermiştir. Ayrıca bu yeni yöntemin mantıklı seçim ve dikgenleştirme kullanarak daha genel bir şebekeye genişletilmesi de mümkündür.

İkinci önerilen çoktürel şebeke (HetNet) yöntemi ise kısıtlı eşevrelilik zamanı varsayımı altında MISO kanalları üzerinde femto hücrelerin özgürlük derecelerini artırabilmek için gerekli olan genel bir çerçeve sunmaktadır. Özgürlük derecesi Pareto optimizsyonu kullanırken en faydalı femto hücre düzenleşimlerini seçerek eniyilenmektedir. S-BIA kullanan femto hücreleri için düzenleşim her hücredeki kullanıcı ve anten sayısını ifade etmektedir. En yerinde düzenleşimler belirlendikten sonra makro baz istasyonunun neden olduğu girişim s-BIA tarafından önceden belirlenen girişim boyutları üzerine hizalanmaktadır. Tezde gösterilmiştir ki iki numaralı çoktürel şebeke yöntemi içinde kullanılan enbüyük eşevrelilik zaman değeri optimal Pareto çözüm vektör sayısını ve her eş için izin verilen $\{[K,M]\}$ düzenleşimlerini değiştirebilmektedir. Belirtmek isteriz ki birden fazla optimal çözüm varken şebeke planlayıcının elindeki özkaynaklara bağlı olarak bu çözümlerden birini seçmesi mümkündür.

Anahtar Kelimeler: Örtülü karışım hizalama, süper sembol uzunluğu, yeniden düzenlenebilir anten, topolojik BIA, hiyerarşik BIA, melez BIA, Pareto en uygun çözümler.

DEDICATION

Dedicated to my parents, family, friends and teachers who have always been supportive

of me during my Doctoral studies

ACKNOWLEDGMENT

My deepest gratitude goes to my supervisor Prof. Dr. Erhan A. İnce for his constant support and wholehearted collaboration in my thesis. His hard work, wisdom and understanding towards this research work has always motivated me and became a factor for my success.

I am also indebted to my friends for their presence which has always encouraged and comforted me.

Last but not least I would like to thank my parents for their love and support. Without them and their support I may not have reached this milestone in my life.

TABLE OF CONTENTS

LIST OF TABLES

LIST OF FIGURES

LIST OF SYMBOLS AND ABBREVIATIONS

σ^2 Variance

I   Identity matrix

p   Cross-correlation

R   Autocorrelation matrix

T   Transposition operator

Tr   Trace operator

R   Covariance matrix

sgn(.)   Point-wise sign function

Vec(.)   Vec operator

w   Filter weights vector

x   Filter input vector

1G   First Generation

2G   Second Generation

3G   Third Generation

4G   Fourth Generation

5G   Fifth Generation

AP   Access Point

AWGN   Additive White Gaussian Noise

BC   Broadcast Channel

BD   Block Diagonalization

BOP   Bi-objective Optimization Problem

BS   Base station

c-BIA	Coordinated Blind Interference Alignment
CDF	Cumulative Distribution Function
CDMA	Code Division Multiple Access
cog-BIA	Cognitive Blind Interference Alignment
CSI	Channel State Information
CSIT	Channel State Information at Trasnmiter
CSIR	Channel State Information at Reciver
DoF	Degree of Freedom
ECF	Epsilon Constraint Framework
EVDO	Evolution Data Optimized
ext-BIA	Extended Blind Interference Alignment
FBS	Femtocell Base Station
FC	Femtocell
FDMA	Frequency Division Multiple Access
FU	Femtocell User
GSM	Global System for Mobile communication system
GPRS	General Packet Radio Service
h-BIA	Hierarchical Blind Interference Alignment
HetNet	Heterogeneous Cellular Network
HSPA	High Speed Packet Access
hybrid-BIA	Hybrid Blind Interference Alignment
IA	Interference Alignment
IC	Interference Channel
ITU	International Telecommunications Union

LTE	Long Term Evolution
LZFB	Linear Zero Forcing Beamformer
MBS	Macrocell Base Station
MC	Macrocell
MIMO	Multiple Input Multiple Output
MISO	Multiple Input Singel Output
MU	Macrocell User
n-BIA	Network Blind Interference Alignment
OFDM	Orthogonal Frequency Division Multiplexing
PDF	Probability Density Function
s-BIA	Standard Blind Interference Alignment
SISO	Singel Input Singel Output
SNR	Signal-to-Noise Ratio
sync-BIA	Syncronized Blind Interference Alignment
TDMA	Time division Multiple Access
TIM	Topological Interference Management
top-BIA	Topological Blind Interference Alignment

Chapter 1

INTRODUCTION

1.1 Introduction

Improving the efficiency of wireless communication systems has been the main concern of researchers within the last few decades. Much thought was put into the study of interference and its effect on cellular networks. Managing the interference in cellular networks is a challenging task and comprises handling the interference between users of a single cell (intracell interference) and managing the interference between neighboring cells (intrecell interfrence). Moreover, the pressing need for high data rates has led to the development of several generations of mobile communication standards (1G to 4G). The first generation (1G) which dealt with analog signals used Frequency Division Multiple Access (FDMA) scheme to allocate a 30 kHz channel per user by splitting the available frequency band into smaller sub-bands. Since each user was allocated one sub-channel for their voice service, tremendous amounts of bandwidth was wasted while providing only the analog voice service. Under 2G digital technologies started to replace the analog ones and Time Division Multiple Access (TDMA) was adopted. This way each user would be able to use the full spectrum during the time allocated to it (time-slot). For the first time, wide geographical regions were split into smaller areas referred to as cellular cells and each hexagonal cell was allocated a Base Station (BS) that would communicate with the mobile subscribers in its coverage. As the mobile phone standard Europe

adopted the Global System for Mobile Communication Systems (GSM) and D-AMPS, an early version of Qualcomm's CDMA known as IS-95, became successfull in the USA. Both GSM and its extended version known as General Pperacket Radio Service (GPRS) brought with them a number of advantages: improved sound quality, better security, and higher total capacity [1, 2] .

The third generation standard was established to increase the spectral efficiency by using Code Division Multiple Access (CDMA) technique which would enable users to perform at the same time in the same frequency band by assigning users orthogonal spreading codes [3, 4] . However, the first 3G standards known as CDMA2000 could not satisfy the growing demands of the customers. Consequently Evolution Data Optimized (EVDO) and High Speed Packet Access (HSPA) techniques have been proposed as alternative solutions to CDMA2000 under 3G.

The 4th Generation Mobile standards started with the International Telecommunications Union (ITU) taking initiative to define the requirements that a 4G network must meet and also the standards that must be followed. Standards such as Long Term Evolution (LTE) or LTE-Advanced (LTE-A) employ the advanced Multiple Input Multiple Output (MIMO) antenna technologies together with Orthogonal Frequency Division Multiplexing (OFDM) transmission to increase the communication efficiency and deliver downlink speeds of 1Gbps when stationary and 100Mbps when mobile [5, 6].

Some loose guidelines that the next generation mobile standards (5G) need to follow, and the challenges that one would face has been outlined in [7–9]. 5G is expected to provide a better mobile broadband (MBB) experience by meeting the requirements of

high spectrum rates (1-20 Gbps), high peak rates, large number of connections and latencies at 1ms and below. It is also expected to be more energy efficient than its predecessors. There's a global race for 5G network developments as countries count on 5G to improve commerce and citizen's lives with broadband. Currently strong companies such as Verizon, Huawei and Erricson are competing to take the lead in 5G.

In early generations (1G and 2G) to avoid the intercell interference between BSs the orthogonal Frequency Reuse (FR) method was employed and the co-channel interferences were treated as noise. Nowadays, high data rates, power efficiency and low latency are the main concerns and dense heterogeneous cellular networks with coexisting macro, micro, femto and pico cells are deployed under the coverage area of conventional BSs. Thus, managing the effect of intercell interference has become crucial in MIMO systems.

Many interference cancellation techniques including the well known linear Zero Forcing (LZF) [10–12] or Block Diagonalization (BD) [13–16] methods have been proposed to manage the interference in MIMO systems. These techniques require full Channel State Information (CSI) and as many antennas as the number of signals they are trying to cancel. Unfortunately in densely populated urban areas and heterogeneous networks this may become impractical since only a limited number of antennas can be employed at the base station (BS) [17] and providing the full CSIT requires the accurate and complex backhul system between BSs. On the other hand, conventional interference avoidance schemes such as TDMA and FDMA drastically reduce the spectral efficiency of cellular networks.

To alleviate these aforementioned problems a new technique known as Interference

Alignment (IA) was first introduced in [18–21]. The key idea behind IA is to align the interference in such a way that it spans minimum possible dimensions out of the available signal space and leaves many interference free dimensions for the desired signals. The number of interference free signal dimensions are known as the Degree of Freedom (DoF) or spatial multiplexing gain and it characterizes the performance of IA at high signal-to-noise ratio (SNR) regime [22].

Main drawback for IA techniques was that, in absence of perfect or partial CSIT the DoF of the network would collapse and hence the transmissions would become unreliable [23]. An interference alignment method which does not require CSIT for the Broadcast Channel (BC) was first proposed in 2011 by Wang, Gou and Jafar [24] and then was elaborated upon by Jafar in [25]. This new technique referred to as the standard Blind Interference Alignment (s-BIA) assumes that a transmitter is equipped with M transmit antennas and there are K receivers, each equipped with a single reconfigurable antenna capable of switching between $M_k = M, \forall k \in \{1, \cdots K\}$ preset modes. The s-BIA approach with $[K, M]$ configuration (K-user $M \times 1$ MISO BC) and no knowledge about CSIT can still align all intracell interference with only a mild assumption on the channel coherence structure and has been shown to achieve $\frac{KM}{K+M-1}$ DoF. The new technique requires that the channel remains unchanged throughout the duration of the transmission. Therefore, coherence time or bandwidth is important when determining whether BIA can be used [26]. This motivates the search for BIA schemes that can provide short super-symbol lengths which will correspond to realistic coherence times. Clearly, it would be interesting to investigate how the s-BIA can be applied under homogeneous cellular networks and what the achievable sum-rate would be.

A mid-point between providing the global CSIT and totally blind schemes is the knowledge of network topology. The basic idea of using topological interference management was first proposed by [27–29]. They suggested using the location information for the users and base stations in a network to enhance the performance of s-BIA. Under the network BIA the users that can be served at the same time were grouped with the aim of minimizing the supersymbol length while the interference between users of each group were treated as noise. Since providing the location information of users and BSs are much easier and requires less synchronization between BSs than providing CSIT, the network topology is a strong feature for blind IA techniques.

In practice, differences in wireless channels for different users due to the random placement of the nodes, path loss, and the existence of obstacles in the wireless medium lead to a partially connected network topology, where a receiver is connected with only a subset of the transmitters. The concept of partially connected cellular networks (PCCN) was first introduced in [30]. In PCCNs, signals of only a small number of BSs can be decoded at each user. Users located close to cell-boundaries will receive data with an acceptable SNR and for those users located near a BS, the signals from neighboring BSs would be weaker and their decoding would deteriorate. It was stated in [30] that, partially connected network can achieve higher DoF compared to a fully-connected network. These schemes cancel both the intracell and intercell interference by relying on receivers with one reconfigurable antenna and by allowing users at the cell edge to be served by all the base stations in their proximity.

Recently in the fifth generation mobile communication standard (5G) heterogeneous networks are studied for achieving higher data rates and power efficiency. Under

heterogeneous networks (HetNets) smaller size cells such as pico and femtocells (FCs) are deployed in the coverage area of macrocells [31, 32]. Under such two-tier networks it is also possible to reduce the load of the macro cell since some of the macro users (MUs) can be serviced by available femtocells [33, 34]. Some open ended issues related to HetNets include servicing the cell-edge users, maximizing the sum-rate and optimizing the achievable DoF.

Femtocells are also referred to as home evolved NodeBs (HetNBs).Their coverage is in the range 10-50 meters and with transmit powers in the range 1-100mW. Femtocells usually operate in the license spectrum of a service provider and are connected to the core network via an IP-based backhaul. HetNets can in principle provide cost-effective data delivery but there are interference issues that need to be addressed. Particularly when we have users close to cell-edges or located in overlapping regions between two or more adjacent MCs. First source of interference is from the neighboring femtocells and the second from the macrocell base station (MBS). When a macrocell user is close to the cell-edge of a femtocell there will be an in-band interference and the macrocell user will get two transmissions: one from the MBS and the other from the nearby femtocell base station (FBS). It is also possible that femtocell users in a particular cell experience interference from the MBS which has a much higher transmit power than those of the FBSs [35].

1.2 Thesis Objectives

This thesis is mainly about interference management in cellular networks where the global CSIT is not available and all cells are working at the same time or in the same frequency band to increase the spectral efficiency. We evaluate and analyze the applications of the Blind Interference Alignment technique over homogeneous and heterogeneous cellular networks where the coherence time of the channel is limited.

The main objectives of this thesis include:

1. Investigating the effect of intercell and intracell interference on s-BIA and studying the possible degree of freedom and the achievable sum-rate under homogeneous cellular networks,

2. Analysis and evaluation of the performance of s-BIA under limited coherence time assumption,

3. Understanding the effects of co-tier and cross-tier interference on sum-rate performance of s-BIA under heterogeneous cellular networks and evaluation of DoF,

4. Evaluate sum-rate and DoF of heterogeneous cellular networks given partial CSIT,

5. Propose new Interference Alignment schemes that uses s-BIA and that could be used over the homogeneous and heterogeneous cellular network. These schemes should try to maximize the DoF while they minimize the supersymbol length (necessary for channels that have short coherence times).

1.3 Thesis Contributions

Our goal in this thesis is to propose new interference alignment schemes that would work under limited coherence time assumption and would give good DoF and sum-rate both for homogeneous and heterogeneous cellular networks. From the work carried out two international conference papers and one journal publication was possible. The first two conference papers were published in 2015 and 16, respectively and have proposed two new schemes to manage the cross and co-tier interference in two-tier HetNets comprised of macrocell and femtocells (heterogeneous setup). These schemes have assumed that MCs and FCs were working at the same time and in the same frequency

band where MCs had access to the global CSIT and s-BIA was employed by each FC to manage intra cell interference. On the other hand, the newly accepted journal paper proposes an approach for handling inter and intracell interference in homogeneous cellular network based on a BIA framework.

Starting by the homogeneous cellular networks the main contributions of this thesis can be listed as:

- *"Hybrid Blind Interference Alignment in Cellular Networks with Limited Coherence Time"* [36], this paper is inspired by the user grouping approach of topological blind interference alignment (top-BIA) which is a semi-blind IA scheme and the fact that the partially connected networks can be advantageous in terms of degree of freedom (DoF) and sum-rate. The hybrid BIA scheme introduced in the paper uses top-BIA to group users that are randomly distributed in a dense small-cell network and aims to reduce the supersymbol length and overcome the DoF loss of the state-of-the-art hierarchical BIA (h-BIA) technique. The proposed scheme is very suitable for channels where coherence time is limited and also could attain a good DoF over a small number of symbol extensions. Both the sum-DoF and the network throughput for hybrid-BIA is greater than that of h-BIA. The paper also shows that h-BIA constitutes a special case of hybrid-BIA.

- *"Interference Management in Two-Tier Heterogeneous Networks Using Blind Interference Alignment"* [35], In order to align the cross-tier interference, in heterogeneous cellular networks, we propose a novel scheme where femtocells are located in a macrocell and each FBS has been paired with a MU and all pairs are operating in different time slots. Within each femtocell BIA with

staggered antenna switching is used. The scheme uses the knowledge of predetermined interference dimensions of the FUs set by BIA and CSIT at MBS to align the MBS interference on the interference dimensions of FUs , hence allowing MBS and FBS to coexist and operate in the same frequency band and/or time slot.

- *"Coherence-time Based Femtocell Configurations and Pareto Optimization to Achieve Maximum DoF in Heterogeneous Networks Using BIA"* [26]. This work extends on our recent publication [35], by aligning the interference from MBS on predetermined interference dimensions of femtocell at each symbol extension where the predetermined dimensions are set by BIA. We focus on the downlink of a two-tier partially connected heterogeneous network with multiple femtocells deployed under the dead zone between two adjacent macro cells. We assume that each MC is serving two MUs and each femtocell would support K number of users. [26] describes a framework in which maximum possible DoF can be determined by femtocell configurations and structure optimization. Since only some femtocell configurations could satisfy the maximum symbol extension condition, the analysis has been carried out by assuming both fixed and unlimited coherence time. In this work Pareto-optimization has been adapted to work out the maximum DoF for the minimum possible number of subtractions at FCs to perform the standard BIA.

1.4 Thesis Outline

The rest of this thesis is organized as follows: Chapter 2 introduces the preliminary informations and necessary definitions in the literature and then tries to review the state of the art for interference management and alignment techniques. In order to set a foundation for our proposed schemes, Chapter 3 will present the standard BIA (s-

BIA) scheme for BC and IC and analyze the implementation of the s-BIA over cellular scenarios. Moreover, the chapter would summarize several well known BIA schemes that are designed to manage intracell and intercell interference in cellular networks.

In Chapter 4, we propose the hybrid BIA scheme for dense small-cell homogeneous cellular network with partial connectivity. This method aims to reduce the supersymbol length and overcome the DoF loss of the state-of-the-art hierarchical BIA (h-BIA) technique. The proposed scheme is evaluated under limited coherence time and its effectiveness for attaining good DoF over a small number of symbol extensions is shown. The chapter also compares and contrast the hybrid-BIA performance with some of the state-of-the-art techniques summarized in Chapter3.

The Chapters 5 and 6 are devoted to aligning the cross-tier interference, in heterogeneous cellular networks. In Chapter 5 we propose a novel scheme where femtocells are located in a macrocell and each FBS has been paired with a MU and all pairs are operating in different time slots. The knowledge of predetermined interference dimensions of the FUs set by BIA and CSIT at MBS are used to align the MBS interference on the FU's, hence allowing MBS and FBS to coexist and operate in the same frequency band and/or time slot. Chapter 6 extends the work described in Chapter 5. Here we focus on the downlink of a two-tier partially connected heterogeneous network with multiple femtocells deployed under overlapping region of two adjacent macro cells where each MC is serving two macrocell users and each femtocell would support K number of users. The chapter describes a framework in which maximum possible DoF can be determined by femtocell configurations and structure optimization. Finally, Chapter 7 draws conclusions and makes suggestions for future work.

Chapter 2

BACKGROUND AND STATE-OF-THE-ART INTERFERENCE ALIGNMENT (IA) TECHNIQUES

2.1 Introduction

This chapter is devoted to explaining the preliminary and necessary definitions for broadcast in cellular networks and it also reviews various state-of-the-art interference alignment techniques in the literature.

2.2 Background for MIMO Systems

MIMO systems which have been deployed in third and forth generation mobile communication standards continue to hold a major role also under 5G. Hence, many researchers still work on analysis of data rates, power efficiency and latency. In what follows we will first express the capacity for a MIMO system and then look at deployment of multiple antennas in cellular networks. Then a summary of concepts such as spatial diversity and multiplexing gain (DoF) would be provided. Finally, basics of conventional interference management techniques such as Linear Zero Forcing and Block Diagonalization in MIMO cellular systems will be discussed and compared with the newly proposed interference alignment schemes.

2.2.1 Multiple Antenna Techniques for Cellular Systems

A block diagram representation of a point-to-point MIMO channel between a transmitter with M_t transmit antennas and a receiver with M_r receive antennas is depicted in Figure 2.1 where the desired and undesired signals are denoted by solid

and dash lines, respectively.
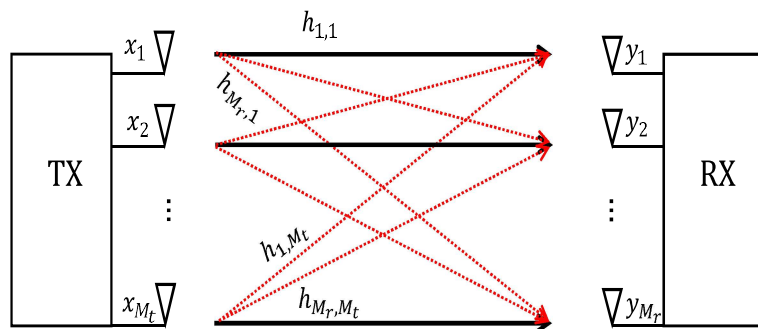
Figure 2.1: Point-to-point MIMO Channel with M_t transmit and M_r receive antennas.

To achieve high capacity MIMO systems use either *multiplexing* or *diversity*. Diversity, uses the fact that if the spatial distance between antennas at either transmitter or receiver are sufficiently large, then independent paths experience different channel responses and the probability of deep fading significantly decreased. For example, in a MIMO system if the same message is transmitted through independent paths then the receiver will have the option of choosing the strongest received signal.

By transmitting independent and separately encoded data signals, known as streams, from each of the multiple transmitting antennas (through the spatial channels), the data rate can also be increased. This effect is known as spatial multiplexing [37].

As in [37], the discrete time representation for the input-output model of the MIMO

channel depicted in Figure 2.1 can be written as:

$$
\begin{bmatrix} y_1 \\ \vdots \\ y_{M_r} \end{bmatrix} = \begin{bmatrix} h_{1,1} & \dots & h_{1,M_t} \\ \vdots & \vdots & \vdots \\ h_{M_r,1} & \dots & h_{M_r,M_t} \end{bmatrix} \begin{bmatrix} x_1 \\ \vdots \\ x_{M_t} \end{bmatrix} + \begin{bmatrix} n_1 \\ \vdots \\ n_{M_r} \end{bmatrix} \tag{2.1}
$$
$$
\underbrace{}_{\mathbf{y}} \qquad \underbrace{}_{\mathbf{H}} \qquad \underbrace{}_{\mathbf{x}} \quad \underbrace{}_{\mathbf{z}}
$$

where $\mathbf{y} = [y_1, y_2, \dots, y_{M_r}]^T \in \mathbb{C}^{M_r \times 1}$ represents the received signal vector,
$\mathbf{H} \in \mathbb{C}^{M_r \times M_t}$ is the narrowband time-invariant channel matrix,
$\mathbf{x} = [x_1, x_2, \dots, x_{M_t}]^T \in \mathbb{C}^{M_t \times 1}$ denotes the transmit symbol vector with M_t
independent input symbols and $\mathbf{z} = [z_1, z_2, \dots, z_{M_r}]^T \in \mathbb{C}^{M_r \times 1}$ corresponds to the
zero-mean circular symmetric complex Gaussian noise vector. Furthermore, if we
apply matrix notation, equation (2.1) can be re-written as:

$$
\mathbf{y} = \mathbf{Hx} + \mathbf{z} \tag{2.2}
$$

The covariance matrix of the transmitted signal vecor $\mathbf{x}$ is given by

$$
\mathbf{R}_{xx} = \mathbb{E}\{\mathbf{xx}^H\} \tag{2.3}
$$

where $\mathbb{E}\{\cdot\}$ represents the expectation and $(\cdot)^H$ the Hermitian operator. Regardless of
the number of transmit antennas (M_t), the total transmitted power is constrained to P
Watts and equals:

$$
P = \text{Tr}(\mathbf{R}_{xx}). \tag{2.4}
$$

Moreover, the covariance matrix of noise vector $\mathbf{z}$ can be formulated as

$$
\mathbf{R}_{zz} = \mathbb{E}\{\mathbf{zz}^H\} \tag{2.5}
$$

If there is no correlation between components of $\mathbf{z}$ assumed, the covariance matrix in

13

(2.5) can be written as

$$\mathbf{R}_{zz} = \mathbb{E}\{\mathbf{z}\mathbf{z}^H\} = N_0\mathbf{I}_{M_r} \tag{2.6}$$

where N_0, represents the identical noise power at each receiver antenna.

If the average power at the output of each receive antenna is denoted as P_r; where $r \in \{1,\ldots,M_r\}$; then average SNR at each receive antenna can be written as

$$\gamma = \frac{P_r}{N_0}. \tag{2.7}$$

If the total received power per antenna is assumed to be equal to the total transmitted power ($P_r = P$), then SNR for each receive antenna independent of the value of M_r would be:

$$\gamma = \frac{P}{N_0}. \tag{2.8}$$

Using equations (2.5) and (2.6) the covariance matrix for the received signal can be expressed as in [38]

$$\mathbf{R}_{\mathbf{yy}} = \mathrm{E}\{\mathbf{y}\mathbf{y}^H\} = \mathbb{E}\{(\mathbf{H}\mathbf{x}+\mathbf{z})(\mathbf{H}\mathbf{x}+\mathbf{z})^H\}$$

$$= \mathbf{H}\mathbb{E}\{\mathbf{x}\mathbf{x}^H\}\mathbf{H}^H + \mathbb{E}\{\mathbf{z}\mathbf{z}^H\} \tag{2.9}$$

$$= \mathbf{H}\mathbf{R}_{xx}\mathbf{H}^H + N_0\mathbf{I}_{M_r}$$

Finally, the total received signal power can be calculated as as the trace of the covariance matrix, i.e. $\mathrm{Tr}(\mathbf{R}_{yy})$.

2.2.2 Capacity for MIMO Channels

Based on the basic principles of Information Theory, the capacity of a deterministic channel can be defined as

$$C = \max_{f(\mathbf{x})} I(\mathbf{x};\mathbf{y}) \text{ bits/channel} \qquad (2.10)$$

where $f(\mathbf{x})$ represents the probability density function (PDF) of the signal vector $\mathbf{x}$, and $I(\mathbf{x};\mathbf{y})$ is the mutual information between random vectors $\mathbf{x}$ and $\mathbf{y}$. The channel capacity can be interpreted as the maximum mutual information that can be achieved by varying the PDF of the transmit signal vector. When $\mathbf{x}$ and $\mathbf{y}$ are continuous random vectors, the mutual information of them can be written as:

$$I(\mathbf{x};\mathbf{y}) = H(\mathbf{y}) - H(\mathbf{y}|\mathbf{x}) \qquad (2.11)$$

Using the statistical independence between two random vectors, $\mathbf{z}$ and $\mathbf{x}$, the above equation would be re-express as

$$I(\mathbf{x};\mathbf{y}) = H(\mathbf{y}) - H(\mathbf{z}) \qquad (2.12)$$

where,

$$H(\mathbf{y}) = \log_2\{\det(\pi e \mathrm{R}_{yy})\}$$

$$\qquad (2.13)$$

$$H(\mathbf{z}) = \log_2\{\det(\pi e N_0 \mathbf{I}_{M_r})\}$$

The covariance matrix $\mathbf{R}_{xx}$ in (2.13) is independent of the channel realizations. Given the channel matrix $\mathbf{H}$, the channel capacity of deterministic MIMO channel can be expressed as:

$$C = \log_2\{\det(\mathbf{I}_{M_r} + \frac{1}{N_0}\mathbf{H}\mathbf{R}_{xx}\mathbf{H}^H)\} \text{ bits/sec/Hz} \qquad (2.14)$$

By constraining the power of the transmit signal and assuming $\mathbf{R}_{xx}$ is a function of the channel matrix, one could maximize the achievable rate as

$$C = \max_{\mathrm{Tr}(\mathbf{R}_{xx}) \leq P} \log_2 \{ \det(\mathbf{I}_{M_r} + \frac{1}{N_0} \mathbf{H}\mathbf{R}_{xx}\mathbf{H}^H) \} \text{ bits/sec/Hz.} \qquad (2.15)$$

2.2.3 Parallel Decomposition of the MIMO Channel

The parallel decomposition would be applied on MIMO channels to decompose it into multiple independent none interfering SISO channels. To clarify this mechanism, consider a given channel matrix $\mathbf{H}$ and its representation based on its singular values:

$$\mathbf{H} = \mathbf{U}\mathbf{\Sigma}\mathbf{V}^H \qquad (2.16)$$

where $\mathbf{U} \in \mathbb{C}^{M_r \times M_r}$ and $\mathbf{V} \in \mathbb{C}^{M_t \times M_r}$ are unitary matrices .i.e. $\mathbf{V}\mathbf{V}^H = \mathbf{I}$. Here, Σ represents the diagonal matrix of size $M_r \times M_t$ which contains the singular values of the channel matrix, i.e. σ_i. Moreover, since singular values and the eigenvectors of the channel matrix are related we can write:

$$\mathbf{H}\mathbf{H}^H = \mathbf{U}\mathbf{\Sigma}\mathbf{\Sigma}^H\mathbf{U}^H = \mathbf{U}\mathbf{\Lambda}\mathbf{U}^H \qquad (2.17)$$

where, the diagonal elements of matrix Λ represent the eigenvalues of matrix $\mathbf{H}\mathbf{H}^H$ as $\lambda_i = \sigma_i^2$. By this definition, the rank of channel matrix $(R_\mathbf{H})$ can be determined based on the number of non-zero singular values of matrix $\mathbf{H}$ or eigenvalues of the hermitian symmetric matrix $\mathbf{H}\mathbf{H}^H \in \mathbb{C}^{M_r \times M_r}$ as

$$\lambda_i = \begin{cases} \sigma_i^2 & , i = \{1, 2, \ldots, M_{min}\} \\ 0 & , i = \{M_{min} + 1, \ldots, M_r\} \end{cases} \qquad (2.18)$$

where, $M_{min} = \min(M_t, M_r)$. Thus the rank is upper bounded as $R_H \le \min(M_t, M_r)$. The rank value would mostly hold for rich scattering channels while for highly correlated channels it will reduce to $R_\mathbf{H} = 1$.

The squared Frobenius norm of a MIMO channel is interpreted as the total power gain of the channel and equals

$$||\mathbf{H}||_F{}^2 = \text{Tr}\left(\mathbf{H}\mathbf{H}^H\right) = \sum_{i=1}^{M_r}\sum_{j=1}^{M_t}|h_{i,j}|^2 \qquad (2.19)$$

Equation (2.19) can also be re-expressed as the linear combination of the square of the singular values or eigenvalues:

$$\begin{aligned}
||\mathbf{H}||_F{}^2 &= ||\mathbf{U}^H\mathbf{H}||_F{}^2 \\
&= \text{Tr}\left(\mathbf{U}^H\mathbf{H}\mathbf{H}^H\mathbf{U}\right) \\
&= \text{Tr}\left(\mathbf{U}^H\mathbf{U}\Lambda\mathbf{U}^H\mathbf{U}\right) \\
&= \text{Tr}(\Lambda) = \sum_{i=1}^{M_{min}}\lambda_i = \sum_{i=1}^{M_{min}}\sigma_i{}^2
\end{aligned} \qquad (2.20)$$

Note that, the Frobenious norm of a matrix would not be changed by multiplication with a unitary matrix [39].

To decompose the deterministic MIMO channel $\mathbf{H}$ into multiple independent SISO channels first the unitary matrix $\mathbf{V}^H$ is used as precoding matrix at transmitter side to shape the input of MIMO system to $\mathbf{x} = \mathbf{V}^H\tilde{\mathbf{x}}$. In a similar manner at the receiver the unitary matrix $\mathbf{U}^H$ would be used to decouple the precoded signals in the previous step.

The received signal after parallel decomposition can be expressed as

$$\tilde{\mathbf{y}} = \mathbf{U}^H (\mathbf{Hx} + \mathbf{z})$$

$$= \mathbf{U}^H (\mathbf{U\Sigma V}^H + \mathbf{z})$$

$$= \mathbf{U}^H (\mathbf{U\Sigma VV}^H \tilde{\mathbf{x}} + \mathbf{z}) \qquad (2.21)$$

$$= \mathbf{U}^H \mathbf{U\Sigma VV}^H \tilde{\mathbf{x}} + \mathbf{U}^H \mathbf{z}$$

$$= \mathbf{\Sigma}\tilde{\mathbf{x}} + \mathbf{U}^H \mathbf{z}$$

Note that the distribution of the noise vector dose not change after multiplying it by a unitary matrix.

A block diagram representation of the processing described above is depicted in Figure 2.2. Note that, since Σ in equation (2.21) is a diagonal matrix with $R_{\mathbf{H}}$ non-zero diagonal elements, the $M_t \times M_r$ MIMO system would be decomposed into $R_{\mathbf{H}}$ parallel independent SISO channels. The $\tilde{x}_i$ and $\tilde{y}_i$ represent input and output of the ith independent channel with gain σ_i. Hence a multiplexing gain of $R_{\mathbf{H}}$ can be achieved by the MIMO channel; i.e. the achievable rate of MIMO channel would be $R_{\mathbf{H}}$ times that of a SISO channel.
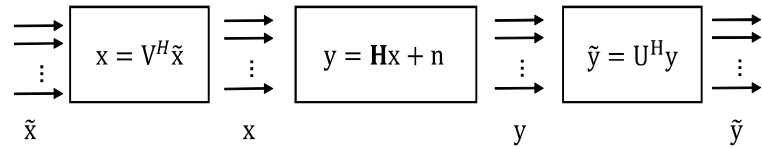
Figure 2.2: Parallel decomposition of MIMO channel using SVD.

Since the transmit power for the ith transmit antenna is given by $P_i = \mathbb{E}\{|x_i|^2\}$, the

capacity of the ith virtual SISO channel could be written as

$$C_i(P_i) = \log_2\{(1 + \frac{P_i}{N_0}\lambda_i)\}, \quad i = 1, 2, \ldots, R_{\mathbf{H}}. \tag{2.22}$$

If that total available power at the transmitter is limited to $\mathbf{R}_{xx} = \sum_{i=1}^{M_t} \mathbb{E}\{|x_i|^2\} = P$ then, the capacity of MIMO channel can be expressed as sum of the capacities of the decomposed SISO channels

$$C(P) = \sum_{i=1}^{R_H} C_i(P_i) = \sum_{i=1}^{R_H} \log_2\{(1 + \frac{P_i}{N_0}\lambda_i)\}. \tag{2.23}$$

Moreover, it can be noted that when the channel matrix is known, the transmitter can allocate different amount of power to each of the decomposed SISO channels based on their eigenvalues. Under this scenario, the capacity can be maximized by solving the following power allocation optimization problem

$$C = \max_{P_i^*} \sum_{i=1}^{R_H} C_i(P_i^*) = \sum_{i=1}^{R_H} \log_2\{(1 + \frac{P_i^*}{N_0}\lambda_i)\}$$

$$\text{Subject to} \sum_{i=1}^{R_H} P_i^* = P \tag{2.24}$$

The solution to the above power allocation problem is known as the Linear Zero Forcing (LZF) with Water Filling (WF).

Note from (2.16) that, in order to determine the precoder and receiver shaping matrices full Channel State Information (CSI), i.e. $\mathbf{H}$ is required. On the other hand when the transmitter has only statistical characterization of the fading channel a reliable communication rate would only be possible over multiple coherence time intervals of the channel. Hence a long-term rate can be obtained by taking the expected value over

all realizations

$$C = \mathbb{E}\left[\log_2\{\det(\mathbf{I}_{M_r} + \frac{1}{N_0}\mathbf{H}\mathbf{R}_{xx}\mathbf{H}^H)\}\right] \quad \text{bits/sec/Hz} \qquad (2.25)$$

When only statistical characterization of the channel is available, the input covariance matrix $\mathbf{R}_{xx}$ should be matched with the channel statistics rather than the channel realization. The reliable communication rate for this case could be written as

$$C = \max_{\text{Tr}(\mathbf{R}_{xx}) \leq P} \mathbb{E}\left[\log_2\{\det(\mathbf{I}_{M_r} + \frac{1}{N_0}\mathbf{H}\mathbf{R}_{xx}\mathbf{H}^H)\}\right] \quad \text{bits/sec/Hz} \qquad (2.26)$$

Finally, if the elements of $\mathbf{H}$ are not known but are sufficiently random (Rayleigh fading model with $\mathcal{CN}(0,1)$), then the optimal covariance matrix would be expressed as in [39]

$$\mathbf{R}_{xx} = \frac{P}{M_t}\mathbf{I}_{M_t} \qquad (2.27)$$

where equal amounts of powers are allocated to each eigenvalue. Then the maximum achievable rate would be

$$C = \mathbb{E}\left[\log_2\{\det(\mathbf{I}_{M_r} + \frac{P}{N_0 M_t}\mathbf{H}\mathbf{H}^H)\}\right] = \mathbb{E}\left[\log_2\{\det(\mathbf{I}_{M_r} + \frac{\text{SNR}}{M_t}\mathbf{H}\mathbf{H}^H)\}\right] \text{bits/sec/Hz.}$$
$$(2.28)$$

2.2.4 Performance Gain of MIMO System at High SNR Regime (DoF)

The multiplexing gain represents the number of interference free signal dimensions and is measured by the Degree of Freedom (DoF). DoF characterizes the multiplexing gain at high SNR regime when the total transmit power approaches to infinity and the noise power and channel coefficients remain constant. Definition of the DoF metric η is as follows:

$$\eta = \lim_{P \to \infty} \frac{C(P)}{\log(P)} \qquad (2.29)$$

20

where, $C(P)$ denotes the sum-capacity and P the total transmit power. The above equation can be re-formulated as:

$$C(P) = \eta \log(P) + o\left(\log(P)\right) \qquad (2.30)$$

where the term $o\left(\log(P)\right)$ can be understood as a function $f(P)$ that tends to zero as the transmit power goes to infinity

$$o\left(\log(P)\right) = \lim_{P \to \infty} \frac{f(P)}{\log(P)} = 0. \qquad (2.31)$$

MIMO fading channel capacity expressed by (2.28) is a function of the distribution of the singular values $[\lambda_i s]$ of the random channel. From Jensen's inequality [39], we know that

$$C = \sum_{i=1}^{R_H} \log_2\{(1 + \frac{\mathrm{SNR}}{M_t}\lambda_i)\} \leq M_{min} \log_2\{(1 + \frac{\mathrm{SNR}}{M_t}\left[\sum_{i=1}^{R_H} \frac{1}{M_{min}}\lambda_i\right])\} \qquad (2.32)$$

The case of equality would be true iff the singular values are all identical.

When the channel matrix **H** is sufficiently random, statistically well-conditioned and channel gain is well distributed across the singular values then DoF at high SNR would be equal M_{min} and the capacity could be expressed as

$$C \approx M_{min} \log_2 \frac{\mathrm{SNR}}{M_t} + \sum_{i=1}^{R_H} \mathbb{E}\left[\log_2 \lambda_i\right] \qquad (2.33)$$

where,

$$\mathbb{E}\left[\log_2 \lambda_i\right] > -\infty. \qquad (2.34)$$

Note that the degrees of freedom is constrained by the minimum of the number of transmit and number of receive antennas $[M_{min} = \min(M_t, M_r)]$. This implies that

for a large capacity, one would need to deploy multiple transmit and multiple receive antennas.

In summary, based on (2.33), one can interpret the DoF metric as the number of signal dimensions where each signal dimension represents an independent interference free Additive White Gaussian Noise (AWGN) SISO channel at high SNR. Moreover, the DoF metric can be referred to as the bandwidth effectivity.

2.2.5 Types of Interference Networks

One essential question that remains to be answered is how to apply the MIMO channel in cellular networks.

When a MIMO channel has more than one transmitter it is necessary to have accurate CSIT. To obtains CSIT first the sequence of orthogonal pilot signals must to be transmitted, then the estimated CSI at each receiver has to be conveyed to each transmitter through the backhaul. Moreover, deployment of MIMO systems in cellular networks is not a straightforward since cellular networks are comprised of both broadcast and interference channels. In this thesis the classification of interference networks are carried out based on the number transmitters (S) they have and the total number of users (K) in the network.

The following shows the possible interference networks based on the values that S can assume:

- ($S = 1$) corresponds to the Broadcast Channel (BC) where a transmitter tries to serve any one of the receivers that are associated with it. Other than the intended, all remaining users will consider this transmitted signal as intracell interference

(refer to Figure 2.3).
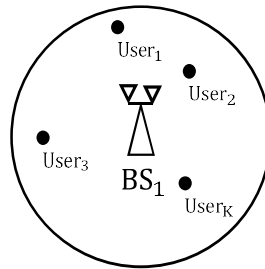
Figure 2.3: MIMO broadcast channel where one transmitter serves multiple users in its coverage area ($S = 1$).

- ($S = K$) corresponds to an Interference Channel (IC) for which each transmitter is paired with a single receiver (number of transmitters and receivers are equal) and serves its paired receiver. Signal(s) from other transmitters are considered as a source of interference (See Figure 2.4).
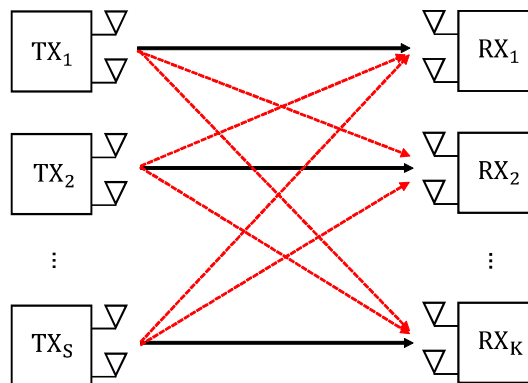
Figure 2.4: K-user MIMO interference channel with equal number of transmitters and receivers where each transmitter serves its corresponding receiver ($S = K$).

- ($1 < S < K$) denotes a cellular network where each transmitter serves multiple receivers. In addition to the intracell interference in BC, this network also suffer from another type of interference. In this case the signals from other transmitter/s are considered as source of interference and referred to as intercell (Figure 2.5).
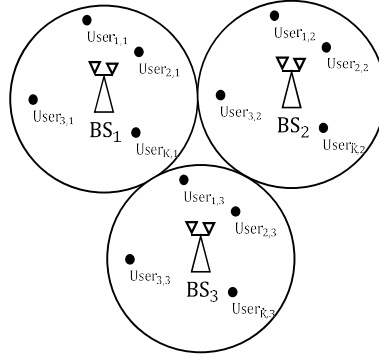
Figure 2.5: MIMO cellular network under which multiple MIMO broadcast channels work side by side at the same time $(1 < S < K)$. Cells may have different or same number of users.

To handle the interference in MIMO cellular networks many methods have been proposed. An straightforward approach to solve this problem is refereed to as MIMO network. As an example consider a cellular network with N BSs each with M_t transmit antennas and one receiver per cell with M_r antennas. In the MIMO network model, all BSs are considered as one transmitter with NM_t antennas serving one user equipped with NM_r antennas. Moreover other interference avoidance methods such as Block Diagonalization (BD) [30, 31] or Linear Zero Forcing Beamforming (LZFB) [28, 29] have been proposed to handle the interference in MIMO cellular networks. However providing global CSIT is a challenging task in MIMO cellular networks, and requires high speed backhaul links for sharing CSIT and synchronization between BSs.

2.2.6 Interference Alignment Concept

In contrast to the above mentioned interference avoidance techniques, to manage the interference in cellular networks a new method referred to as Interference Alignment (IA) is proposed in [40–44]. The key idea behind IA is to align the interference in such a way that it spans minimum possible dimensions out of the available signal space and leaves many interference free dimensions for the desired signals. The IA scheme

requires full CSI to construct the beamforming and receiver filters. For instance, the problem of MIMO interference channel has been tackled as an K-users $M \times M$ MIMO Interference Channel (IC). This method has been applied on a network comprised of K transmitters each equipped with M antennas and serving its corresponding receiver with M antennas. In this scheme, the ith receiver can decode the message transmitted by the ith transmitter while the interference signals transmitted by other transmitters ($j \neq i$) would be properly aligned. It has been shown that this scheme can achieve $\frac{KM}{2}$ DoF or $M/2$ interference free dimensions for desired signals of each user [22]. The above mentioned IA scheme can be represented as follows:

$$\lim_{n \to \infty} \dim \left(\text{Proj} \, \mathbf{I}_i^c \, \text{span} \left(\mathbf{U}_i^n \mathbf{H}_{i,i}^n \mathbf{V}_i^n \right) \right) = \frac{1}{2} \mathrm{M} n \; \forall k \in \{1, 2, \ldots K\}. \qquad (2.35)$$

where $\mathbf{H}_{i,j}^n$ represent the channel matrix between the jth transmitter and the ith receiver while $\mathbf{U}_i^n$ and $\mathbf{V}_i^n$ denote the beamformer matrix and receiver filters of transmitter and receiver i during the n channel uses. Moreover, $\mathbf{I}_i$ represent the interference signal subspace at receiver i as:

$$\mathbf{I}_i = \text{span} \left(\mathbf{U}_i^n [\mathbf{H}_{i,1}^n \mathbf{V}_1^n, \ldots, \mathbf{H}_{i,i-1}^n \mathbf{V}_{i-1}^n, \mathbf{H}_{i,i+1}^n \mathbf{V}_{i+1}^n, \ldots, \mathbf{H}_{i,K}^n \mathbf{V}_K^n] \right) \qquad (2.36)$$

where $(\text{Proj} \, \mathbf{I}_{\mathcal{A}}^c \, \mathcal{B})$ represents the vector space spanned by the projection of vector $\mathcal{B}$ over the null-space of vector $\mathcal{A}$. As it shown in (2.36) the IA framework requires full CSI at transmitters and receivers to be applicable in cellular network [45].

2.3 Analysis of the state-of-the-art

To mitigate the effect of interference over cellular networks various interference management techniques have been proposed. This section will review the interference management techniques which may be classified under Interference Alignment (IA). Firstly, a summary of traditional interference avoidance techniques that could be

applied over different MIMO interference channels (BC,IC and X-channel) is provided and their theoretical DoF region and the amount of CSIT required by each technique will be reviewed. Secondly, the feasibility of using the state-of-art blind-IA (BIA) technique in order to reduce the amount of CSIT required will be discussed. Thirdly, assuming deployment of small-cells under a dense cellular network, the applications of IA and BIA techniques to handle the two main sources of interference: 1) intracell interference 2) intercell interference will be pointed out. Finally, the evolution of cellular networks from homogeneous to heterogeneous will be explained and applications of BIA over heterogeneous cellular networks to handle co-tier and cross-tier interference will be detailed.

Theoretical limits for capacities of different channels have been provided under information theory. However, the closed form solutions for capacities of many MIMO systems still has not been established. Instead for most cases researchers have used the Degree of Freedom (DoF) metric to measure and evaluate the multiplexing gain of MIMO systems.

The DoF of MISO BC with M transmit antennas and $K = M$ users each equipped with a single antenna, was evaluated in [46–48] and it has been shown that M DoF can be achieved given full CSI both at transmitter and receiver. In [49], the achievable DoF for a MISO broadcast channel with two users ($K=2$) that has M_{r_1} and M_{r_2} receive antennas respectively and a transmitter with M transmit antennas has been evaluated. [49] has showed that the $\max(M, M_{r_1} + M_{r_2})$ DoF can be achieved when the global CSI is available. However, for large number of transmitters or receivers with multiple receive antennas analyzing the achievable DoF would start to become a challenge.

The achievable DoF of a MIMO Interference Channel (IC) with $S = K$ transmitter/receiver pairs (each equipped with M_t and M_r antennas) has been provided in [20]. This work has showed that for $S \leq R$ where $R = \frac{\max(M_t, M_r)}{\min(M_t, M_r)}$ the achievable DoF would equal $\min(M_t, M_r) \cdot S$ and for $S > R$, $\min(M_t, M_r) \cdot \frac{R}{R+1}$ DoF would be attained. It was pointed out that when transmitters and receivers are equipped with same number of antennas ($M_t = M_r$), then the achieved DoF would become $M_t/2$.

It is worth underlining once more that the aforementioned DoF gains could be achieved if and only if global CSIT is available and in absence of perfect CSIT, the DoF gains would collapse. As an example, consider a MISO broadcast channel with no CSIT over which a conventional orthogonal resource allocation strategy is being applied. Under such a scenario the achievable DoF would collapse to 1.

The DoF regions for MIMO BC and MIMO IC and their extensions in the absence of CSIT have been presented in [50] and [51] respectively. In practical settings however, channel side information at transmitter may not be available, may be delayed or may be degraded. In the literature a great deal of research exist that tries to analyze the achievable DoF of different channel configurations where different level of CSIT is available [52–57].

Moreover, even when CSIT is available the channel states may change during the course of transmission. This type of transmission is referred to as the Compound Channel(CCh). Under linear beamforming, the achievable DoF for a compound broadcast channel (CBC) has been evaluated in [58] and authors in [59] has showed that more than 1 DoF could be achieved when the channel varies only between a finite set of channel sates. The DoF region of compound BC and IC configurations have

been presented in [60] and therein it was shown that the DoF for compound MISO BC would equal $\frac{KM}{K+M-1}$ when the transmitter has M transmit antennas and each of the K users have a single receive antenna and the channel state of each user changes only between set of finite states. Similarly, the DoF region for a compound IC assuming only a real channel has been studied in [60] and it was shown that the achieved DoF gain would be equal to $\frac{K}{2}$.

After driving the DoF regions for the different channel configurations, the next step would be to investigate how one can achieve the derived upper bounds while using different interference management techniques over cellular networks. In [10–16], it was shown that the full multiplexing gain would be achieved by applying LZF and BD beamforming over MISO and MIMO channels. Moreover, it was demonstrated that if the number of transmitters increases designing a scheme capable of achieving the optimal DoF would become computationally expensive.

In contrast to the aforementioned interference avoidance schemes, the possibility of using Interference Alignment(IA) technique to achieve the optimal DoF has also been investigated. The feasibility condition for IA was first derived in [61, 62]. Afterwards the achievable DoF over an IC using IA has been derived in [22, 63, 64]. To achieve maximum DoF these schemes all have assumed perfect knowledge of CSI at transmitter and receiver.

Main drawback of most IA techniques is that, global channel state information should be available at all nodes [65]. In the literature it was shown that this would be difficult to achieve since overhead of CSI feedback would be high [66]. In absence of perfect channel state information or with partial CSIT the DoF of the network would start to

deteriorate and the transmissions would become unreliable [23]. Assuming no CSIT and using predefined channel correlations the feasibility of IA over the BC was first presented in [24]. Later in [67–70] it was shown that artificial generation of the channel correlations using pattern-reconfigurable antennas was quite possible.

A pattern-reconfigurable antenna is an antenna that can dynamically change its radiative properties (radiation pattern, frequency and polarization) between a set of finite states using micro-electromechanical switches. A reconfigurable antenna is known to require less space than multiple regular antennas since it can switch between multiple modes using only a single Radio Frequency (RF) chain.

Application of blind IA (IA with no CSIT) over the BC was first proposed in [24] and later on elaborated upon in [25]. This new technique is known as standard Blind Interference Alignment (s-BIA) and assumes a K-user, $M \times 1$ MISO BC ($[K,M]$ configuration) in which the BS is equipped with M transmit antennas and each receiver has a single reconfigurable antenna capable of switching between M preset modes. With no knowledge about CSIT, s-BIA can align all intracell interference with only a mild assumption on the channel coherence structure and has been shown to achieve $\dfrac{KM}{K+M-1}$ DoF. Moreover, in [71] the linear achievable DoF of MIMO BC using BIA with multiple reconfigurable antennas at each receiver has been studied. The literature also points out that BIA that uses more than one transmitter could be quite difficult to analyze.

Achievable DoF of s-BIA over a SISO IC has been investigated in [72–76] and in [40, 77] the s-BIA have been applied under the K-user $M \times 1$ MISO Interference Channel (IC) where users were assumed to have different number of preset modes. The s-BIA

technique requires that the channel remains unchanged throughout the duration of the transmission. Therefore, coherence time or bandwidth becomes an important measure when determining whether s-BIA can be utilized or not [26]. Hence, reserchers are motivated to come up with BIA schemes that have short supersymbol lengths. which will correspond to realistic coherence times.

The ever increasing demand for mobile broadband applications and services has led to massive network densification. Most cellular system architectures are both economically and ecologically limited to handle such expansion. The concept of small-cell networks (SCNs) based on the idea of dense deployment of self-organizing, low-cost,low-power base stations (BSs) has been a promising alternative that has been utilized for some time. The performance of s-BIA under cellular and clustered systems was first analyzed in [78]. It was shown that although s-BIA can totally cancel the intracell interference, the rates of users located at the cell edges would deteriorate due to the intercell interference coming from the neighboring cells.

A straight forward approach to cope with both intra and intercell interference in cellular networks (each cell with $[K, M]$ configuration) would be to apply a technique known as extended BIA (ext-BIA) [79]. This scheme assumes no data-sharing between the base stations and can fully remove the intercell interference at the expense of longer supersymbol lengths. Alternatively, an approach where data sharing has been employed could be found in [80].

In both [78] and [81] it is mentioned that if the BIA codes of the neighboring cells are synchronized (sync-BIA), then the intercell interference can considerably be reduced. Moreover a comparison between s-BIA and LZFB has been provided in [81].

In [80], it was shown that a new scheme known as coordinated BIA (c-BIA) could also be applied to align intra and intercell interference in cellular networks. However, the supersymbol lengths for c-BIA were seen to be much longer than the ones required by ext-BIA.

A compromise between IA techniques with global CSIT and the ones which are totally blind would be to use the knowledge of network topology. Idea of using the topological interference management (TIM) was first proposed in [27–29] where the authors have suggested using location information of the users and base stations in a network to enhance the performance of IA by treating interference as noise [82, 83]. An analysis of TIM for linear, square, and hexagonal cellular arrays has been carried out in [84,85]. It was shown that when channel gains remain constant throughout the transmission period, TIM would be equivalent to the index coding problem [86, 87]. Moreover, [85] has showed that knowledge of the network topology can be used to differentiate between users that are subject to intercell interference (shared users) and those who can treat the interference as noise (private users).

BIA using network topology was presented in [30] and it was pointed out that full connectivity may not be possible in several practical scenarios and partially-connected networks in general may achieve higher DoFs. Network BIA (n-BIA) [30] which is a general interference alignment technique for cellular networks has assumed a partially-connected network topology and can differentiate between its private users that can see intercell interference as noise and its shared users that are connected to all BSs in their proximity. In [30] it was shown that n-BIA can achieve optimal-DoF under symmetric cellular networks. However, this theoretical upper bound could only be achieved iff the cell-edge users (shared users) could switch between preset modes that are equal to

the total number of transmit antennas in the neighboring cells.

To manage the intercell interference seen by shared users in a partially-connected cellular network an alternative BIA based method was proposed in [77]. This DoF-oriented BIA scheme would relax the orthogonality among users which have the smallest number of preset modes and assumes that they can be represented as one virtual user-group with preset mode that is equal to the sum of all user's modes in that group. Afterwards, s-BIA can be applied in the network for creation of the precoder matix. Each member of the virtual group has to decode the transmitted signals for all members of the group before extracting their own desired signals.

SNR-BIA for a multi-cell network was introduced in [88] and tries to jointly optimize the transmitter connections and the user grouping to reduce the noise accumulation due to the zero forcing subtractions of s-BIA. SNR-BIA has been inspired by what has been presented in [77] and [89]. In [88], it was demonstrated that SNR-BIA is more robust to user mobility and would have an increased sumrate when compared against c-BIA, s-BIA and ext-BIA schemes.

It was noted that, under various scenarios users were only able to switch between a limited number of preset modes which was dictated by their hardware configurations. For BIA schemes presented in [30], [77] and [88] the shared users were assumed to be capable of switching between more than their actual preset modes and this would help them to acquire a higher DoF which is only possible in theory.

Motivated by sync-BIA and ext-BIA, [79] has proposed a new BIA scheme that makes use of topological information in a cellular network. This scheme is known as

topological BIA (top-BIA) and enhances the performance of s-BIA under various user distributions. In [79], users that can be served at the same time are grouped with the aim of minimizing the supersymbol length. Moreover, in this scheme users are only served by their corresponding BSs and can only switch between preset modes dictated by their hardware configurations. It was shown that under different user distributions, top-BIA would uniformly outperform both sync-BIA and ext-BIA. Even though in [79] the initial network is partially-connected (signals of only a small number of BSs can be seen by each user), in essence the groups of users determined by the top-BIA can be treated as a fully-connected network under s-BIA.

Finally, [45] has proposed a new BIA technique known as hierarchical blind interference alignment (h-BIA) that could be applied over the IC and has showed its extension to cellular networks with finite coherence time. Initially, h-BIA would form proper groups of users and then interference between users of the same group (inter-user interference, IUI) and subsequently between different groups (inter-group interference, IGI) is managed via s-BIA. h-BIA requires full connectivity among users and all available BSs. In [45] it was shown that while h-BIA could significantly reduce the length of the supersymbol length it would incur some DoF loss.

The use of heterogeneous networks (HetNets) which are comprised of macro and femto cells has been proposed in [31, 32]. It was assumed that the femtocells (FCs) are randomly deployed under the coverage area of a macrocell (MC) and some users were served by FCs to reduced the load on MCs [33, 34]. Furthermore, issues such as how to serve the cell-edge users in practical systems and how to maximize the sum-rate and achievable DoF were addressed in [90].

Interference management over heterogeneous networks assuming global CSIT has been addressed by [91–93]. These references point out that to manage intracell, intercell, co-tier and cross-tier interferences a tremendous amount of information must be fed back via the backhaul links. Since under many scenarios this may be impractical use of cognitive small cells have been proposed by [94–97] to address a solution to this problem.

Recently, BIA has also been applied in some two-tier macro-femto cellular networks. [79] has used knowledge of network topology to propose several heuristic BIA schemes while trying to reduce the supersymbol lengths and maintaining a good DoF. In [23], Kronecker product representation has been used to design a BIA scheme for managing the interference in a two-tier HetNet where several femto BSs each with only one FU were allocated under the coverage area of a MC. Although the schemes proposed in [79] and [23] can cancel all types of interference, since each user could only switch between its actual preset modes these schemes are generally sub-optimal as far as DoF gain is concerned.

To maximize the sum-DoF of a heterogeneous network, an extended version of n-BIA was proposed in [98]. In this scheme, macro users (MUs) were considered as private users and would receive signals only from their corresponding MBS while femto users (FUs) were considered as shared users and were able to align the received signals from their FBS and the interfering MBS.

Trying to maximize the sum-DoF of the macro-tier (with no CSIT assumption), the linear DoF region of the two-tier macro-femto network has been derived in [99]. To achieve this upper bound, a cognitive BIA scheme (cog-BIA) [99] was proposed .

Therein, the femto-tier would achieve non zero-DoF while the macro-tier still would

achieve the same optimal DoF as if the femto-tier was not present.

Chapter 3

BLIND INTERFERENCE ALIGNMENT FRAMEWORK AND ITS APPLICATIONS

3.1 Introduction

Most Interference Alignment (IA) techniques prior to Blind IA (BIA) required perfect knowledge of the Channel State Information at the Transmitter (CSIT). To meet this requirement one would need high-capacity backhaul links and accurate synchronization, which would require a large amount of network resources. Blind Interference Alignment (BIA) which is also known as standard BIA (s-BIA) was first proposed in [24] and would assume no CSIT. s-BIA was first applied over the K-user $M \times 1$ MISO Broadcast Channel (BC) and it would align all intracell interference with only a mild assumption on the channel coherence structure. The maximum achievable DoF for s-BIA was shown to equal $\frac{KM}{K+M-1}$. As stated in [77, 100] s-BIA was later extended for the K-user $M \times 1$ MISO Interference Channel (IC) assuming an asymmetric antenna configuration (users have different number of preset modes $M_k \leq M, M \geq 2$). Therein it was also demonstrated that when preset modes for users are identical then K-user $M \times 1$ IC will achieve the same DoF that K-user, $M \times 1$ MISO BC does. As stated in [40], for fully-connected IC networks sum-DoF would not scale with number of transmitters but instead would depend on the preset modes of each user.

The remaining sections of this chapter will first describe the construction of beamforming matrix plus the generic supersymbol structure when s-BIA is adopted under BC and IC. This will then be followed by an analysis of the achievable DoFs and derivation of the closed-form expressions for the sumrate under MISO BC and IC. Thirdly, the chapter will show how the sumrates could be calculated under two different power allocation strategies: Mainly 1) uniform power allocation [24] and 2) constant power allocation [78, 81]. At the end, the chapter will show how BIA can be applied under different cellular scenarios.

3.2 Blind Interference Alignment for K-user $M \times 1$ MISO BC

3.2.1 System Model for MISO BC

Consider a broadcast channel where a BS has M transmit antennas and K active users each with a single reconfigurable antenna. Assume that the reconfigurable antenna of each user can switch between M preset modes, same as the number of transmitter's antennas. The transmitted signal at time t can then be represented as $\mathbf{x}(t) = [u_1, \ldots, u_M]^T \in \mathbb{C}^{(M \times 1)}$, where u_i, $i \in \{1, \ldots, M\}$ denotes the transmitted symbol by the ith transmit antenna at the base station. Based on this definition, the received signal of the kth user at time t would be:

$$y^{[k]}(t) = \mathbf{h}^{[k]}\left(n^{[k]}(t)\right)\mathbf{x}(t) + z^{[k]}(t) \tag{3.1}$$

where, $\mathbf{h}^{[k]}\left(n^{[k]}(t)\right) \in \mathbb{C}^{(1 \times M)}$ is the channel vector between BS and k^{th} user at time t with channel mode $n^{[k]}(t)$. Channel state at time t for k^{th} user can assume any one of the M possible modes and $z^{[k]}(t) \in \mathcal{CN}(0, 1)$ denotes the zero mean, unit variance additive white Gaussian noise. It is assumed that the transmitter does not have any information about channel sate information at transmitter (no CSIT) and the channel

stays constant during the course of transmission for sufficient number of channel uses or time slots. In addition, the channel coefficients in the channel vector **h** are assumed to be independent and identically distributed (*i.i.d.*), zero mean and unit variance, complex Gaussian random variables. This would guarantee that any M channels would be linearly independent. Moreover, the transmit signal $\mathbf{x}(t)$ is subject to the average constraint power $\mathbb{E}\|\mathbf{x}(t)\|^2 \leq P$ for $t \geq 1, t \in \mathbb{N}$.

3.2.2 *K*-user 2×1 MISO BC

To clarify the construction of beamforming matrix plus the generic supersymbol structure under BC this subsection will introduce the toy example depicted in Figure 3.1. Under 2×1 2-user MISO BC the transmitter has $M = 2$ antennas and each user has a single reconfigurable antenna capable of switching between two different modes. Based on the derivarions in [71], the maximum achievable DoF by this setting in absence of CSIT would be $4/3$.
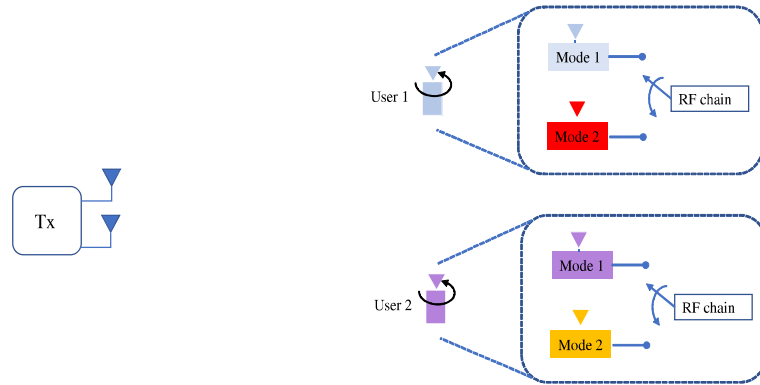
Figure 3.1: Representation for 2×1 2-user MISO BC with one reconfigurable antenna at each receiver.

To achieve this upper bound a BS would need to transmit the following signals using a

supersymbol of length three symbol extensions:

$$\mathbf{X} = \begin{bmatrix} \mathbf{x}(1) \\ \mathbf{x}(2) \\ \mathbf{x}(3) \end{bmatrix} = \begin{bmatrix} \mathbf{I} \\ \mathbf{I} \\ \mathbf{0} \end{bmatrix} \mathbf{x}_1^{[1]} + \begin{bmatrix} \mathbf{I} \\ \mathbf{0} \\ \mathbf{I} \end{bmatrix} \mathbf{x}_1^{[2]} \tag{3.2}$$

where, $\mathbf{X} = \left[\mathbf{x}(1)^T \mathbf{x}(2)^T \mathbf{x}(3)^T \right]^T \in \mathbb{C}^{3M \times 1}$ represents the transmitted signal during the entire supersymbol of three channel uses and in (3.2), $\mathbf{x}_q^{[k]} = \left[u_{q,1}^{[k]}, u_{q,2}^{[k]} \right]^T$ denotes the qth symbol vector transmitted to the kth user (in this particular example $q = 1$). Elements of the transmitted symbol vectors can in general be denoted as $u_{q,\tau}^{[k]}$ and represent the symbols transmitted by the τth transmit antenna of the BS ($\tau \in \{1, 2\}$) to the kth user during symbol vector q. Hence, for the toy example depicted in Figure 3.1 each $\mathbf{x}_q^{[k]}$ carries 2 DoF. Even though for the 2×1 2-user MISO BC example $q = 1$, in general the number of symbol vectors q (also referred to as alignment blocks), for each user depends on the number of transmit antennas M and the active users K as $q = (M-1)^{(K-1)}$. In addition, $\mathbf{I}$ and $\mathbf{0}$ respectively represents the 2×2 identity and zero matrices. For the toy-example introduced, received signal at user-1 during three channel uses (entire supersymbol length) would be as follows:

$$\begin{bmatrix} y^{[1]}(1) \\ y^{[1]}(2) \\ y^{[1]}(3) \end{bmatrix} = \underbrace{\begin{bmatrix} \mathbf{h}^{[1]}(1)^T \\ \mathbf{h}^{[1]}(2)^T \\ \mathbf{0} \end{bmatrix}}_{\text{rank}=2} \mathbf{x}_1^{[1]} + \underbrace{\begin{bmatrix} \mathbf{h}^{[1]}(1)^T \\ \mathbf{0} \\ \mathbf{h}^{[1]}(1)^T \end{bmatrix}}_{\text{rank}=1} \mathbf{x}_1^{[2]} + \begin{bmatrix} z^{[1]}(1) \\ z^{[1]}(2) \\ z^{[1]}(3) \end{bmatrix} \tag{3.3}$$

As shown by equation (3.3) and according to Table 3.1, by this transmission strategy, the desired signal for user-1 would occupy a two-dimension space in a full rank matrix (rank 2) while the desired signals for user-2 (interference seen by user-1) are aligned over one of three available dimensions at user-1 (in vector space $[1\,0\,1]^T$ in the given

example).

Table 3.1: Supersymbol structure for the 2-user 2×1 MISO BC where each row represent the preset mode pattern structure of a user.

Time slot	1	2	3
User1	$\mathbf{h}^{[1]}(1)$	$\mathbf{h}^{[1]}(2)$	$\mathbf{h}^{[1]}(1)$
User2	$\mathbf{h}^{[2]}(1)$	$\mathbf{h}^{[2]}(1)$	$\mathbf{h}^{[2]}(2)$

It can be easily seen that in the first time slot user-1 receives the summation of desired symbol $\mathbf{x}_1^{[1]}$ and the interference signal $\mathbf{x}_1^{[2]}$ while using the initial preset mode. On the other hand, symbols $\mathbf{x}_1^{[1]}$ and $\mathbf{x}_1^{[2]}$ are transmitted in an orthogonal manner within time slots 2 and 3. This strategy enables user-1 to measure the desired signal transmitted to user-2 as the source of interference in third time slot by using the same preset mode in the first time slot. This would allow user-1 to simply remove the interference received in the first time slot by subtracting the third received signal from sum of the desired signal plus the interference. This procedure is generally referred to as the zero forcing cancellation and the received signal of user-1 after this process can be formulated as:

$$
\tilde{\mathbf{y}}^{[1]} = \begin{bmatrix} y^{[1]}(1) - y^{[1]}(3) \\ y^{[1]}(2) \end{bmatrix} = \underbrace{\begin{bmatrix} \mathbf{h}^{[1]}(1)^T \\ \mathbf{h}^{[1]}(2)^T \end{bmatrix}}_{\mathbf{H}^{[1]}} \mathbf{x}_1^{[1]} + \underbrace{\begin{bmatrix} z^{[1]}(1) - z^{[1]}(3) \\ z^{[1]}(2) \end{bmatrix}}_{\tilde{\mathbf{z}}^{[1]}} \tag{3.4}
$$

where, $\tilde{\mathbf{y}}^{[k]} \in \mathbb{C}^{M \times 1}, \mathbf{H}^{[k]} = \left[\mathbf{h}^{[k]}(1)^T \, \mathbf{h}^{[k]}(2)^T \right]^T \in \mathbb{C}^{2 \times 2}$ and $\tilde{\mathbf{z}}^{[k]} \in \mathbb{C}^{M \times 1}$ respectively represent the received signal, the effective channel matrix and the noise vector of the kth user for $k \in \{1, 2\}$ after zero forcing cancellation. Finally, user-1 can solve the following 2×2 interference free system of equations and can attain 2 DoF by extracting

two desired symbols of $\mathbf{x}_1^{[1]}$

$$\tilde{\mathbf{y}}^{[1]} = \mathbf{H}^{[1]}\mathbf{x}_1^{[1]} + \tilde{\mathbf{z}}^{[1]}. \tag{3.5}$$

The interference subtraction in time slot one of (2.5) would result in an unwanted increment in the noise power of user-1.

Throughout a similar procedure user-2 can also achieve 2 DoF. The desired signals of $\mathbf{x}_1^{[2]}$ can be extracted during symbol extensions $\{1,3\}$ and the interference signal $\mathbf{x}_1^{[1]}$ can be measured during symbol extension 2 and later can be subtracted from the first received signal.

For the 2-user 2×1 BC example, each user can achieve 2 DoF within three time slots or over a supersymbol of length 3. Therefore, the normalized sum-DoF per symbol extension would be 4/3. This value coincides with the theoretical upper bound of the sum-DoF under no CSIT scenario. Table 3.2 summarizes the transmitted symbols and preset modes for users when $K = 2$ and $M = 2$:

Table 3.2: Transmitted signals and preset mode patterns for 2-user, 2×1 MISO BC.

Time slot	Tx for User 1	Tx for User 2	User`s 1 Mode	User`s 2 Mode
1	$\mathbf{x}_1^{[1]}$	$\mathbf{x}_1^{[2]}$	1	1
2	$\mathbf{x}_1^{[1]}$	0	2	1
3	0	$\mathbf{x}_1^{[2]}$	1	2

Block 1 — (time slots 1–2)

Block 2 — (time slots 2–3)

For the more general K-user 2×1 MISO BC scenario, the supersymbol structure is as depicted in Table 3.3. Similar to the 2-user, 2×1 MISO BC here the transmitter will transmit only one symbol vector $\mathbf{x}_q^{[k]} = \left[u_{q,1}^{[k]} \; u_{q,2}^{[k]} \right]^T$, to each of the K users and each

user can attain 2 DoF (one from each transmit antenna). With K users, the supersymbol would have $K + 1$ symbol extensions (time slots or channel uses) and is comprised of two main blocks which are known as Block-1 or interference block and Block-2 or interference-free block. Block-1 occupies one channel use and Block-2 needs K symbol extensions.

Within the first symbol extension or Block-1, the desired signal vectors of all K users, $\left\{ \mathbf{x}_1^{[1]}, \mathbf{x}_1^{[2]}, \ldots, \mathbf{x}_1^{[K]} \right\}$, are transmitted while each user selects its corresponding first channel mode as $\mathbf{h}^{[k]}(1) \ \forall k \in [1:K]$. Hence the transmit signal during the first symbol extension can be written as:

$$\mathbf{x}(1) = \sum_{k=1}^{K} \mathbf{x}_1^{[k]} \tag{3.6}$$

Table 3.3: Supersymbol and preset mode patterns for K-user 2×1 MISO BC s-BIA.

	Time slot	Tx for user 1	Tx for user 2	...	Tx for user K	User 1	User 2	...	User K
Block 1	1	$\mathbf{x}_1^{[1]}$	$\mathbf{x}_1^{[2]}$	...	$\mathbf{x}_1^{[K]}$	$\mathbf{h}^{[1]}(1)$	$\mathbf{h}^{[2]}(1)$	...	$\mathbf{h}^{[K]}(1)$
	2	$\mathbf{x}_1^{[1]}$	0	...	0	$\mathbf{h}^{[1]}(2)$	$\mathbf{h}^{[2]}(1)$	...	$\mathbf{h}^{[K]}(1)$
	3	0	$\mathbf{x}_1^{[2]}$	...	0	$\mathbf{h}^{[1]}(1)$	$\mathbf{h}^{[2]}(2)$	...	$\mathbf{h}^{[K]}(1)$
Block 2	⋮	⋮	⋮	⋱	⋮	⋮	⋮	⋱	⋮
	$K+1$	0	0	...	$\mathbf{x}_1^{[K]}$	$\mathbf{h}^{[1]}(1)$	$\mathbf{h}^{[2]}(1)$	...	$\mathbf{h}^{[K]}(2)$

To construct a full-rank matrix for each user, the second channel mode $\mathbf{h}^{[k]}(2)$, $\forall k \in [1:K]$ should be used over an extra symbol extension. Therefore, the kth user will switch to the second channel mode at $t = k + 1$ channel use.

As in the 2-user case, during the first symbol extension the kth user would suffer from $K - 1$ interference signals intended for other users, i.e. $\mathbf{x}_1^{[j]}, j \neq k$. The kth user can benefit from the additional symbol extension of other users by remaining in the same channel mode $\mathbf{h}^{[k]}(1)$ $(t \neq (k+1))$ and simply measuring interference signals of $K - 1$

other users and subtracting them from the received signal of user k in the first symbol extension. To achieve this, Block-2 which is over K symbol extensions can be used to transmit the intended symbols of all users in an independent manner:

$$\mathbf{x}(t) = \mathbf{x}_1^{[t-1]}, \quad 2 < t \leq K+1 \tag{3.7}$$

Finally, the received signal of kth user after zero forcing subtraction can be written as:

$$\tilde{\mathbf{y}}^{[k]} = \begin{bmatrix} y^{[k]}(1) - \sum_{\substack{t=2 \\ t \neq k+1}}^{K+1} y^{[k]}(t) \\ y^{[k]}(k+1) \end{bmatrix} = \underbrace{\begin{bmatrix} \mathbf{h}^{[k]}(1)^T \\ \mathbf{h}^{[k]}(2)^T \end{bmatrix}}_{\tilde{\mathbf{H}}^{[k]}} \mathbf{x}_1^{[k]} + \underbrace{\begin{bmatrix} z^{[k]}(1) - \sum_{\substack{t=2 \\ t \neq k+1}}^{K+1} z^{[k]}(t) \\ z^{[k]}(k+1) \end{bmatrix}}_{\tilde{\mathbf{z}}^{[k]}} \tag{3.8}$$

Equation (3.8) can also be represented using matrix notation as follows:

$$\tilde{\mathbf{y}}^{[k]} = \mathbf{H}^{[k]}\mathbf{x}_1^{[k]} + \tilde{\mathbf{z}}^{[k]} \tag{3.9}$$

where, $\tilde{\mathbf{z}}^{[k]} = \mathcal{CN}(0, \mathbf{R}_{\tilde{z}})$ and $\mathbf{R}_{\tilde{z}}$ represents the covariance matrix of the noise as $\mathbf{R}_{\tilde{z}} = \text{diag}(K-1, 1)$.

To recap, the beamforming vector of the kth user over a 2×1 MISO BC would have $Q_k = 1$ alignment block in which 2 DoF can be achieved by each user and the users switch between $M = 2$ preset modes. Since each user gets 2 DoF over $K+1$ symbol extensions the sum DoF per symbol extension would be equal to $\frac{\sum_{k=1}^{K} Q_k M_k}{K+1} = \frac{2K}{K+2-1}$. This value coincides with the optimal DoF value stated in [71] for the K-user 2×1 MISO BC.

3.2.3 K-user 3×1 MISO BC

When the number of transmit antennas is higher, the construction of the supersymbol becomes more challenging. The main idea is that, during each alignment block the

43

channel state of the desired user has to change among $M = 3$ modes in order to provide 3×3 full-rank matrix and the channel states of remaining $K - 1$ users need to remain constant. This can be done by constructing the supersymbol comprised of two concatenated blocks: Mainly Block-1 and Block-2. Block-1 is designed to ensure the alignment between transmitted symbols while Block-2 is for guaranteeing the independence between desired signals (avoids having overlaps between desired signals).

To clarify the change in the supersymbol structure when transmit antennas are more than 2, Table 3.4 has shown the supersymbol for a 2-user 3×1 MISO BC scenario and the reader should compare this with the supersymbol structure depicted in Table 3.2.

Table 3.4: Symbol vectors and preset channel modes for 2-user, 3×1 MISO BC.

Time slot	Tx for User 1		Tx for User 2		User 1	User 2
1	$\mathbf{x}_1^{[1]}$	0	$\mathbf{x}_1^{[2]}$	0	$\mathbf{h}^{[1]}(1)$	$\mathbf{h}^{[2]}(1)$
2	$\mathbf{x}_1^{[1]}$	0	0	$\mathbf{x}_2^{[2]}$	$\mathbf{h}^{[1]}(2)$	$\mathbf{h}^{[2]}(1)$
3	0	$\mathbf{x}_2^{[1]}$	$\mathbf{x}_1^{[2]}$	0	$\mathbf{h}^{[1]}(1)$	$\mathbf{h}^{[2]}(2)$
4	0	$\mathbf{x}_2^{[1]}$	0	$\mathbf{x}_2^{[2]}$	$\mathbf{h}^{[1]}(2)$	$\mathbf{h}^{[2]}(2)$
5	$\mathbf{x}_1^{[1]}$	0	0	0	$\mathbf{h}^{[1]}(3)$	$\mathbf{h}^{[2]}(1)$
6	0	$\mathbf{x}_2^{[1]}$	0	0	$\mathbf{h}^{[1]}(3)$	$\mathbf{h}^{[2]}(2)$
7	0	0	$\mathbf{x}_1^{[2]}$	0	$\mathbf{h}^{[1]}(1)$	$\mathbf{h}^{[2]}(3)$
8	0	0	0	$\mathbf{x}_2^{[2]}$	$\mathbf{h}^{[1]}(2)$	$\mathbf{h}^{[2]}(3)$

Block 1 spans time slots 1–4; Block 2 spans time slots 5–8. Columns correspond to $q_1^{[1]}$, $q_2^{[1]}$, $q_1^{[2]}$, $q_2^{[2]}$.

Under the 3×1 MISO BC each of the two users would have 2 alignment blocks, $q \in \{1, 2\}$, and within each alignment block 3 DoF can be achieved by switching the reconfigurable antenna between $M = 3$ preset modes. The first alignment block for user-1 ($q_1^{[1]}$) utilizes the symbol extensions $\{1, 2, 5\}$ while the second one ($q_2^{[1]}$) is over symbol extensions $\{3, 4, 6\}$. In each alignment block, the first two symbols extensions are provided by Block-1 and the final symbol extension by Block-2. Note from Table 3.4 that, while user-1 alters its channel mode three times within the first alignment

44

block the channel state of user-2 would remain constant at $\mathbf{h}^{[2]}(1)$ and during the second alignment block of user-1 the channel state of user-2 remains constant at $\mathbf{h}^{[2]}(2)$. In addition, during each alignment block the symbol vector $\mathbf{x}_q^{[k]}$ $\forall k \in \{1,2\}$, $q \in \{1,2\}$ is transmitted $M = 3$ times. To guarantee the alignment between transmitted signal vectors in Block-1, user-1 must switch its corresponding channel between $M - 1$ preset modes as $\{\mathbf{h}^{[1]}(1)\mathbf{h}^{[1]}(2)\}$ in each alignment block while the channel of user-2 remains constant. This pattern is then repeated twice once for each alignment block. On the other hand user-2 must employ the channel pattern: $\{\mathbf{h}^{[2]}(1), \mathbf{h}^{[2]}(1), \mathbf{h}^{[2]}(2), \mathbf{h}^{[2]}(2)\}$. Finally, to ensure independence of the symbols in Block-2, the last symbol of each alignment block $\mathbf{x}_q^{[k]}$ $\forall k \in \{1,2\}$, $q \in \{1,2\}$ is transmitted in an orthogonal manner, once per symbol extension. Therefore, the transmitted signal for this toy example can be written as:

$$
\mathbf{X} = \begin{bmatrix} \mathbf{I} & \mathbf{0} \\ \mathbf{I} & \mathbf{0} \\ \mathbf{0} & \mathbf{I} \\ \mathbf{0} & \mathbf{I} \\ \mathbf{I} & \mathbf{0} \\ \mathbf{0} & \mathbf{I} \\ \mathbf{0} & \mathbf{0} \\ \mathbf{0} & \mathbf{0} \end{bmatrix} \begin{bmatrix} \mathbf{x}_1^{[1]} \\ \mathbf{x}_2^{[1]} \end{bmatrix} + \begin{bmatrix} \mathbf{I} & \mathbf{0} \\ \mathbf{0} & \mathbf{I} \\ \mathbf{I} & \mathbf{0} \\ \mathbf{0} & \mathbf{I} \\ \mathbf{0} & \mathbf{0} \\ \mathbf{0} & \mathbf{0} \\ \mathbf{I} & \mathbf{0} \\ \mathbf{0} & \mathbf{I} \end{bmatrix} \begin{bmatrix} \mathbf{x}_1^{[2]} \\ \mathbf{x}_2^{[2]} \end{bmatrix} \tag{3.10}
$$

where, $\mathbf{x}_q^{[k]} = \begin{bmatrix} u_{q,1}^{[k]} u_{q,2}^{[k]} u_{q,3}^{[k]} \end{bmatrix}^T$ represents the transmitted signal vector during the qth alignment block, $q \in \{1,2\}$, of the kth user, $k \in \{1,2\}$, and can provide 3 DoF. Moreover, $\mathbf{I}$ and $\mathbf{0}$ respectively denote the 3×3 identity and zero matrices.

Hence, the received signal within the first alignment block of user-1 can be written as:

$$
\begin{bmatrix} y^{[1]}(1) \\ y^{[1]}(2) \\ y^{[1]}(5) \end{bmatrix} = \underbrace{\begin{bmatrix} \mathbf{h}^{[1]}(1)^T \\ \mathbf{h}^{[1]}(2)^T \\ \mathbf{h}^{[1]}(3)^T \end{bmatrix}}_{\text{rank}=3} \mathbf{x}_1^{[1]} + \underbrace{\begin{bmatrix} \mathbf{h}^{[1]}(1)^T \mathbf{x}_1^{[2]} \\ \mathbf{h}^{[1]}(2)^T \mathbf{x}_2^{[2]} \\ 0 \end{bmatrix}}_{\text{rank}=2} \begin{bmatrix} z^{[1]}(1) \\ z^{[1]}(2) \\ z^{[1]}(5) \end{bmatrix} \tag{3.11}
$$

Note that the desire symbol $\mathbf{x}_1^{[1]}$ is transmitted over a rank-3 (full rank) matrix and the interference signals $\mathbf{x}_1^{[2]}$ and $\mathbf{x}_2^{[2]}$ occupy only a 2-dimensional space by aligning over a rank-2 matrix.

For user-1 to cancel the interference received during symbol extensions $\{1\}$ and $\{2\}$, the symbol extensions $\{7\}$ and $\{8\}$ are used to perform zero forcing subtraction as depicted below:

$$
\tilde{\mathbf{y}}^{[1]} = \begin{bmatrix} y^{[1]}(1) - y^{[1]}(7) \\ y^{[1]}(2) - y^{[1]}(8) \\ y^{[1]}(5) \end{bmatrix} = \underbrace{\begin{bmatrix} \mathbf{h}^{[1]}(1)^T \\ \mathbf{h}^{[1]}(2)^T \\ \mathbf{h}^{[1]}(3)^T \end{bmatrix}}_{\tilde{\mathbf{H}}^{[1]}} \mathbf{x}_1^{[1]} + \underbrace{\begin{bmatrix} z^{[1]}(1) - z^{[1]}(7) \\ z^{[1]}(2) - z^{[1]}(8) \\ z^{[1]}(5) \end{bmatrix}}_{\tilde{\mathbf{z}}^{[1]}} \tag{3.12}
$$

where, $\tilde{\mathbf{z}}^{[1]} = \mathcal{CN}(0, \mathbf{R}_{\tilde{z}})$ with $\mathbf{R}_{\tilde{z}} = \text{diag}(3,3,1)$ and $\tilde{\mathbf{H}}^{[1]} = \left[\mathbf{h}^{[1]}(1)^T \mathbf{h}^{[1]}(2)^T \mathbf{h}^{[1]}(3)^T \right]^T$ represents the effective channel matrix of user-1.

Throughout the same procedure user-1 can achieve another 3 DoF over its second alignment block which is over symbol extensions $\{3,4,6\}$. User-2 which has two alignment blocks $(Q_2 = 2)$ over symbol extensions $\{1,3,7\}$ and $\{2,4,8\}$ will also get 3 DoF for each of its alignment blocks. Hence, $Q_k M_k = 2 \cdot 3, k \in \{1,2\}$ DoF is achieved by each user over 8 symbol extensions which results in $\dfrac{\Sigma_{k=1}^2 Q_k M_k}{8} = 3/2$ sum-DoF per symbol extension.

As the number of users increases the transmission strategy becomes more challenging. However as seen by the 2-user 3×1 MISO BC toy example given in Table 3.4, the idea to guarantee the alignment between users is to periodically repeat the $M - 1 = 2$ channel modes of the kth user ($\mathbf{h}^{[k]}(1)$ and $\mathbf{h}^{[k]}(2)$) during the alignment Block-1 while other $K - 1$ users maintain their channel modes. Pattern $\{\mathbf{h}^{[1]}(1), \mathbf{h}^{[1]}(2)\}$ replicated twice for user-1 and pattern $\{\mathbf{h}^{[2]}(1), \mathbf{h}^{[2]}(1), \mathbf{h}^{[2]}(2), \mathbf{h}^{[2]}(1)\}$ used once for user-2 are known as building blocks for each user and Figure 3.2 shows the building block structure of the K-user for 3×1 MISO BC.
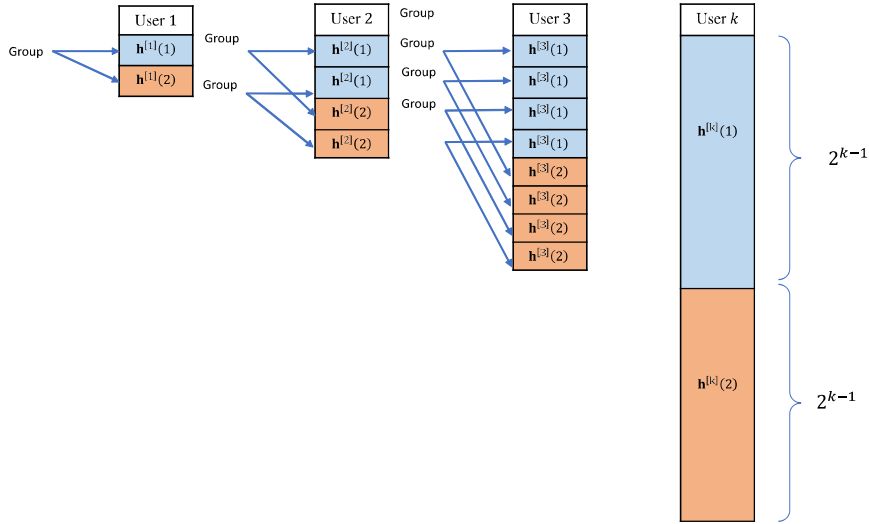
Figure 3.2: Building block structure for K-user, 3×1 MISO BC.

As can be seen from Figure 3.2 during Block-1 the building block of the kth user contains 2^k symbol extensions when it's antenna is switching between $M - 1 = 2$ modes and the channel modes $\mathbf{h}^{[k]}(1)$ and $\mathbf{h}^{[k]}(2)$ are each repeated $2^{(k-1)}$ times. Meanwhile the remaining $K - 1$ users retain their current channel modes. Since, the Kth user has the largest building block, the length of Block-1 is 2^K symbol extensions. Within this duration, each user can replicate its building block, $2^{(K-k)}$ times where

$p \in \{1, \ldots, 2^{(K-k)}\}$ represents the pth building block of the kth user.

Since each building block is comprised of 2 channel modes the beamforming matrix can be formed by grouping each two channel modes within them. By this scheme the alignment between transmitted signals will be guaranteed due to the structure of Block-1. As shown by Figure 3.2 for the kth user the Block-1 provides $2^{(K-k)}$ building blocks, where each contains 2^K symbol extensions. Hence $2^{(k-1)}$ groups over a single building block and total of $2^{(K-1)}$ groups over the length of Block-1 can be formed for this user.

To complete the beamforming design, Block-2 is constructed by adding the third channel mode, $\mathbf{h}^{|k|}(3)$ to the end of each group of the kth user. To do so, Block-2 allocates $2^{(K-1)}$ symbol extensions per user and total of $K \times 2^{(K-1)}$ symbol extensions for the K users. Since within the duration of Block-2 each symbol $\mathbf{x}_q^{[k]}$, $q \in \{1, \ldots, 2^{(K-1)}\}$, occupies only one symbol extension, the orthogonality between symbols of each user would be guaranteed . This transmission strategy is beneficial in two ways; firstly the neither the desired signals nor the interference signals overlap among themselves and secondly the received interference signals during Block-1 can be measured by the desired user in Block-2 to perform the zero-forcing subtraction necessary for extracting the desired symbols.

For the K-user, 3×1 MISO BC scenario each user can achieve 3 DoF per alignment block in which the channel is switching between $M = 3$ preset modes. Since each user has $Q_k = 2^{(K-1)}$ alignment blocks and K active user are served by the transmitter $M_k Q_k = 3 \times 2^{(K-1)}$ DoF would be attained by each user and the sum-DoF would be equal to $3 \times K \times 2^{(K-1)}$. Since Block-1 and Block-2 each has lengths 2^K and $K \times 2^{(K-1)}$

respectively, the normalized sum-DoF for the standard BIA with K-user, 3×1 MISO BC can be represented as:

$$\text{DoF} = \frac{\sum_{k=1}^{K} Q_k M_k}{2^K + K \times 2^{(K-1)}} = \frac{3 \times K \times 2^{(K-1)}}{2^K + K \times 2^{(K-1)}} = \frac{3K}{K+2} \qquad (3.13)$$

3.3 Blind Interference Alignment for K-user $M \times 1$ MISO BC and IC

Up to this point, foundation of the standard BIA scheme for some special cases of MISO BC has been explained. This section will describe the general framework for both the BC [24] and the IC [77] assuming M transmit antennas and K active users.

The key condition for achieving blind interference alignment in a K-user, $(M \times 1)$ MISO BC or K-user, $(M \times 1)$ MISO IC is that, over the duration of M_k symbols, $\forall k \in \{1, 2, \ldots, K\}$, the channel of the desired user changes in each symbol duration while the channels of undesired users remain constant. This way, the streams for the desired user will be distinguishable and all streams will align into a single dimension at the unintended users.

Hence to satisfy this key condition, the kth receiver should use a reconfigurable antenna capable of switching between M_k predetermined sequence of antenna switching modes (also known as preset mode patterns) to artificially generate a desired channel pattern over M_k series of channel uses referred to as an alignment block. Since each user may have more than one alignment block, we use the notation $q_i^{[k]}$ to represent the ith alignment block for the kth user where $i \in \{1, \ldots, Q_k\}$ and Q_k represents the total number of alignment blocks of each user and equals:

$$Q_k = \prod_{\substack{i=1 \\ i \neq k}}^{K} (M_i - 1), \quad \forall k \in \{1, 2, \ldots, K\}. \qquad (3.14)$$

49

To achieve high DoF, users will try to share as many temporal channel uses with each other while each receiver is still able to cancel the interference seen from the other users. This can be done by considering the general case as two independent problems known as, alignment problem and linear independency problem. To satisfy this requirement, a transmit precoder matrix needs to be constructed by concatenation of the two main blocks;the interference-free block and the interference block. The interference block requires T_K time slots and the interference-free block $\sum_{k=1}^{K} Q_k$ time slots respectively. Within each time slot of the interference block, signal vectors of all K users are transmitted simultaneously. On the other hand the interference-free block is designed to ensure the orthogonality between desired signal vectors, hence during each time slot, signal vector of only one user is transmitted. The precoder matrix constructed by the s-BIA has symbol length of

$$\text{SL}_{\text{s-BIA}} = T_K + \sum_{k=1}^{K} Q_k = \prod_{i=1}^{K} (M_k - 1) + \sum_{k=1}^{K} Q_k \text{ time slots.} \tag{3.15}$$

Interestingly, as stated in [40], for fully-connected IC networks the sum-DoF would not scale with number of transmitters. In a scenario where M_f represents the transmit antennas for the fth BS and $\mathcal{K}_f$ the set of users served by the fth transmitter, the sum-DoF for the network will only depend on the preset modes of each receiver given (3.16) is satisfied.

$$M_f \geq \max_{k \in \mathcal{K}_f} M_k \tag{3.16}$$

Below we consider a toy-example as depicted by Figure 3.3 where 2-user, $M \times 1$ MISO IC has been assumed. User-1 and user-2 are assumed to switch between $M_1 = 3$ and $M_2 = 2$ modes respectively and transmitter(s) have $M_f \geq M_k$ antennas.
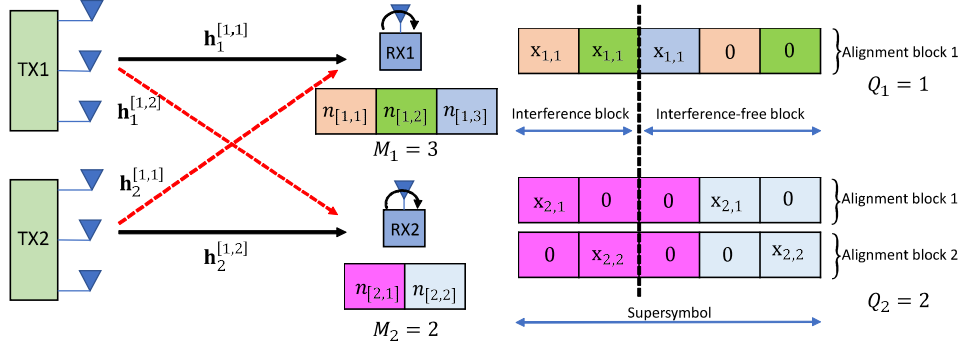
Figure 3.3: Two-user $M \times 1$, MISO-IC

In Figure 3.3, $\mathbf{h}_j^{[k,f]}$ represents the channel gain between the jth BS and receiver k served by transmitter f where $k, f \in \{1, 2\}$. Using (3.15), the constructed precoder matrix for this toy-example would have a supersymbol length of $\text{SL}_{\text{s-BIA}} = 5$ time slots and the transmitted signal $\mathbf{X}$ for the two users could be represented as:

$$
\mathbf{X} = \underbrace{\begin{bmatrix} \mathbf{I}_3 \\ \mathbf{I}_3 \\ \mathbf{I}_3 \\ \mathbf{0}_3 \\ \mathbf{0}_3 \end{bmatrix}}_{\text{Precoder for user-1}} \underbrace{\begin{bmatrix} \mathbf{x}_1^{[1]} \end{bmatrix}}_{\mathbf{x}_1} + \underbrace{\begin{bmatrix} \mathbf{I}_{3\times 2} & \mathbf{0}_{3\times 2} \\ \mathbf{0}_{3\times 2} & \mathbf{I}_{3\times 2} \\ \mathbf{0}_{3\times 2} & \mathbf{0}_{3\times 2} \\ \mathbf{I}_{3\times 2} & \mathbf{0}_{3\times 2} \\ \mathbf{0}_{3\times 2} & \mathbf{I}_{3\times 2} \end{bmatrix}}_{\text{Precoder for user-2}} \underbrace{\begin{bmatrix} \mathbf{x}_1^{[2]} \\ \mathbf{x}_2^{[2]} \end{bmatrix}}_{\mathbf{x}_2}
$$

$$
= \begin{bmatrix} \mathbf{I}_3 \\ \mathbf{I}_3 \\ \mathbf{I}_3 \\ \mathbf{0}_3 \\ \mathbf{0}_3 \end{bmatrix} \begin{bmatrix} u_1^{[1]} \\ u_2^{[1]} \\ u_3^{[1]} \end{bmatrix} + \begin{bmatrix} \mathbf{I}_{3\times 2} & \mathbf{0}_{3\times 2} \\ \mathbf{0}_{3\times 2} & \mathbf{I}_{3\times 2} \\ \mathbf{0}_{3\times 2} & \mathbf{0}_{3\times 2} \\ \mathbf{I}_{3\times 2} & \mathbf{0}_{3\times 2} \\ \mathbf{0}_{3\times 2} & \mathbf{I}_{3\times 2} \end{bmatrix} \begin{bmatrix} u_1^{[2]} \\ u_2^{[2]} \\ u_3^{[2]} \\ u_4^{[2]} \end{bmatrix}.
$$

(3.17)

where, $\mathbf{x}_1 \in \mathcal{A}_1^{[M_1(M_2-1)]\times 1}$ represents the transmitted signal for user-1 which can be decoupled to $\mathbf{x}_1 = [\mathbf{x}_1^{[1]^T}, \ldots, \mathbf{x}_{(M_2-1)}^{[1]^T}]^T$ with $\mathbf{x}_q^{[1]} \in \mathcal{A}_1^{M_1 \times 1}$ for $q \in \{1, \ldots, Q_1\}$. On the other hand, $\mathbf{x}_2 \in \mathcal{A}_2^{[M_2(M_1-1)]\times 1}$ denotes the transmitted signal for user-2 and can be decoupled to $\mathbf{x}_2 = [\mathbf{x}_1^{[2]^T}, \ldots, \mathbf{x}_{(M_1-1)}^{[2]^T}]^T$ with $\mathbf{x}_q^{[2]} \in \mathcal{A}_1^{M_2 \times 1}$ for $q \in \{1, \ldots, Q_2\}$. It is clear from (3.17) that the precoder matrices of user-1 and user-2 each has $Q_1 = 1$ and $Q_2 = 2$ alignment blocks where each alignment block is of 5 time slots and can be

written as a block column vector made up of identity (**I**) and zero (**0**) matrices. Here each alignment block is responsible for transmitting one signal $\mathbf{x}_q^{[k]}$ with $k \in \{1, 2\}$ and $q \in \{1, \ldots, Q_k\}$ within the duration of the supersymbol length.

For the given toy-example, the transmitted signals and preset mode pattern of each receiver are summarized in Table 3.5.

Table 3.5: Transmitted signals and preset mode patterns for 2-user s-BIA [$M_1 = 3$, $M_2 = 2$].

Time slot	T_1's Signal	T_2's Signal	R_1's Mode	R_2's Mode	
1	$\mathbf{x}_1^{[1]}$	$\mathbf{x}_1^{[2]}$	1	1	Interference block
2	$\mathbf{x}_1^{[1]}$	$\mathbf{x}_2^{[2]}$	2	1	
3	$\mathbf{x}_1^{[1]}$	$\mathbf{0}$	3	1	Interference-free block
4	$\mathbf{0}$	$\mathbf{x}_1^{[2]}$	1	2	
5	$\mathbf{0}$	$\mathbf{x}_2^{[2]}$	2	2	

Note that the desired signal of user-1, $\mathbf{x}_1^{[1]} \in \mathcal{A}_1^{M_1 \times 1}$, is transmitted M_1 times within the duration of its alignment block (3 time slots) where the first $(M_1 - 1)$ desired signals are transmitted during the length of interference block (first $(M_1 - 1)(M_2 - 1)$ time slots) and the M_1^{th} desired signal is transmitted in the first time slot of the interference-free block (3rd time slot). Meanwhile as shown in Table 3.5, user-1 changes its channel pattern by switching between M_1 modes during the first $M_1 = 3$ time slots ($\{n^{[1]}(1) = 1, n^{[1]}(2) = 2, n^{[1]}(3) = 3\}$) while user-2 maintains its initial channel mode ($\{n^{[2]}(1) = 1, n^{[2]}(2) = 1, n^{[2]}(3) = 1\}$). On the other hand, in the first M_1 time slots, user-2 only uses the first $M_1 - 1$ time slots to transmit its own signals. In the M_1^{th} slot, user-2 keeps silent and receives unpolluted interference-free $\mathbf{x}_1^{[1]}$ signal which can be used to subtract the interference in the previous $M_1 - 1$ time slots. After $M_1(M_2 - 1)$ time slots, each signal $\mathbf{x}_q^{[2]}, q \in \{1, 2\}$ is transmitted once more. In summary, the preset mode pattern of the toy example introduced in Figure 3.3 can be denoted as $\langle M_1, M_2 \rangle = \langle 3, 2 \rangle$, where

channel switching pattern of each user during 5-symbol extensions is as follows:

$$n^{[1]} = (1,2,3,1,2) \, , \, n^{[2]} = (1,1,1,2,2)$$

For the example discussed, the received signal for user-1 during the first alignment block can be written as:

$$\mathbf{y}_1^{[1]} = \underbrace{\begin{bmatrix} \mathbf{h}_1^{[1,1]}(1) \\ \mathbf{h}_1^{[1,1]}(2) \\ \mathbf{h}_1^{[1,1]}(3) \\ \mathbf{0}_{1 \times 3} \\ \mathbf{0}_{1 \times 3} \end{bmatrix}}_{\text{rank} = 3} \begin{bmatrix} \mathbf{x}_1^{[1]} \end{bmatrix} + \underbrace{\begin{bmatrix} \mathbf{h}_2^{[1,1]}(1) & \mathbf{0}_{1 \times 2} \\ \mathbf{0}_{1 \times 2} & \mathbf{h}_2^{[1,1]}(2) \\ \mathbf{0}_{1 \times 2} & \mathbf{0}_{1 \times 2} \\ \mathbf{h}_2^{[1,1]}(1) & \mathbf{0}_{1 \times 2} \\ \mathbf{0}_{1 \times 2} & \mathbf{h}_2^{[1,1]}(2) \end{bmatrix}}_{\text{rank} = 2} \begin{bmatrix} \mathbf{x}_1^{[2]} \\ \mathbf{x}_2^{[2]} \end{bmatrix} + \begin{bmatrix} z_1(1) \\ z_1(2) \\ z_1(3) \\ z_1(4) \\ z_1(5) \end{bmatrix} \tag{3.18}$$

Equation (3.18) points out that the desired signal of user-1 occupies 3 dimensions while the interference signals from user-2 are aligned into a 2D space (one per alignment block). Finally, user-1 will subtract unpolluted signals received during the interference-free block from its polluted desired signals that are availeble during the interference block. This interference subtraction procedure is known as Zero Forcing (ZF) and for our example is as follows:

$$\mathbf{y}_1^{[1]} = \begin{bmatrix} y^{[1]}(1) - y^{[1]}(4) \\ y^{[1]}(2) - y^{[1]}(5) \\ y^{[1]}(3) \end{bmatrix} = \begin{bmatrix} \mathbf{h}_1^{[1,1]}(1) \\ \mathbf{h}_1^{[1,1]}(2) \\ \mathbf{h}_1^{[1,1]}(3) \end{bmatrix} \mathbf{x}_1^{[1]} + \begin{bmatrix} z^{[1]}(1) - z^{[1]}(4) \\ z^{[1]}(2) - z^{[1]}(5) \\ z^{[1]}(3) \end{bmatrix} \triangleq \mathbf{H}_1 \mathbf{x}_1^{[1]} + \mathbf{z}_1^{[1]}$$

$$\tag{3.19}$$

Hence by following this procedure, user-1 can solve the $M_1 \times M_1$ system of equations in (3.19) and can extract M_1 desired signals over its alignment block (Q_1). In a similar manner, user-2 can extract M_2 interference-free signals per alignment block ($Q_2 = 2$). Overall, a total of ($Q_1 M_1 + Q_2 M_2$) interference free signals can be achieved over the supersymbol length of 5 time slots which leads to a sum-DoF of

$(1 \cdot 3 + 2 \cdot 2)/(5) = 7/5$. Moreover, due to the ZF subtraction procedure introduced in (3.19) the noise power in the first $M_1 - 1$ received signals has been doubled which results in decreasing the sum-rate of s-BIA scheme. For the 2-user, $M \times 1$ MISO-IC example the noise covariance matrix of user-1 is an identity matrix with diagonal elements $N_0 \cdot \text{diag}(2\mathbf{I}_{M_1-1}, 1)$ and the normalization factor of $\sqrt{2}$.

The general framework of the s-BIA scheme for constructing both the preset mode patterns and precoder matrices, independent of the number of transmitters in the network is summarized in Table 3.6.

Table 3.6: K-user s-BIA with preset modes $\{M_1, \dots, M_k\}$

Slot Number	Symbols $1 \cdots (k-1)$	Symbol k	Rx k
1 $\vdots$ T_{k-1}	Interference block for $(k-1)$ users	$\mathbf{x}_1^{[k]}$ $\vdots$ $\mathbf{x}_{T_{k-1}}^{[k]}$	1 $\vdots$ 1
$\vdots$	$\vdots$	$\vdots$	$\vdots$
$T_{k-1}(M_k-2)+1$	Interference block for $(k-1)$ users	$\mathbf{x}_1^{[k]}$ $\vdots$ $\mathbf{x}_{T_{k-1}}^{[k]}$	M_k-1 $\vdots$ M_k-1
T_k+1 $\vdots$ T_k+Q_1	first $(k-1)$ users interference-free block	0 $\vdots$ 0	1 $\vdots$ M_k-1
$\vdots$ $T_k+Q_1+\dots+Q_{k-2}+1$ $\vdots$ $T_k+Q_1+\dots+Q_{k-1}$		$\vdots$ 0 $\vdots$ 0	$\vdots$ 1 $\vdots$ M_k-1
$T_k+Q_1+\dots+Q_{k-1}+1$ $\vdots$ $T_k+Q_1+\dots+Q_k$	0 $\vdots$ 0	$\mathbf{x}_1^{[k]}$ $\vdots$ $\mathbf{x}_{T_{k-1}}^{[k]}$	M_k $\vdots$ M_k

Consider k^{th} user, $k \in \{1, \dots, K\}$, with M_k preset modes with $M_k \leq M$ (M denotes the maximum number of transmit antennas) where the set of preset modes M_k for receivers ($k \in \{1, \cdots, K\}$) are denoted as $\mathcal{N} = \{M_1, \dots, M_K\}$. The desired symbols of user-k are denoted as $\mathbf{x}_{[k]} = [\mathbf{x}_1^{[k]T} \dots \mathbf{x}_{Q_k}^{[k]T}]^T$. Each $\mathbf{x}_q^{[k]}$ where $q \in \{1, 2, \dots, Q_k\}$ has a signal

54

constellation of size $M_k \times 1$.

Similar to the 2-user example of Figure 3.3, the precoder matrix for the K-user case can also be constructed by again concatenating the interference and interference-free blocks. Throughout the interference block duration, the kth receiver operates at mode-1 for T_{k-1} time slots and switches to mode-2 for the next T_{k-1} time slots, and would continue to switch its mode up to mode-$(M_k - 1)$ (please refer to Table 3.6). During the interference free block, user-k would be in preset mode-M_k to receive its desired signal vectors and in the remaining time slots it would operate in the same preset mode it was using in the interference block while receiving the undesired interfering signal(s).

This transmission strategy is beneficial since neither the desired nor the interference signals overlap with each other. Also, the interference signals received during the interference block can be measured by the desired user in the interference-free block to eliminate the interference via ZF. In general, through the s-BIA scheme the kth user has to perform $(K - 1)$ subtraction in each time slot of its interference-free block, $M_k(K - 1)$ subtractions per alignment block and the total of $M_k(K - 1)Q_k$ subtractions to cover all alignment blocks. After canceling the aligned interference, the qth received desired signal of kth receiver from transmitter f can be expressed as:

$$\mathbf{y}_q^{[k]} = \begin{bmatrix} \mathbf{h}_f^{[k,f]}(1) \\ \vdots \\ \mathbf{h}_f^{[k,f]}(M_k-1) \\ \mathbf{h}_f^{[k,f]}(M_k) \end{bmatrix} \mathbf{x}_q^{[k]} + \begin{bmatrix} z_{k,u}(1) - z_{k,u}(T_k+Q_1+1) - & \cdots & -z_{k,u}(T_k+Q_1+\ldots+Q_{k-1}+1) \\ \vdots & \vdots & \vdots \\ z_{k,u}(M_k-1) - z_{k,u}(T_k+Q_1+M_k-1) - & \cdots & -z_{k,u}(T_k+Q_1+\ldots+Q_{k-1}+M_k-1) \\ & z_{k,u}(M_k) & \end{bmatrix} \triangleq \mathbf{H}_k \mathbf{x}_q^{[k]} + \mathbf{z}_q^{[k]}$$

$$(3.20)$$

where the $\mathbf{z}_q^{[k]} \in \mathbb{R}^{M_k \times 1}$ is the received noise vector and due to the number of subtractions within each time slot of the interference-block the received signal would

suffer from a noise increase. The covariance matrix for the noise is as follows:

$$N_0 \cdot \begin{bmatrix} K\mathbf{I}_{M_k-1} & \mathbf{0} \\ \\ \mathbf{0} & 1 \end{bmatrix} \tag{3.21}$$

where the normalization factor equals $\sqrt{K}$. Moreover, $\mathbf{H}_k \in \mathbb{R}^{M_k \times M_k}$ represents the effective channel matrix of user-k and since it has got full rank, the M_k information symbols belonging to $\mathbf{x}_q^{[k]}$ can linearly be decoded. Finally, with Q_k alignment blocks for user-k and M_k desired symbols per alignment block, k^{th} user of s-BIA would achieve M_kQ_k DoF over SL time slots. Therefore, the sum-DoF for the K-user scenario can be calculated as:

$$\text{sum-DoF}_{\text{s-BIA}} = \frac{\sum_{k=1}^{K} M_kQ_k}{T_K + \sum_{k=1}^{K} Q_k} = \frac{\sum_{k=1}^{K} \frac{M_k}{M_k-1}}{1 + \sum_{k=1}^{K} \frac{1}{M_k-1}}. \tag{3.22}$$

Note that, in K-user MISO BC, because $M_k = M, \forall k \in \{1, 2, ..., K\}$ the equation (3.22) is going to match with the sum-DoF formula given in [24] as:

$$D_{[K,M]} = \frac{KM(M-1)^{(K-1)}}{(M-1)^K + K(M-1)^{(K-1)}} = \frac{KM}{K+M-1}. \tag{3.23}$$

In short, the preset mode pattern for the s-BIA can be denoted as:

$$\langle M_1, M_2, \dots, M_K \rangle$$

3.4 Sumrate for MISO BC

In previous sections the achievable DoF of the standard BIA in MISO BC and IC has been described, in what follows the closed form expressions for the achievable sumrates of MISO BC at finite SNR regime will be explained. As stated earlier, since each alignment block is comprised of M symbol extensions the channel state changes among M preset modes. The first $M - 1$ symbol extensions of each alignment block

56

are known as Block-1 and are subject to interference from remaining $K - 1$ users. On the other hand, the last symbol extension of each alignment block corresponding to the Mth channel mode is provided by Block-2, where the transmission of signals are carried out in an orthogonal manner. Recall that, the $K - 1$ interference terms received in each symbol extension of Block-1 can be measured in Block-2 and subsequently removed through the zero forcing subtraction procedure. However this subtraction results in increased noise power in the first $M - 1$ symbol extensions provided by Block-1. The received signal of the kth user after interference subtraction during q^{th} alignment block would be:

$$\tilde{\mathbf{y}}^{[k]} = \begin{bmatrix} \tilde{y}^{[k]}[1] \\ \vdots \\ \tilde{y}^{[k]}[M-1] \\ \tilde{y}^{[k]}[M] \end{bmatrix} = \begin{bmatrix} \mathbf{h}^{[k]}(1)^T \\ \vdots \\ \mathbf{h}^{[k]}(M-1)^T \\ \mathbf{h}^{[k]}(M)^T \end{bmatrix} \mathbf{x}_q^{[k]} + \begin{bmatrix} z^{[k]}[1] - \sum_{\substack{j=1 \\ j \neq k}}^{K} z^{[k]}[j] \\ \vdots \\ z^{[k]}[M-1] - \sum_{\substack{j=1 \\ j \neq k}}^{K} z^{[k]}[j] \\ z^{[k]}[M] \end{bmatrix} \tag{3.24}$$

Note that in the above equation, the temporal index represents the location of the symbol extension in the alignment block. Given (2.24), each user can solve $M \times M$ system of equations and can achieve M degrees of freedom:

$$\tilde{\mathbf{y}}^{[k]} = \mathbf{H}^{[k]} \mathbf{x}_q^{[k]} + \tilde{\mathbf{z}}^{[k]}, \tag{3.25}$$

$\mathbf{H}^{[k]}$ represents the channel matrix of user-k and equals:

$$\mathbf{H}^{[k]} = \left[\mathbf{h}^{[k]}(1)^T \, \mathbf{h}^{[k]}(2)^T \ldots \mathbf{h}^{[k]}(M)^T \right]^T \in \mathbb{C}^{M \times M}, \tag{3.26}$$

$\mathbf{x}_q^{[k]} \in \mathbb{C}^{M \times 1}$ denotes the desired symbol and $\tilde{\mathbf{z}}^{[k]} \sim \mathcal{CN}(0, \mathbf{R}_{\tilde{z}})$ represents the noise vector after zero forcing subtraction with covariance matrix $\mathbf{R}_{\tilde{z}}$ as follow:

$$R_{\tilde{z}} = \begin{bmatrix} K\mathbf{I}_{M-1} & \mathbf{0} \\ \\ \mathbf{0} & 1 \end{bmatrix}. \tag{3.27}$$

In general, each user has $(M-1)^{K-1}$ alignment blocks within the length of the supersymbol, thus the ratio of alignment blocks of each user per supersymbol length would equal:

$$B_r = \frac{(M-1)^{K-1}}{SL_{s-BIA}} = \frac{(M-1)^{K-1}}{(M-1)^K + K(M-1)^{(K-1)}} = \frac{1}{M+K-1}. \tag{3.28}$$

3.4.1 Utilizing Power Allocation Strategies to Optimize Sumrates

The power allocation strategy should be designed by considering the difference between the number of transmitted symbols in each time slot of Block-1 and Block-2. If π represents the ratio of power allocated to each symbol of Block-1 over each symbol of Block-2, then this ratio can be used to optimize the power allocation strategy.

In general the average power allocated to each symbol based on the power ratio π is as follows:

$$P_{sym} = \frac{SL_{s-BIA}}{MK\pi\mathcal{L}_{Block-1} + M\mathcal{L}_{Block-2}}P = \frac{M+K-1}{MK((M-1)\pi+1)}P. \tag{3.29}$$

Moreover, the normalized rate per symbol extension of the kth user given the power ratio π would be:

$$R^{[k]} = B_r \mathbb{E}\left[\log\left(\det\left(\mathbf{I} + P_{sym}\mathbf{H}^{[k]}\mathbf{H}^{[k]^+}\mathbf{R}_{\tilde{z}}^{[k]^{-1}}\right)\right)\right] =$$

$$\frac{1}{M+K-1}\mathbb{E}\left[\log\left(\det\left(\mathbf{I} + \frac{M+K-1}{MK((M-1)\pi+1)}P\mathbf{H}^{[k]}\mathbf{H}^{[k]^+}\mathbf{R}_{\tilde{z}}^{[k]^{-1}}\right)\right)\right] \tag{3.30}$$

where, $\mathbf{H}^{[k]}$ is same as (3.25) and $\mathbf{R}_{\tilde{z}}^{[k]}$ is the covariance matrix of noise after zero forcing subtraction:

$$\mathbf{R}_{\tilde{z}} = \begin{bmatrix} (\frac{1}{\pi} + K - 1)\mathbf{I}_{M-1} & 0 \\ \\ 0 & 1 \end{bmatrix} \tag{3.31}$$

3.4.2 Constant Power Allocation

Constant power allocation strategy which was proposed in [78,81] assigns same power to each symbol extension, i.e. $\pi^{-1} = K$ to avoid any fluctuation between Block-1 and Block-2. [78,81] has showed that with constant power at each slot the sumrate would be maximized at finite SNR .When constant power allocation is employed, the normalized rate for the kth user could be written as:

$$R_{[k]}^{s-BIA} = \frac{1}{M+K-1} \mathbb{E}\left[\log\left(\det\left(\mathbf{I} + \frac{P}{M}\mathbf{H}^{[k]}\mathbf{H}^{[k]^+}\mathbf{R}_{\tilde{z}}^{[k]^{-1}}\right)\right)\right] \tag{3.32}$$

where $\mathbf{H}^{[k]}$ is same as (3.26) and $\mathbf{R}_{\tilde{z}}^{[k]}$ is the covariance matrix of noise after zero forcing subtraction:

$$\mathbf{R}_{\tilde{z}} = \begin{bmatrix} (2K-1)\mathbf{I}_{M-1} & \mathbf{0} \\ \\ \mathbf{0} & 1 \end{bmatrix}. \tag{3.33}$$

3.4.3 Uniform Power Allocation

Recall that under MISO BC, during Block-1, MK symbols are simultaneously transmitted in each time slot, while in Block-2 only M symbols per time slot are transmitted in an orthogonal manner. When equal power is allocated to each symbols of Block-1 and Block-2 and when average power constraint at transmitter is

$\{\|\mathbf{x}[t]^2\|\} \leq P$, then power allocated to each symbol extension would equal:

$$
\begin{aligned}
P_{sym} &= \frac{SL_{s-BIA}}{MK\mathcal{L}_{Block-1} + M\mathcal{L}_{Block-2}}P \\
&= \frac{(M-1)^K + K(M-1)^{K-1}}{MK(M-1)^K + MK(M-1)^{K-1}}P \\
&= \frac{M+K-1}{M^2K}P.
\end{aligned}
\tag{3.34}
$$

Normalized rate of the kth user under uniform power allocation would therefore be:

$$
\begin{aligned}
R_{[k]}^{s-BIA} &= B_r\mathbb{E}\left[\log\left(\det\left(\mathbf{I} + P_{sym}\mathbf{H}^{[k]}\mathbf{H}^{[k]+}\mathbf{R}_{\tilde{z}}^{[k]^{-1}}\right)\right)\right]. \\
&= \frac{1}{M+K-1}\mathbb{E}\left[\log\left(\det\left(\mathbf{I} + \frac{M+K-1}{M^2K}P\mathbf{H}^{[k]}\mathbf{H}^{[k]+}\mathbf{R}_{\tilde{z}}^{[k]^{-1}}\right)\right)\right].
\end{aligned}
\tag{3.35}
$$

3.5 DoF of s-BIA Under Limited Coherence Time

Recall that while using s-BIA under the K-user $M \times 1$ MISO BC ($[K, M]$ configuration) a base station can transmit $S_{[K,M]}$ interference free symbols through a finite number of symbol extensions $SL_{[K,M]}$ and no channel knowledge is required at the transmitter to null the interference between users. As mentioned earlier, the DoF of a BS using s-BIA can be obtained by taking the ratio of the total number of transmitted interference free symbols and the number of channel uses

$$
D_{[K,M]} = \frac{S_{[K,M]}}{SL_{[K,M]}} = \frac{KM(M-1)^{(K-1)}}{(M-1)^K + K(M-1)^{(K-1)}} = \frac{KM}{K+M-1}.
\tag{3.36}
$$

A large $SL_{[K,M]}$ value implies a large coherence time which in practice most of the time is not available. For small-cell networks where FCs are deployed in a dense cellular network most of the FCs are assumed to be utilized inside buildings and therefor FUs can be considered as indoor users. As defined by 3GPP LTE-A [31, 34, 101], indoor users are assumed to have average speeds in the range $0 - 15$ km/h and have coherence times (T_c) that are in the range 10 ms $- 15$ ms respectively. Assuming a symbol

duration T_s of 1 ms, the maximum number of symbol extensions $T_{\max}$ in any FC is given as $T_{\max} = T_c/T_s$. When $SL_{[K,M]} > T_{\max}$ the FC with $[K,M]$ s-BIA configuration cannot perform and the DoF would be zero whereas when $SL_{[K,M]} \leq T_{\max}$, the DoF would be none-zero. In general, the achievable DoF in a FC using s-BIA with $[K,M]$ configuration under a given $T_{\max}$ can be formulated as:

$$D_{[K,M]}(T_{\max}) = \frac{\left\lfloor \dfrac{T_{\max}}{SL_{[K,M]}} \right\rfloor S_{[K,M]}}{T_{\max}}. \tag{3.37}$$

Distinguished from other IA schemes, in s-BIA scheme, blind interference cancellation is achieved at the receivers via simple subtractions of received symbols at different time slots at the cost of amplified noise powers. A user belonging to a BS with $[K,M]$ configuration would require

$$E_{[K,M]} = (K-1)(M-1)^K \tag{3.38}$$

subtractions. It should be noted that high K and M values can significantly increase the processing times and noise power. Minimizing the number of subtractions can indirectly decrease the number of users and antennas, K and M, thus also the number of symbol extensions $SL_{[K,M]}$, and antenna switching times M.

3.6 Applications of General Blind Interference Alignment Scheme

To set the foundation for our proposed scheme, this section briefly introduces various BIA schemes throughout Sections 3.6.1–3.6.4 assuming a small-cell down-link (DL) cellular network.

3.6.1 Syncronized BIA

Consider a cellular system, where s-BIA is implemented in each cell independently (similar to MISO BC). In such a scenario, neighboring cells are considered as a

source of intercell interference. Since the s-BIA has been designed to handle the intracell interference, its throughput would be drastically limited by adjacent cells. The effect of intercell interference in this scenario was evaluated in [78] and [81]. Interestingly, it was pointed out that if the BIA codes of the BSs of neighboring cells are synchronized (sync-BIA), the effect of intercell interference can be considerably reduced. Both in [78] and [81] it was pointed out that after zero forcing at each user, those users in different cells using the same user index will face intercell interference and the rest will be aligned successfully. Figure 3.4(a) depicts a three-cell cellular system where each cell has $[K, M] = [2, 2]$ configuration and s-BIA is implemented in each cell independently. Users in each cell are denoted by black and red color indexes and the precoder for the three BSs is as depicted in Figure 3.4(b). Users of any cell are only subject to the intercell interference from the same color index users of neighboring cells and will not sense any intracell interference. In this scenario, as users in each cell move from the center toward the cell boundary they experience more intercell interference. Achievable sum-rate of the kth user in cell f of the cth cluster can be written as:

$$
R_{[k,fc]}^{\text{sync-BIA}} = \frac{1}{K+M-1} \cdot \mathbb{E}\left[\log\left(\det\left(\mathbf{I} + \frac{(M+K-1)P}{M^2 K} \mathbf{H}_{fc}^{[k,fc]} \mathbf{H}_{fc}^{[k,fc]^+} \mathbf{R}_z^{-1} \right) \right) \right]
$$

(3.39)

where,

$$
\mathbf{R}_z^{-1} = N_0 \mathbf{I} + \sum_{\substack{j=1 \\ j \neq f}}^{F} P \tilde{\mathbf{H}}_{jc}^{[k,fc]} \tilde{\mathbf{H}}_{jc}^{[k,fc]^+} + \sum_{\substack{s=1 \\ s \neq c}}^{C} \sum_{\substack{j=1 \\ j \neq f}}^{F} P \tilde{\mathbf{H}}_{js}^{[k,fc]} \tilde{\mathbf{H}}_{js}^{[k,fc]^+}
$$

(3.40)

$$
\tilde{\mathbf{H}}_{fc}^{[k,fc]} = \sqrt{g(d_{fc}^{[k,fc]})} \times \left[\frac{1}{\sqrt{K}} \mathbf{h}_{fc}^{[k,fc]}(1), \ldots \frac{1}{\sqrt{K}} \mathbf{h}_{fc}^{[k,fc]}(M-1), \mathbf{h}_{fc}^{[k,fc]}(M) \right]^T
$$

(3.41)

$$
\tilde{\mathbf{H}}_{js}^{[k,fc]} = \sqrt{g(d_{js}^{[k,fc]})} \times \left[\mathbf{h}_{js}^{[k,fc]}(1), \ldots \mathbf{h}_{js}^{[k,fc]}(M-1), \mathbf{h}_{js}^{[k,fc]}(M) \right]^T
$$

(3.42)
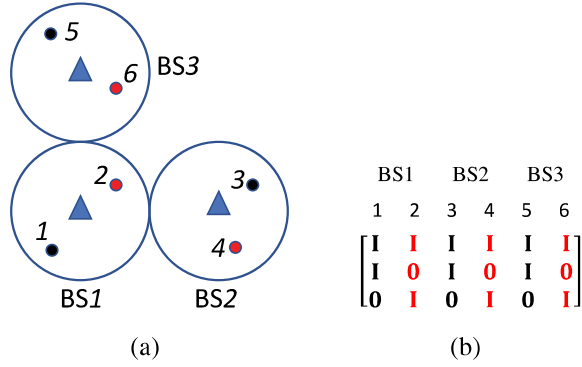
Figure 3.4: Synchronized BIA for three cells two-user setting, with M=2. (a) three cells network. (b) sync-BIA precoder for BSs.

3.6.2 Extended BIA

A straight forward approach to cancel both the intracell and intercell interferences is through the use of extended BIA (ext-BIA) proposed in [79]. The precoder matrix is constructed similar to the s-BIA when the whole cluster is considered as a big cell with M transmit antennas and FK users. Each user is served by its own BS using a predetermined supersymbol structure. Between the BSs there is no data sharing. Figure 3.5, depicts the three cells scenario under which each cell has $[K,M] = [2,2]$ configuration and its corresponding precoder matrix.
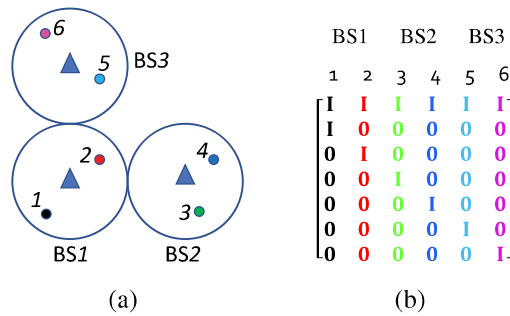

Figure 3.5: Extended BIA for a three cells two-user setting with 2 transmit antennas per BS. (a) three cells network. (b) ext-BIA precoder for BSs 1-3.

The achievable sum-rate for the kth user in cell f of the cth cluster with ext-BIA can be

63

written as:

$$R_{[k,fc]}^{\text{ext-BIA}} = \frac{1}{FK+M-1} \cdot \mathbb{E}\left[\log\left(\det\left(\mathbf{I} + \frac{(M+FK-1)P}{M^2K}\mathbf{H}_{fc}^{[k,fc]}\mathbf{H}_{fc}^{[k,fc]^+}\mathbf{R}_z^{-1}\right)\right)\right]$$

(3.43)

where,

$$\mathbf{R}_z^{-1} = N_0\mathbf{I} + \sum_{\substack{s=1 \\ s\neq c}}^{C}\sum_{\substack{j=1 \\ j\neq f}}^{F} P\tilde{\mathbf{H}}_{js}^{[k,fc]}\tilde{\mathbf{H}}_{js}^{[k,fc]^+}.$$

(3.44)

$\tilde{\mathbf{H}}_{fc}^{[k,fc]}$ is similar to (3.41) with $\sqrt{FK}$ as the normalization term and $\tilde{\mathbf{H}}_{js}^{[k,fc]}$ is same as (3.42).

3.6.3 Topological BIA

There is always a trade-off between the performance of sync-BIA and ext-BIA based on the user distribution in the network. When users are located close to the BSs in each cell, they experience low intercell interference. In this case, the sync-BIA performs better compared to the ext-BIA which tries to eliminate all weak intercell interference in expense of a longer supersymbol length. On the other hand, when users in cells are located closer to the cell boundaries, they receive strong intercell interference from neighboring BSs. In this case ext-BIA can achieve higher normalized user-rate than sync-BIA by canceling all inter and itracell interference.

Instead of the above mentioned fully blind schemes, authors in [79] proposed to use a semi-blind IA scheme in which they would exploit the location information of the users and base stations in the network. They grouped suitable users that can be served at the same time as a single user, then the precoder would consider each cluster in the network as one big cell and construct the precoder for each group by using the s-BIA framework. This approach is uniformly superior in performance than sync-BIA and

ext-BIA for any possible user distribution by minimizing the required supersymbol length.

The user grouping can be done by first defining a group indicator matrix B which labels the suitable users for grouping. The matrix B initially equals an all-ones matrix of size $(FK \times FK)$. Afterwards, the corresponding elements of interference limited users and the users in the same cell which cannot be grouped due to the intracell interference are replaced by 0 values.
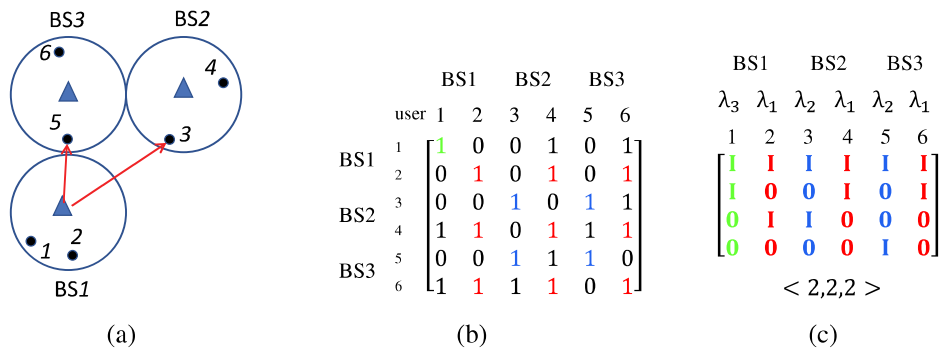
Figure 3.6: (a) top-BIA for a three cells two-user setting with 2 transmit antennas per BS where BS1 cause interfering on user 5 in cell 3 and user 3 in cell 2. (b) Grouping indicator matrix B for top-BIA. (c) top-BIA precoder for BSs 1-3.

An example demonstrating the top-BIA can be observed in Figure 3.6. Note that BS1 casts strong interference to user-3 in BS2. Therefor, as shown by grouping indicator matrix and indicated by 0s, users 1 and 2 in BS1 could not be grouped with user-3 $\big($refer to Figure 3.6(b)$\big)$. Similarly, transmission of BS1 would cause interference on user-5 in BS3. Hence, for the same reasons, users 1 and 2 can not be grouped with user-5. Moreover, due to the intracell interference issues, users that are located in a same cell cannot make a group, and corresponding elements of matrix B would be set to 0s. As pointed out by matrix B, for this toy example users 1 and 2, users 3 and 4 and users 5 and 6 should not be grouped with each other. Finally, it can be seen that, matrix

B is symmetric and since each user can be grouped with itself, the diagonal elements of matrix B would be identical and equals unity.

Given matrix B, top-BIA could be employed to determine group of users that can be served simultaneously via s-BIA. In general, the grouping problem is NP-Hard. However, top-BIA would provide a simpler solution by utilizing a heuristic algorithm. To avoid high complexity top-BIA avoids examining all possibilities and might result in a sub-optimal solution.

Once the grouping indicator matrix is obtained, top-BIA would examine the proper sub-matrices of B and compare them with the 1s matrix before grouping the users. An F cell cluster where each cell has K users would result in a matrix B of size $(FK \times FK)$. Note that, the size of any group is upper bounded by F meaning that users sharing a cell cannot be grouped together. Since the best scenario is when a group has F users top-BIA would start by examining the size $(F \times F)$ sub-matrices of B (with symmetric row and column indexes) that are all 1s. When this condition is met, top-BIA will group the corresponding users and after removing related columns and rows would re-evaluate with a matrix of reduced size $[(FK - F) \times (FK - F)]$. On the other hand when the condition is not met, then the algorithm will lower the size to $(F - 1) \times (F - 1)$ and step through the same process once again. Finally, set of grouped users denoted as $\Lambda = \{\lambda_1, \lambda_2 \ldots \lambda_{|\Lambda|}\}$ is obtained where λ_i and $|\Lambda|$ respectively represent groups formed and the cardinality of the set Λ.

For example, in Figure 3.6(b), the sub-matrix formed by the indices $\{2, 4, 6\}$ is all-ones and top-BIA would group them together as λ_1. Then top-BIA removes 2nd, 4th and 6 rows and columns of B and continues to examine the remaining matrix. If there are no

other 3×3 sub-matrix that is all 1s then it will start to search for 2×2 sub-matrices. In our example the next two groups obtained by top-BIA are $\{3,5\}$ as λ_2 and $\{1\}$ as λ_3. Finally, a group set is formed as $\Lambda = \{\{2,4,6\},\{3,5\},\{1\}\}$ which can be seen in Figure 3.6(b) (same color indicates users of same group). Once user-groups are formed, transmit precoders depicted in Figure 3.6(c) can be constructed.

To construct the grouping indicator matrix, the long term SINR value corresponding to each BS-user pair is calculated and compared with a threshold to determine the 1 or 0 elements. For a given user distribution, the threshold value should be chosen so that top-BIA scheme can achieve higher throughput than Sync-BIA and Ext-BIA.

Initially the threshold value would be set to the minimum of SINR values. Then the network throughput of top-BIA and other blind IA schemes would be calculated. Afterwards, for each new iteration threshold value is updated with the next smallest SINR and this process will continue until the top-BIA can achieves higher network throughput in comparison to other BIA schemes. Threshold updating will be stopped once the throughput of top-BIA starts to descend.

Under top-BIA, k^{th} user in f^{th} cell of the cth cluster would have a sum-rate as:

$$R_{[k,fc]}^{\text{top-BIA}} = \frac{1}{|\Lambda|+M-1} \cdot \mathbb{E}\left[\log\left(\det\left(\mathbf{I} + \frac{(M+|\Lambda|-1)P}{M^2 K}\mathbf{H}_{fc}^{[k,fc]}\mathbf{H}_{fc}^{[k,fc]^{+}}\mathbf{R}_z^{-1}\right)\right)\right]$$

(3.45)

where,

$$\mathbf{R}_z^{-1} = N_0\mathbf{I} + \sum_{\substack{j=1 \\ j\neq f}}^{F} P\tilde{\mathbf{H}}_{jc}^{[k,fc]}\tilde{\mathbf{H}}_{jc}^{[k,fc]^{+}} + \sum_{\substack{s=1 \\ s\neq c}}^{C}\sum_{\substack{j=1,j\neq f, \\ j\in L^{[k,fc]}}}^{F} P\tilde{\mathbf{H}}_{js}^{[k,fc]}\tilde{\mathbf{H}}_{js}^{[k,fc]^{+}}.$$

(3.46)

$\tilde{\mathbf{H}}_{fc}^{[k,fc]}$ and $\tilde{\mathbf{H}}_{js}^{[k,fc]}$ are as in (3.41) and (3.42) and the normalization term for

$\tilde{\mathbf{H}}_{fc}^{[k,fc]}$ equals $\sqrt{|\Lambda| - 1}$. In addition $L^{[k,fc]}$ represents the set of BSs as source of intercell interference which transmit at the same time with the kth user.

3.6.4 Hierarchical BIA

Hierarchical blind interference alignment (h-BIA) aims to reduce the supersymbol length without sacrificing much on DoF. The approach tries to group the users and aims to preferably have same number of users with similar user's modes in each group. Inter-user interference (IUI) between receivers of the same group are managed first by utilizing pattern n_1 obtained via s-BIA. Subsequently, inter-group interference (IGI) between different groups are handled by making use of pattern n_2 (also obtained using s-BIA). Both patterns n_1 and n_2 are dependent on the user grouping detailed below:

Consider a cluster with $K_T = FK$ total users where F denotes the number of cell in the cluster and K the number of users in each cell. Independent of number of transmitters, K_T receivers are divided into K_G groups when each group has $K_E = K_T/K_G$ users. The kth user in the ith group is denoted as $[k,i]$ where $i \in [1 : K_G]$ and $k \in [1 : K_E]$. If receiver $[k,i]$ has $M_{[k,i]}$ preset modes, then $M_{[k,i]}$ is divided by M_{G_i} groups if it is divisible. $M_{E_{[k,i]}} = M_{[k,i]}/M_{G_i}$ and denotes the kth user preset mode belonging to the user-group i.

Set of all $M_{E_{[k,i]}} \forall k \in [1 : K_E]$, form the group mode set $\mathcal{N}_i = \{M_{E_{[1,i]}}, \ldots M_{E_{[k,i]}} \ldots M_{E_{[K_E,i]}}\}$. The preset mode patter n_1 for each group is constructed according to the group mode set ($\mathcal{N}_i, \forall i \in [1 : K_G]$) as:

$$n_1 = \langle M_{E_{[1,i]}}, \ldots M_{E_{[k,i]}} \ldots M_{E_{[K_E,i]}} \rangle.$$

While aligning IUI, if all user-groups use the same pattern n_1 for users in a group then the interference signal intended for another user in other groups using a pattern other than n_1 would also be aligned. Therefore the grouping condition can be stated as:

$$\mathcal{N}_1 = \mathcal{N}_2 = \cdots = \mathcal{N}_{K_G}. \tag{3.47}$$

In general, where user-groups have different $\mathcal{N}_i$ sets, to satisfy the above mentioned condition the common $\mathcal{N}_i$ set is designates as the union of the individual $\mathcal{N}_i$ set for all groups. Hence, the preset mode pattern n_1 for all groups can be constructed by taking the union of all group mode sets:

$$\mathcal{U} = \bigcup_{i=1}^{K_G} \mathcal{N}_i = \{M_{E_1}, \ldots M_{E_k} \ldots M_{E_{|u|}}\}. \tag{3.48}$$

Pattern n_2 is constructed to align the inter group interference (IGI). Since there are K_G groups, each with M_{G_i} preset modes, pattern n_2 is formed as:

$$n_2 = \langle M_{G_1}, \ldots M_{G_i} \ldots M_{G_{K_G}} \rangle. \tag{3.49}$$

As before, signals that are interfering can be aligned using the designed preset mode patterns. The preset mode pattern for user k in i^{th} group is constructed by taking a Cartesian product of patterns n_1 and n_2:

$$\mathbf{n}_{[k,i]} = (\text{pattern } n_1 \text{ of receiver } k \text{ in each group}) \times (\text{pattern } n_2 \text{ for users in group } i)$$
$$\tag{3.50}$$

To clarify the workings of h-BIA we provide an example where 4 users with respective preset modes of 8, 8, 4, 4 are considered. To satisfy the above-mentioned grouping condition, users are partitioned into two groups where the users in each group have preset modes 8 and 4 ($K_G = 2$, $K_E = 2$). Since number of preset modes of

69

each group are divisible by 2, preset mode group values are set as $M_{G_1} = M_{G_2} = 2$. By this partitioning each group would have similar group-mode-sets as $\mathcal{N}_i = \{8/2, 4/2\} = \{4, 2\}, \forall i \in \{1, 2\}$. Recalling that s-BIA requires 7 time slots for $\langle 4, 2 \rangle$ configuration, pattern n_1 for the union-group-set $\mathcal{U} = \mathcal{N}_i$ can be written as:

$$(1, 2, 3, 4, 1, 2, 3), \text{ for users } [1, i]$$
$$(1, 1, 1, 1, 2, 2, 2), \text{ for users } [2, i], \quad \forall i \in \{1, 2\}$$

(3.51)

Pattern n_2 is designed according to the preset mode group values ($M_{G_1} = M_{G_2} = 2$) using standard BIA with structure $\langle 2, 2 \rangle$ and is as follows:

$$(1, 2, 1), \text{ for users } [k, 1]$$
$$(1, 1, 2), \text{ for users } [k, 2], \quad \forall k \in \{1, 2\}$$

(3.52)

From (3.51) and (3.52) the preset pattern mode for each individual user can be generated as:

$$\mathbf{n}_{[k,i]} = \begin{cases} (1, 2, 3, 4, 1, 2, 3) \times (1, 2, 1) \text{ user } [1, 1] \text{ with } M_{[1,1]} = 8 \\[2mm] (1, 1, 1, 1, 2, 2, 2) \times (1, 2, 1) \text{ user } [2, 1] \text{ with } M_{[2,1]} = 4 \\[2mm] (1, 2, 3, 4, 1, 2, 3) \times (1, 1, 2) \text{ user } [1, 2] \text{ with } M_{[1,2]} = 8 \\[2mm] (1, 1, 1, 1, 2, 2, 2) \times (1, 1, 2) \text{ user } [2, 2] \text{ with } M_{[2,2]} = 4 \end{cases}$$

(3.53)

Based on pattern-n_1, the precoder matrices for group-1 (G_1) and group-2 (G_2) can be written as:

$$\mathbf{x}_{G_1} = \begin{bmatrix} \mathbf{I}_8 \\ \mathbf{I}_8 \\ \mathbf{I}_8 \\ \mathbf{I}_8 \\ \mathbf{0}_8 \\ \mathbf{0}_8 \\ \mathbf{0}_8 \end{bmatrix} \mathbf{x}_{[1,1]} + \begin{bmatrix} \mathbf{I}_{8\times4} & \mathbf{0}_{8\times4} & \mathbf{0}_{8\times4} \\ \mathbf{0}_{8\times4} & \mathbf{I}_{8\times4} & \mathbf{0}_{8\times4} \\ \mathbf{0}_{8\times4} & \mathbf{0}_{8\times4} & \mathbf{I}_{8\times4} \\ \mathbf{0}_{8\times4} & \mathbf{0}_{8\times4} & \mathbf{0}_{8\times4} \\ \mathbf{I}_{8\times4} & \mathbf{0}_{8\times4} & \mathbf{0}_{8\times4} \\ \mathbf{0}_{8\times4} & \mathbf{I}_{8\times4} & \mathbf{0}_{8\times4} \\ \mathbf{0}_{8\times4} & \mathbf{0}_{8\times4} & \mathbf{I}_{8\times4} \end{bmatrix} \mathbf{x}_{[2,1]},$$

$$\mathbf{x}_{G_2} = \begin{bmatrix} \mathbf{I}_8 \\ \mathbf{I}_8 \\ \mathbf{I}_8 \\ \mathbf{I}_8 \\ \mathbf{0}_8 \\ \mathbf{0}_8 \\ \mathbf{0}_8 \end{bmatrix} \mathbf{x}_{[2,1]} + \begin{bmatrix} \mathbf{I}_{8\times 4} & \mathbf{0}_{8\times 4} & \mathbf{0}_{8\times 4} \\ \mathbf{0}_{8\times 4} & \mathbf{I}_{8\times 4} & \mathbf{0}_{8\times 4} \\ \mathbf{0}_{8\times 4} & \mathbf{0}_{8\times 4} & \mathbf{I}_{8\times 4} \\ \mathbf{0}_{8\times 4} & \mathbf{0}_{8\times 4} & \mathbf{0}_{8\times 4} \\ \mathbf{I}_{8\times 4} & \mathbf{0}_{8\times 4} & \mathbf{0}_{8\times 4} \\ \mathbf{0}_{8\times 4} & \mathbf{I}_{8\times 4} & \mathbf{0}_{8\times 4} \\ \mathbf{0}_{8\times 4} & \mathbf{0}_{8\times 4} & \mathbf{I}_{8\times 4} \end{bmatrix} \mathbf{x}_{[2,2]}.$$

Finally, the precoding matrix requiring 21 time slots based on pattern n_2 can be expressed as:

$$\mathbf{x} = \begin{bmatrix} \mathbf{I}_{56} \\ \mathbf{I}_{56} \\ \mathbf{0}_{56} \end{bmatrix} \mathbf{x}_{G_1} + \begin{bmatrix} \mathbf{I}_{56} \\ \mathbf{0}_{56} \\ \mathbf{I}_{56} \end{bmatrix} \mathbf{x}_{G_2}$$

When the grouping condition in (3.47) is met then user-groups have same number of users (K_E) and users with same index in each group have same modes $(M_{E_k} = M_{E_{[k,i]}}, \forall i \in [1 : K_G], \forall k \in [1 : K_E])$. Hence, the sum-DoF for the h-BIA can be calculated as the product of $(\text{sum-DoF}_{\text{s-BIA}}$ achieved by pattern $n_1)$ and $(\text{sum-DoF}_{\text{s-BIA}}$ achieved by pattern $n_2)$:

$$\text{sum-DoF}_{\text{h-BIA}} = \frac{\sum_{k=1}^{K_E} \frac{M_{E_k}}{M_{E_k}-1}}{1 + \sum_{k=1}^{K_E} \frac{1}{M_{E_k}-1}} \times \frac{\sum_{i=1}^{K_G} \frac{M_{G_i}}{M_{G_i}-1}}{1 + \sum_{i=1}^{K_G} \frac{1}{M_{G_i}-1}}. \tag{3.54}$$

The supersymbol length $\text{SL}_{\text{h-BIA}}$ can also be calculated as the product of $(\text{SL}_{\text{s-BIA}}$ with pattern $n_1)$ and $(\text{SL}_{\text{s-BIA}}$ with pattern $n_2)$:

$$\text{SL}_{\text{h-BIA}} = \left(\prod_{k=1}^{K_E}(M_{E_k}-1) + \sum_{k=1}^{K_E} \prod_{\substack{p=1 \\ p\neq k}}^{K_E}(M_{E_p}-1) \right) \times \left(\prod_{i=1}^{K_G}(M_{G_i}-1) + \sum_{i=1}^{K_G} \prod_{\substack{q=1 \\ q\neq i}}^{K_G}(M_{G_q}-1) \right). \tag{3.55}$$

It can be noted that within the duration of supersymbol length, the number of

71

interference-free signals for the desired user $[k, i]$ can be calculated as:

$$d_{[k,i]} = M_{[k,i]} \prod_{\substack{p=1 \\ p \neq k}}^{K_E} (M_{E_p} - 1) \prod_{\substack{q=1 \\ q \neq k}}^{K_G} (M_{G_q} - 1) \qquad (3.56)$$

Comparing the results for s-BIA and h-BIA under complete grouping condition, we see that h-BIA can significantly reduce the supersymbol length however it suffers from a minor loss in sum-DoF. Equations (3.57) and (3.58) represent the reduction rate in supersymbol length and the sum-DoF loss ratio when $M_{E_k} = \sqrt{M}$, $M_{G_i} = \sqrt{M}$ for $i \in [1 : K_G]$, $k \in [1 : K_E]$ and $K_G = \sqrt{K}$.

$$\frac{\text{SL}_{\text{s-BIA}}}{\text{SL}_{\text{h-BIA}}} =\sim O \underbrace{\left((\sqrt{M} - 1)^{K - 2(\sqrt{K} - 1)} (\sqrt{M} + 1)^K \right)}_{\text{SL reduction rate}}. \qquad (3.57)$$

$$\frac{\text{sum-DoF}_{\text{h-BIA}}}{\text{sum-DoF}_{\text{s-BIA}}} = 1 - \underbrace{\frac{2(\sqrt{M} - 1)(\sqrt{K} - 1)}{(\sqrt{M} + \sqrt{K} - 1)^2}}_{\text{sum-DoF loss}}. \qquad (3.58)$$

In case of an incomplete grouping, pattern n_1 is designed based on $\mathcal{U}$ given in (3.48) and the length of supersymbol ($\text{SL}_{\text{h-BIA}}$) would be:

$$\text{SL}_{\text{h-BIA}} = \left(\prod_{k=1}^{|\mathcal{U}|} (M_{E_k} - 1) + \sum_{k=1}^{|\mathcal{U}|} \prod_{\substack{p=1 \\ p \neq k}}^{|\mathcal{U}|} (M_{E_p} - 1) \right) \times \left(\prod_{i=1}^{K_G} (M_{G_i} - 1) + \sum_{i=1}^{K_G} \prod_{\substack{q=1 \\ q \neq i}}^{K_G} (M_{G_q} - 1) \right), \qquad (3.59)$$

consequently the sum-DoF would be:

$$\text{sum-DoF}_{\text{h-BIA}} = \frac{\sum_{k=1}^{|\mathcal{U}|} \frac{M_{E_k}}{M_{E_k} - 1}}{1 + \sum_{k=1}^{|\mathcal{U}|} \frac{1}{M_{E_k} - 1}} \times \frac{\sum_{i=1}^{K_G} \frac{M_{G_i}}{M_{G_i} - 1}}{1 + \sum_{i=1}^{K_G} \frac{1}{M_{G_i} - 1}}$$

$$- \underbrace{\sum_{i=1}^{K_G} \sum_{M_{E_k} \in \mathcal{U} \setminus M_i} \frac{\frac{M_{E_k}}{M_{E_k} - 1}}{1 + \sum_{p=1}^{|\mathcal{U}|} \frac{1}{M_{E_p} - 1}} \times \frac{\frac{M_{G_i}}{M_{G_i} - 1}}{1 + \sum_{q=1}^{K_G} \frac{1}{M_{G_q} - 1}}}_{\text{incomplete grouping sum-DoF loss}}. \qquad (3.60)$$

In (3.60), DoF loss represents the difference in sum-DoF for complete and incomplete

groupings in which all groups have a common M_E set as $\mathcal{U}$.

In what follows, we first re-state the sum-rate formula for h-BIA under one cell scenario and then formulate the sum-rate for a cellular setup with many cells.

Let us first consider a cell that has a single transmitter with M transmit antennas and K users with $M_k = M, \forall k \in [1:K]$ preset modes. While constructing the preset mode pattern for h-BIA, K_G groups will be obtained from a total of K users resulting in K_E users per group ($K_E = K/K_G$), and M preset modes are also partitioned into M_G groups ($M_E = M/M_G$). Assuming equal power allocation [78], as in [45] the sum-rate for the single cell scenario would be:

$$
R^{\text{h-BIA}} = \sum_{i=1}^{K_G} \sum_{k=1}^{K_E} \frac{1}{(M_E + K_E - 1)(M_G + K_G - 1)} \mathbb{E} \left[\log \left(\det \left(\mathbf{I} + \frac{P}{M} \tilde{\mathbf{H}}^{[k,i]} \tilde{\mathbf{H}}^{[k,i]^+} \mathbf{R}_z^{-1} \right) \right) \right]
$$

(3.61)

where

$$
\mathbf{R}_{\tilde{z}} = \begin{bmatrix} \mathbf{R}_{\tilde{z}_1} & & & \mathbf{0} \\ & \ddots & & \\ & & \mathbf{R}_{\tilde{z}_1} & \\ \mathbf{0} & & & \mathbf{R}_{\tilde{z}_2} \end{bmatrix}.
$$

(3.62)

and

$$
\tilde{\mathbf{H}}^{[k,i]} = \left[\mathbf{h}^{[k,i]}(1)^T, \ldots, \mathbf{h}^{[k,i]}(M-1)^T, \mathbf{h}^{[k,i]}(M)^T \right]^T.
$$

(3.63)

In (3.62), $\mathbf{R}_{\tilde{z}_1}$ denotes the noise variance matrix of groups 1 to $(M_G - 1)$ after IUI and IGI cancellation and $\mathbf{R}_{\tilde{z}_2}$ represents the noise variance matrix of the M_G^{th} group which is not affected by IGI.

$$
\mathbf{R}_{\tilde{z}_1} = \begin{bmatrix} (2K_G - 1)(2K_E - 1)\mathbf{I}_{M_E-1} & \mathbf{0}_{(M_E-1)\times 1} \\ \\ \mathbf{0}_{1\times(M_E-1)} & 2K_G - 1 \end{bmatrix}
$$

(3.64)

73

$$\mathbf{R}_{\tilde{z}_2} = \begin{bmatrix} (2K_E - 1)\mathbf{I}_{M_E - 1} & \mathbf{0}_{(M_E - 1) \times 1} \\ \\ \mathbf{0}_{1 \times (M_E - 1)} & 1 \end{bmatrix}. \tag{3.65}$$

The results of the single cell scenario can be extended to a fully-connected homogeneous cellular network setting with F transmitters each with M transmit antennas and K_T receivers which can switch between M preset modes. This way, each transmitter can serve its corresponding K_f receivers. As opposed to the previous scenario, here it is assumed that the average transmit power for all transmitters is limited to P and each transmitter uses maximum power for transmitting symbols to their desired receivers. Therefore, in this scenario the increment in the noise variance due to the use constant power allocation does not occur. Assuming uniform power allocation, the achievable sum-rate of the kth user ($k \in [1 : K_E]$) in group i ($i \in [1 : K_G]$), can be written as:

$$R_{[k,i]}^{\text{h-BIA}} = \frac{1}{(M_E + K_E - 1)(M_G + K_G - 1)} \times \mathbb{E}\left[\log\left(\det\left(\mathbf{I} + \tilde{P}\tilde{\mathbf{H}}_{[k,i]}^{f_{[k,i]}} \tilde{\mathbf{H}}_{[k,i]}^{f_{[k,i]}+} \mathbf{R}_z^{-1} \right) \right) \right] \tag{3.66}$$

where, $\tilde{P} = \frac{(M_E + K_E - 1)(M_G + K_G - 1)P}{K_T M^2}$ and $f_{[k,i]}$ denotes the transmitter which serves user k in group i ($[k,i]$). $\tilde{\mathbf{H}}_{[k,i]}^{f_{[k,i]}}$ is channel between $[k,i]$ and transmitter $f_{[k,i]}$ as follows:

$$\tilde{\mathbf{H}}_{[k,i]}^{f_{[k,i]}} = \sqrt{g(d_{[k,i]}^{f_{[k,i]}})} \left[\mathbf{h}_{[k,i]}^{f_{[k,i]}}(1)^T, \ldots, \mathbf{h}_{[k,i]}^{f_{[k,i]}}(M-1)^T, \mathbf{h}_{[k,i]}^{f_{[k,i]}}(M)^T \right]^T \tag{3.67}$$

and $\mathbf{R}_{\tilde{z}}$ represents the noise variance matrix and can be written as:

$$\mathbf{R}_{\tilde{z}} = \begin{bmatrix} \mathbf{R}_{\tilde{z}_1} & & & \mathbf{0} \\ & \ddots & & \\ & & \mathbf{R}_{\tilde{z}_1} & \\ \mathbf{0} & & & \mathbf{R}_{\tilde{z}_2} \end{bmatrix} \tag{3.68}$$

where

$$\mathbf{R}_{\tilde{z}_1} = \begin{bmatrix} K_T \mathbf{I}_{M_E-1} & \mathbf{0}_{(M_E-1)\times 1} \\ \mathbf{0}_{1\times(M_E-1)} & K_G \end{bmatrix} \tag{3.69}$$

and

$$\mathbf{R}_{\tilde{z}_2} = \begin{bmatrix} K_E \mathbf{I}_{M_E-1} & \mathbf{0}_{(M_E-1)\times 1} \\ \mathbf{0}_{1\times(M_E-1)} & 1 \end{bmatrix}. \tag{3.70}$$

Note that, although the sum rate from (3.66) increases by using more transmitters (due to an increase in total transmit power), the sum-DoF does not change.

3.6.5 Hierarchical BIA Under Limited Coherence Time

Since the standard blind interference alignment scheme requires that the channel stays constant during the course of transmission, coherence time or number of allowable symbol extensions becomes an important issue to consider. In general when coherence time is limited there are three ways to reduce the number of symbol extensions (SL) to satisfy the requirement of BIA schemes: 1) to reduce the number of served users (K), 2) to reduce the number of preset modes used by each user (M_k), 3) utilizing orthogonalization approaches such as TDMA and FDMA and employing the hierarchical BIA scheme. Section 3.5 has explained what would be the effects of changing number of served users and transmit antennas on the achievable DoF of a single BS with $[K,M]$ configuration under a BC using s-BIA with limited coherence time assumption. This subsection aims to evaluate the achievable DoF of hierarchical-BIA (h-BIA) scheme under limited coherence time and explains how optimization can constrain the supersymbol length not to exceed the available coherence time.

As stated earlier, one way of reducing the supersymbol length is to reduce M_k. This

can be done using the optimization defined in (45) of [45] which is also known as the conventional preset mode pattern design (CPD). In this method the supersymbol length is adjusted by reducing the preset modes for each user to meet the coherence time limitation (T_{max}). Moreover, CPD method aims to serve all the users simultaneously, therefore changing the number of served users (K) is not considered in this method. Here the true used preset modes of the kth user is denoted by M'_k while this user is able to switch between M_k different preset modes. The CPD optimization problem has previously been defined in [45] as:

$$\max \quad \text{sum-DoF} = \frac{\sum_{k=1}^{K} \frac{M'_k}{M'_k - 1}}{1 + \sum_{k=1}^{K} \frac{1}{M'_k - 1}}$$

$$\text{s.t.} \quad \text{SL} = \left(\prod_{k=1}^{K} (M'_k - 1) + \sum_{k=1}^{K} \prod_{\substack{p=1 \\ p \neq k}}^{K} (M'_p - 1) \right) \leq T_{max} \tag{3.71}$$

$$2 \leq M'_k \leq M_k \ \forall k \in [1:K].$$

As stated in [45], the design of the preset mode patterns could be made more efficient if h-BIA is used. Considering h-BIA with appropriate grouping where $\mathcal{U}$ and $\mathcal{M}_G$ sets are defined as $\{M_{G_1}, \ldots M_{G_i} \ldots M_{G_{K_G}}\}$ and $\{M_{E_1}, \ldots M_{E_k} \ldots M_{E_{|u|}}\}$, the newly formed optimization problem can be expressed as:

$$\max \quad \text{sum-DoF}_{\text{h-BIA}}$$

$$\text{s.t.} \quad \text{SL}_{tot} \leq T_{max}$$

$$1 \leq M_{G_i} \leq \left\lfloor \frac{\min\limits_k M'_{[k,i]}}{2} \right\rfloor \ \forall i \in [1:K_G] \tag{3.72}$$

$$1 \leq M_{E_{[k,i]}} \leq \left\lfloor \frac{M'_{[k,i]}}{M_{G_i}} \right\rfloor \ \forall i \in [1:K_G], k \in [1:K_E]$$

where $M'_{[k,i]}$ represents the actual used preset modes of user $[k,i]$ and sum-DoF$_{\text{h-BIA}}$ and SL$_{tot}$ are same as in equations (3.54) and (3.55) respectively. In (3.72), M_{G_i} values

are limited to be greater than 2 otherwise user $[k,i]$ would not be able to construct patter $n1$ and accordingly, h-BIA wouldn't be able to align the IUI. Moreover, when $K_G = 1$ and $M_{G_1} = 1$ this optimization problem represents the CPD problem. The optimization problem in (3.72) is a complex integer problem with many constraints and hence a sub-optimal solution to this problem can be obtained using an algorithm known as Dynamic Supersymbol Design (DSD) (for details refer to [45]).
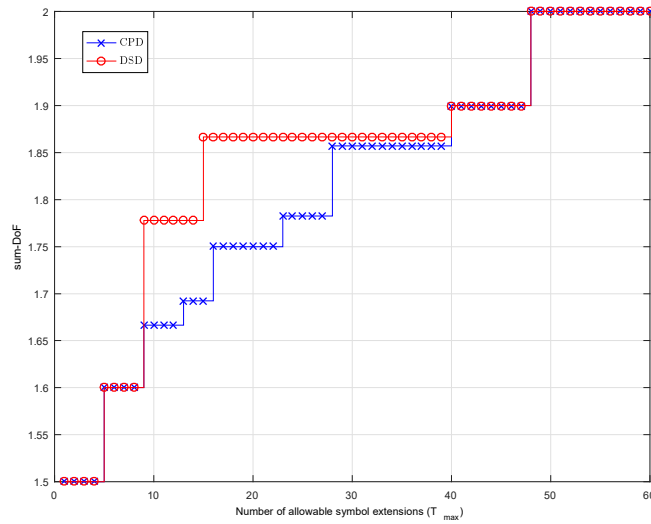
Figure 3.7: Comparing achievable DoF of s-BIA with that of h-BIA under limited coherence time.

Figure 3.7 shown the result of optimization problems in (3.71) and (3.72). The sum-DoF attained for CPD and DSD algorithms assume 4 users ans a preset mode set with values $\{6, 6, 4, \text{ and } 4\}$.

As can be seen in Figure 3.7, DSD achieves 16/9 DoF with $T_{max} = 10$ and increased to 28/15 when $T_{max} = 15$. DoF of 16/9 within the duration of 9 symbol extensions corresponds to the solution when four (4) users are split into two groups each with two (2) users and each user with only 4 actually used preset modes $\left(M_k' = 4, \forall k \in \{1,2,3,4\}, (\mathcal{M}_G, \mathcal{U}) = \left(\{2,2\}, \{2,2\} \right) \right)$. The DoF of 28/15 within the

77

duration of 15 symbol extensions is achieved when $\left(\mathcal{M}_G, \mathcal{U}\right) = \left(\{3,2\}, \{2,2\}\right)$. Comparing CPD and DSD results one can see that, the DSD would achieve higher sum-DoFs for coherence times that are upper bounded by $T_{max} \in [10\text{–}35]$. Finally the two optimization problems results in a similar sum-DoF when T_{max} exceeds 35.

Chapter 4

HYBRID BLIND INTERFERENCE ALIGNMENT IN HOMOGENEOUS CELLULAR NETWORKS WITH LIMITED COHERENCE TIME

4.1 Introduction

The work presented in this chapter is inspired by the user grouping approach of top-BIA and the fact that partially connected networks can be advantageous in terms of DoF and sum-rate. After grouping the users in a cellular network (as in top-BIA) our proposed hybrid BIA scheme would apply h-BIA on the grouped users to reduce the supersymbol length and overcome the DoF loss of the h-BIA. The chapter is organized as follows: The system model is described in Section 4.2. The proposed hybrid blind interference alignment scheme is explained in detail in Section 4.3 and to clarify its workings a toy example is provided. Afterwards, Section 4.4 provides the simulation parameters and examines DoF and throughput for the methods discussed et al.

4.2 Notation and System Model

In the proposed method scalars are denoted by lowercase letters, vectors by boldface lowercase letters and matrices by boldface capital letters. $[1:n]$ denotes a set $\{1, 2, \ldots, n\}$ and $\mathcal{A} \backslash \mathcal{B}$ denotes the set of elements that are members of $\mathcal{A}$ and not $\mathcal{B}$.

We consider a MISO BC cellular network comprised of C clusters, each with F small-cells and total of $N = CF$, base stations (BSs). Each BS has M transmit antennas and

serves K users and each user is equipped with one re-configurable antenna that can switch between $M_k \leq M$, $M \geq 2$ different modes. For any chosen mode, a user will see a channel that is independent of all other channels experienced in other antenna modes. BSs are assumed to transmit at a fixed power level and are randomly located by the end users. Power control is not considered in this paper and furthermore it is assumed that information on associations and clustering is available.

The received signal for the kth user in f^{th} cell of the cth cluster can be expressed as:

$$
y^{[k,fc]}(t) = \sqrt{g(d_{fc}^{[k,fc]})} \mathbf{h}_{fc}^{[k,fc]}(n_{[k,fc]}) \mathbf{x}_{fc}(t) + \sum_{\substack{j=1 \\ j \neq f}}^{F} \sqrt{g(d_{jc}^{[k,fc]})} \mathbf{h}_{jc}^{[k,fc]}(n_{[k,fc]}) \mathbf{x}_{jc}(t)
$$

$$
+ \sum_{\substack{s=1 \\ s \neq c}}^{C} \sum_{j=1}^{F} \sqrt{g(d_{js}^{[k,fc]})} \mathbf{h}_{js}^{[k,fc]}(n_{[k,fc]}) \mathbf{x}_{js}(t) + z^{[k,fc]}(t)
$$

$$(4.1)$$

with $k \in \{1,2,...,K\}$; $f,j \in \{1,2,...,F\}$; $c,s \in \{1,2,...,C\}$, and $n_{[k,fc]} \in \{1,2,...,M_k\}$. $\mathbf{x}_{fc}(t) \in \mathbb{C}^{M \times 1}$ is the transmitted signal vector at time t from f^{th} cell in c^{th} cluster and $g(d_{js}^{[k,fc]})$ is the distance based path loss model. $d_{js}^{[k,fc]}$ and $\mathbf{h}_{js}^{[k,fc]}(m) \in \mathbb{C}^{1 \times M}$ represent the distance and small scale fading channel with preset channel mode $n_{[k,fc]}$ between k^{th} user in the fth cell of the cluster c and the jth cell of the cluster s. $z^{[k,fc]}(t) \sim \mathcal{CN}(0,N_0)$ denotes the independent and identically distributed circular symmetric complex Gaussian noise with variance N_0. Finally, each transmitter is constrained to have average transmit power as $\mathbb{E}[\|\mathbf{x}_{fc}(t)\|^2] \leq P$.

4.3 Proposed Hybrid BIA Scheme

Herein the authors propose a hybrid blind interference alignment (hybrid-BIA) scheme which aims to reduce the DoF loss that h-BIA suffers from and at the same time the proposed scheme tries to minimize the supersymbol length (symbol extensions required). Hybrid-BIA is inspired by the user grouping approach used by

top-BIA [79], and the fact that partially-connected networks can be beneficial in terms of DoF and sumrate [30].

The proposed hybrid-BIA scheme has a two-step structure. In step-1, the information on the positions of users and BSs in the network are utilized for grouping the users that can be simultaneously served. This can be done by applying the top-BIA scheme which has been described in detail in subsection 3.6.3. Grouping the users throughout the top-BIA scheme helps to reduce the number of actual users from K_T to $|\Lambda|$ and converts the given initial network to a fully-connected network. In step-2, the hybrid-BIA will apply h-BIA (introduced in subsection 3.6.4) on the set of user-groups $\lambda_i, \forall i \in \Lambda$ (rather than the individual users) to align the inter and intra user-groups interferences. This approach would reduce the supersymbol length and the DoF loss that h-BIA alone would encounter.

The system model considered is a homogeneous cellular network comprised of F small-cells each with one BS. We assume each cell has $[K_f, M]$ configuration where, $f \in [1 : F]$ and $M \geq 4$[1] and the total of $K_T = \sum_{f=1}^{F} K_f$ users in the network.

Hybrid-BIA can be applied under different scenarios such as: 1) on a dense clustered cellular network where the user association of each BS is known, 2) in partially-connected network where the transmission of each BS dose not cause intercell interference on private users of the neighboring cells.

In scenario-1 where user and BS association is known, the proposed hybrid-BIA scheme applies the top-BIA to examine possible user-groups by changing the SINR

---

[1]Minimum M for h-BIA should be 4 to guarantee that 2 user-groups each with 2 users and each user with 2 preset modes is obtained.

threshold value (THR) at each iteration. The iterations will continue till the top-BIA achieves a higher sum-rate than sync-BIA and ext-BIA. In the second step, h-BIA is applied to the user-groups formed by top-BIA. For scenario-2 since shared and private users have been predefined by the network, without any iteration the proposed hybrid-BIA scheme applies top-BIA to determine the user-groups and then it employs h-BIA on the user-groups formed. Algorithms 1 and 2 summarize the pseudocodes for the two scenarios described above. To clarify the strong points of the proposed

---

Algorithm 1 Pseudocode for the proposed hybrid-BIA for a dense clustered network

1: At iteration-1 ($n = 1$) initialize the threshold THR by the minimum pairwise SINR value,
2: Form the grouping indicator matrix B using THR value,
3: Find the set of user-groups $\Lambda = \{\lambda_1, \lambda_2, \ldots, \lambda_{|\Lambda|}\}$ by examining the proper submatrices of B,
4: Calculate $R_n^{\text{top-BIA}}$ using (3.45) as the throughput of a cluster at n^{th} iteration,
5:   **if** $R_n^{\text{top-BIA}} \geq max\{R^{\text{sync-BIA}}, R^{\text{ext-BIA}}\}$ **and** $R_n^{\text{top-BIA}} < R_{n-1}^{\text{top-BIA}}$ **then**
6:     **stop.**
7:   **else**
8:     Set threshold THR to the next minimum pairwise SINR value,
9:     **return** to step 2:,
10:   **end if**
11: Apply h-BIA on the set of user-groups (Λ),
12: Calculate $R^{\text{hybrid-BIA}}$ using (4.2) as the throughput of a cluster.

Algorithm 2 Pseudocode for the proposed hybrid-BIA under partially-connected networks

1: Form the grouping indicator matrix B,
2: Find the set of user-groups $\Lambda = \{\lambda_1, \lambda_2, \ldots, \lambda_{|\Lambda|}\}$ by examining the proper submatrices of B,
3: Apply h-BIA on the set of user-groups (Λ),
4: Calculate $R^{\text{hybrid-BIA}}$,
5: Calculate sum-DoF of hybrid-BIA at a cluster.

---

hybrid-BIA scheme, we will first examine the performances of sync-BIA, ext-BIA, top-BIA and h-BIA schemes on a simple toy example (refer to Figure 4.1) and afterwards calculate the achievable DoF, supersymbol length, and the sum-rate for the proposed scheme. Finally, we will compare the achieved sum-DoF and supersymbol length of hybrid-BIA with the results obtained using the BIA schemes introduced in sections 3.6.1–3.6.4.

As the toy-model consider a partially-connected network as depicted in Figure 4.1, with two cells ($F = 2$) each with $[K_f = 3, M = 4]$ configuration $\forall f \in \{1, 2\}$ and total
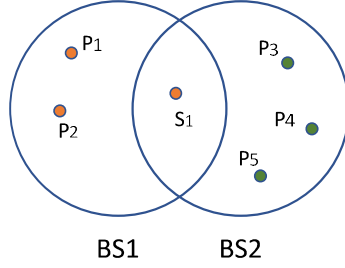
Figure 4.1: Toy example for a partially-connected network where each cell has $[K = 3, M = 4]$ configuration.

of $K_T = 6$ users. Assume that users $\{P_1, P_2, S_1\}$ belong to cell-1 and are served by BS1 and $\{P_3, P_4, P_5\}$ belong to cell-2 and are served by BS2. In each cell, the users that are located close to the BS receive a strong signal hence the interference from the other BS can be considered as noise. These users are referred to as private users and denoted as P_i. The remaining users which are able to receive transmission from all BSs in their proximity are referred to as shared users and are denoted as S_i.

Sections that follow calculate the achievable DoF and supersymbol length for the five different BIA scheme under the above toy example as:

A When sync-BIA is used, the precoder matrix of each cell which has $[K, M] = [3, 4]$ configuration will be constructed independently as in s-BIA. Hence, each user in each cell will have $Q_i = 9$ alignment blocks, $\forall i \in \{1, 2, 3\}$, and is expected to achieve $M_i Q_i = 36$ interference-free signals over a supersymbol length of 54 time slots. However, due to the intercell interference shared user S_1 will have zero DoF and only the private users can contribute to the sum-DoF. Since DoF for a single private user is $36/54 = 0.6$ then the sum-DoF achieved with five private users would be $5(36/54) = 3.\overline{3}$.

B Under ext-BIA scheme, the whole network can be considered as a single cell with $[K, M] = [6, 4]$ configuration. For each user there would be $Q_i = 243$ alignment

blocks, $\forall i \in [1 : K_T]$, and in total there would be $M_iQ_i = 972$ interference-free symbols over a supersymbol length of 2187 time slots. Accordingly, the sum-DoF would be $\left(\sum_{i=1}^6 M_iQ_i\right)/2187 = 2.\overline{6}$.

C When top-BIA scheme is deployed, K_T users are partitioned into $|\Lambda| = 4$ user-groups as $\lambda_1 = \{P_1, P_3\}$, $\lambda_2 = \{P_2, P_4\}$, $\lambda_3 = \{P_5\}$ and $\lambda_4 = \{S_1\}$ as depicted in Figure 4.2(a). Following the user grouping, the interference between $|\Lambda| = 4$ user-groups are handled by constructing a precoder matrix using s-BIA for a single cell with $[K, M] = [|\Lambda|, 4]$ configuration. By this scheme, each group of users has $Q_{\lambda_i} = 27$ alignment blocks, $\forall \lambda_i \in [1 : |\Lambda|]$ which is same as the number of alignment blocks of each individual user ($Q_k = 27, \forall k \in [1 : K_T]$) in the network. The length of the precoder constructed by top-BIA requires 189 time slots which would result in $\left(\sum_{i=1}^{K_T} M_iQ_i\right)/189 = 3.43$ sum-DoF.

D Hierarchical blind interference alignment (h-BIA) will partition the K_T users into $K_G = 2$ groups where each group contains $K_E = 3$ users with $M_{[k,i]} = 4$ preset modes, $\forall k \in [1 : K_E]$ and $i \in [1 : K_G]$. Since preset modes of users from each group are divisible by 2, preset mode group values are set to $M_{G_1} = M_{G_2} = 2$. Through this partitioning both groups would have similar group mode sets: $\mathcal{N}_i = \{4/2, 4/2, 4/2\} = \{2, 2, 2\}, \forall i \in \{1, 2\}$. Hence, pattern n_1 based on the union group mode set $\mathcal{N}_i$ will be constructed according to s-BIA with $\langle 2, 2, 2 \rangle$ ($[K, M] = [3, 2]$) configuration within 4 time slots. Similarly pattern n_2 is designed according to the preset mode group values ($M_{G_1} = M_{G_2} = 2$) using s-BIA with $\langle 2, 2 \rangle$ ($[K, M] = [2, 2]$) configuration within 3 time slots. Referring to (3.54) and (3.55) the sum-DoF for h-BIA would be $\langle 2, 2, 2 \rangle \langle 2, 2 \rangle = (6/4)(4/3) = 2$ within $(4) \times (3) = 12$ time slots.

E The proposed hybrid-BIA scheme suggests to apply the h-BIA on user-groups generated by top-BIA algorithm. For the toy example given in Figure 4.1 the top-BIA partitions $K_T = 6$ users into $|\Lambda| = 4$ user-groups. The proposed scheme considers this set of user-groups, $\Lambda = \{\lambda_1, \lambda_2, \lambda_3, \lambda_4\}$, as users of a fully-connected network as depicted in Figure 4.2(a), where each group has $M_{\lambda_i} = 4$ preset modes. h-BIA will then partition the $|\Lambda| = 4$ users into $K_G = 2$ groups where each group contains $K_E = 2$ users with $M_{[k,i]} = 4$, $k \in [1 : K_E]$ and $i \in [1 : K_G]$, preset modes. Since preset modes of users from each group are divisible by 2, preset mode group values are set to $M_{G_1} = M_{G_2} = 2$. By this partitioning both groups would have similar group sets: $\mathcal{N}_i = \{4/2, 4/2\} = \{2,2\}$, $\forall i \in \{1,2\}$. Hence pattern n_1 based on the union of group mode sets $\mathcal{N}_i$ will be constructed according to s-BIA with $\langle 2,2 \rangle$ ($[K,M] = [2,2]$) configuration within 3 time slots. Similarly, pattern n_2 is designed according to the preset mode group values ($M_{G_1} = M_{G_2} = 2$) again using s-BIA with $\langle 2,2 \rangle$ ($[K,M] = [2,2]$) configuration within 3 time slots. Then, according to (3.56) each group of users λ_i $\forall i \in [1 : |\Lambda|]$ and consequently each individual user $k \in [1 : K_T]$ achieves respectively $d_{\lambda_i} = 4$ and $d_k = 4$ interference-free signals. Since the constructed precoder matrix by this scheme based on equation (3.55) requires 9 time slots (refer to Figure 4.2(b)), the hybrid-BIA achieves $\left(\sum_{i=1}^{K_T} M_i Q_i\right)/9 = \left(\sum_{i=1}^{K_T} d_i\right)/9 = (24/9) = 2.6\overline{6}$ sum-DoF.

Table 4.1 summarizes the achievable sum-DoFs and supersymbol lengths of all mentioned BIA algorithms for the toy-example of Figure 4.1. Figures 4.3(a) and 4.3(b) depict the sum-DoF and supersymbol length curves for the aforementioned BIA techniques in a two-cell scenario as the number of users in each cell is varied from 3 to 14. Note that, when $|\Lambda| = K$ sum-DoF achieved is optimal for hybrid-BIA

and at $|\Lambda| = FK$ performance of hybrid-BIA will converge to that of h-BIA. Even though top-BIA with $|\Lambda| = K$ appears to have the best sum-DoF, the supersymbol length required by top-BIA is much larger than the one for hybrid-BIA.
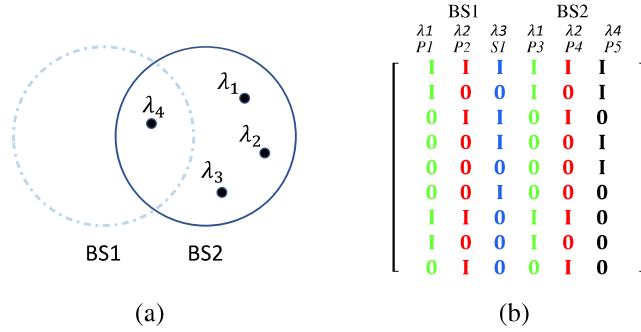

Figure 4.2: Fully connected network with 4 user-groups. (a) 2-cell network with $K_T = 6$ users partitioned into $|\Lambda| = 4$ user-groups. (b) Proposed hybrid-BIA precoder for BSs.

Table 4.1 summarizes the achievable sum-DoFs and supersymbol lengths of all mentioned BIA algorithms for the toy-example of Figure 4.1.

Table 4.1: Sum-DoF and supersymbol length comparison

	sync-BIA	ext-BIA	top-BIA	h-BIA	hybrid-BIA
Supersymbol length	54	2187	189	12	9
Sum-DoF	3.33	2.66	3.42	2	2.66

Figures 4.3(a) and 4.3(b) depict the sum-DoF and supersymbol length curves for the aforementioned BIA techniques in a two-cell scenario as the number of users in each cell is varied from 3 to 14. Note that, when $|\Lambda| = K$ sum-DoF achieved is optimal for hybrid-BIA and at $|\Lambda| = FK$ performance of hybrid-BIA will converge to that of h-BIA. Even though top-BIA with $|\Lambda| = K$ appears to have the best sum-DoF, the supersymbol length required by top-BIA is much larger than the one for hybrid-BIA.

In what follows, we will first formulate the throughput of the proposed hybrid-BIA
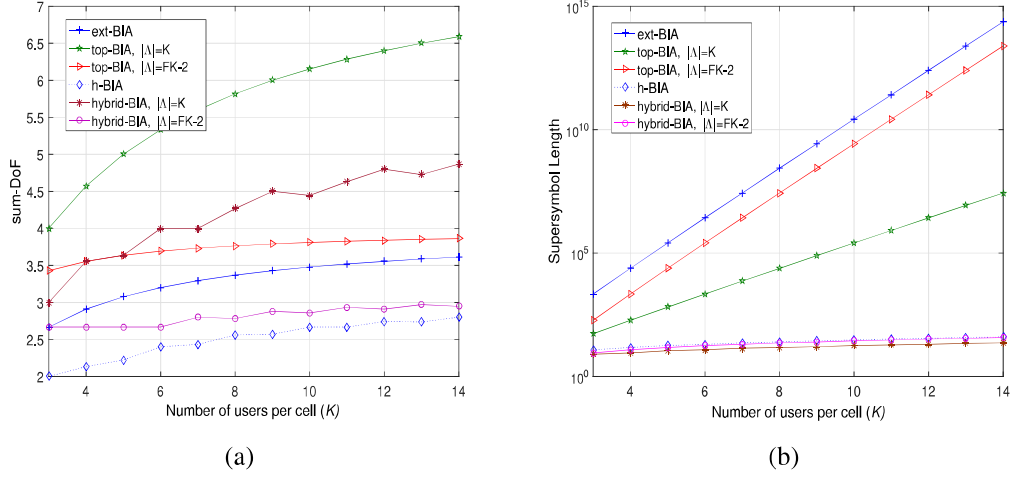
Figure 4.3: sum-DoF and Supersymbol Length Comparison: (a) sum-DoF vs number of users per cell, (b) Supersymbol length vs number of users per cell.

scheme. Later in Section 4.4 we will evaluate the throughput of hybrid-BIA and compare it against the other BIA schemes introduced et al. Assuming uniform power allocation, the achievable sum-rate of user-k in user-group λ_l ($l \in [1 : K_E]$) and in h-BIA group i ($i \in [1 : K_G]$), can be written as:

$$R_{[k,i]}^{\text{hybrid-BIA}} = \frac{1}{(M_E + K_E - 1)(M_G + K_G - 1)} \times \mathbb{E}\left[\log\left(\det\left(\mathbf{I} + \tilde{P}\tilde{\mathbf{H}}_{[k,i]}^{f_{[k,i]}} \tilde{\mathbf{H}}_{[k,i]}^{f_{[k,i]}}{}^{+} \mathbf{R}_z^{-1}\right)\right)\right] \tag{4.2}$$

where, $\tilde{P} = \frac{(M_E + K_E - 1)(M_G + K_G - 1)P}{|\Lambda|M^2}$ and $f_{[k,i]}$ is the transmitter which serves user k in group i and $\tilde{\mathbf{H}}_{[k,i]}^{f_{[k,i]}}$ is channel between $[k,i]$ and transmitter $f_{[k,i]}$.

$$\tilde{\mathbf{H}}_{[k,i]}^{f_{[k,i]}} = \sqrt{g(d_{[k,i]}^{f_{[k,i]}})} \left[\mathbf{h}_{[k,i]}^{f_{[k,i]}}{}^{T}(1), \dots \mathbf{h}_{[k,i]}^{f_{[k,i]}}{}^{T}(M-1), \mathbf{h}_{[k,i]}^{f_{[k,i]}}{}^{T}(M)\right]^{T} \tag{4.3}$$

and $\mathbf{R}_{\tilde{z}}$ represents the noise variance matrix and can be denoted as:

$$\mathbf{R}_{\tilde{z}} = \begin{bmatrix} \mathbf{R}_{\tilde{z}_1} & & & \mathbf{0} \\ & \ddots & & \\ & & \mathbf{R}_{\tilde{z}_1} & \\ \mathbf{0} & & & \mathbf{R}_{\tilde{z}_2} \end{bmatrix} \tag{4.4}$$

87

where,

$$\mathbf{R}_{\tilde{z}_1} = \begin{bmatrix} |\Lambda| \mathbf{I}_{M_E - 1} & \mathbf{0}_{(M_E - 1) \times 1} \\ \mathbf{0}_{1 \times (M_E - 1)} & K_G \end{bmatrix} \qquad (4.5)$$

and

$$\mathbf{R}_{\tilde{z}_2} = \begin{bmatrix} K_E \mathbf{I}_{M_E - 1} & \mathbf{0}_{(M_E - 1) \times 1} \\ \mathbf{0}_{1 \times (M_E - 1)} & 1 \end{bmatrix}. \qquad (4.6)$$

From top-BIA, the range of values for $|\Lambda|$ will vary from K to FK. Then, for hybrid-BIA with $|\Lambda| = K$ the sum-rate would be maximized and the values for the diagonal elements of $\mathbf{R}_{\tilde{z}_1}$ would be minimized. Hence, when $|\Lambda| = K$ the system will encounter the least noise increase due to a small number of subtractions.

In [99], a cognitive-BIA (cog-BIA) scheme for heterogeneous networks has also been proffered for eliminating the intracell interference of each tier plus the inter-tier interference. Since hybrid-BIA does not require any data sharing between BSs, authors believe that it would be possible to apply the hybrid-BIA scheme in heterogeneous network. Independent of their tiers users can be grouped together using top-BIA and be served by their respective BSs by applying h-BIA. hybrid-BIA can also be applied to partially connected IC networks when condition in (3.16) holds.

4.4 Throughput Evaluation

In this section, first the sum-rate performance of h-BIA will be evaluated and compared against that of the s-BIA assuming a single cell scenario. This would be done to demonstrate that, the sum-rate and sum-DoF of h-BIA would be less than that of the s-BIA even in a single cell scenario over a wide range of SNR values. Later on, the paper will compute the cumulative distribution functions (CDF) for the throughput of the proposed hybrid-BIA scheme and the other state of the art schemes introduced in subsections 3.3–3.6.4 assuming a clustered small-cell network.

Eventually the performance of the proposed hybrid-BIA scheme would be examined under different number of user-groups (formed by top-BIA) assuming a cellular network with the same structure as in Figure 4.1. Finally, in section 4.5 the achievable sum-DoF and supersymbol length of the proposed hybrid-BIA and h-BIA schemes would be compared under a symmetric cellular network where the number private users per cell is the same.

Figure 4.4 depicts the sum-rate comparison between h-BIA and s-BIA under a Gaussian channel with $C\mathcal{N}(0,1)$, assuming a single cell scenario with $[K,M] = [4,4]$ configuration where h-BIA parameters are taken as $K_G = 2, K_E = 2, M_G = 2, M_E = 2$. For this scenario the sum-rate comparison has been carried out assuming two different power allocation strategies: namely uniform and constant power allocation [81], [78]. [78] has pointed out that constant power allocation could improve the sum-rate of BIA schemes. Figure 4.4 shows that for both uniform and constant power allocation the sum-rate for h-BIA is uniformly lower than that of s-BIA. Moreover, in high SNR regime the achievable DoF for h-BIA is also lower than that of s-BIA. These results agree with what has been stated in [45] and is further confirmed by the less steep slope for the h-BIA curves.

Figure 4.5 shown the CDF versus throughput graphs of all five aforementioned BIA schemes evaluated at the center cluster of a clustered cellular network where each cluster has F small-cells and each small-cell has $[K_f, M]$ configuration with $f \in [1:F]$. The total number of users in a cluster were taken as $K_T = \sum_{f=1}^{F} K_f$.

The system parameters assumed for the throughput comparison of the BIA schemes in Figure 4.5 have been summarized in Table 4.2. The total throughput in the center
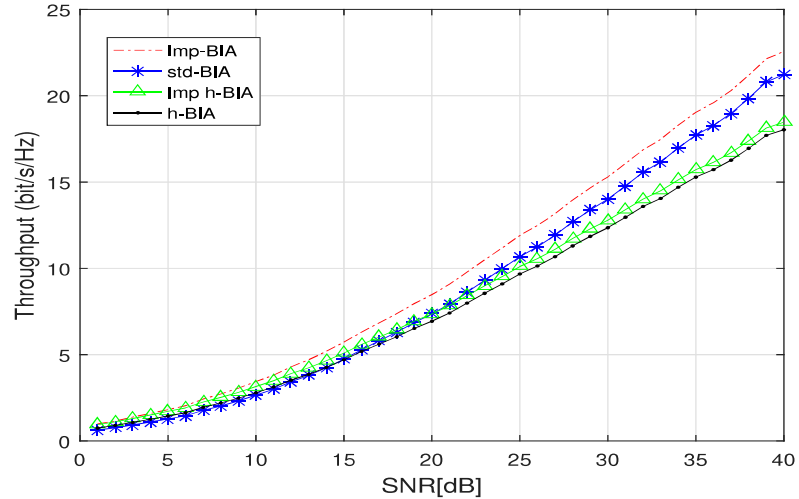
Figure 4.4: Throughput comparison between s-BIA and h-BIA under uniform and constant power allocation assuming a single cell with $[K,M] = [4,4]$ configuration and h-BIA parameters $K_G = K_E = M_G = M_E = 2$.
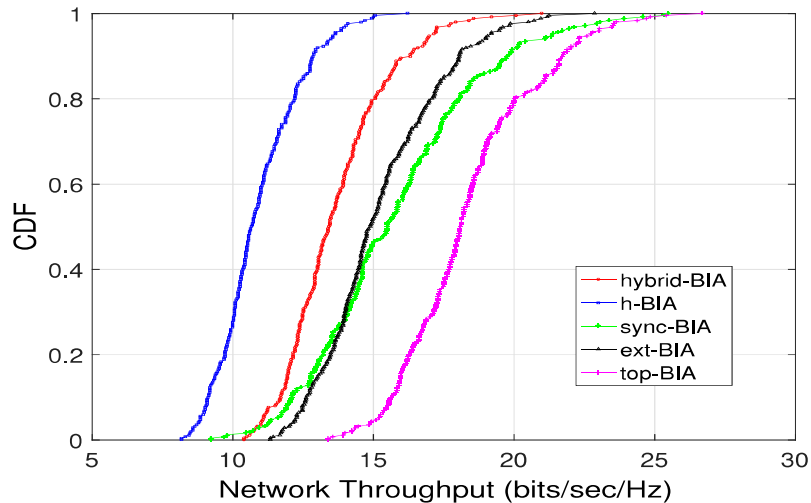
Figure 4.5: Cumulative distribution function (CDF) for the throughput of BIA schemes compared.

cluster has been evaluated via Monte Carlo simulations. During simulations, 250 realizations of the user distribution at the center cluster and 500 channel realizations for location of each user have been generated in order to calculate the CDF. Before comparing sum-rates for h-BIA and hybrid-BIA with other methods introduced in the paper, the noise covariance matrices (3.68) and (4.4) has been re-expressed as in (3.44) and (3.46). Also, the normalization terms have been set equal to square root of

Table 4.2: Simulation parameters for homogeneous cellular networks.

Number of clusters	9
Number of cells per cluster	2
Number of users per cell	4^2
Inter-cluster distance	250m
Effective coverage of each cell	30m
Number of transmit antennas at each BS	4
Number of switching modes at each user	4
Transmit power of each BS	20 dBm
Noise power	-104 dBm
Pathloss model	$15.3 + 37.6 \cdot \log_{10}(d)$
Small scale fading	Rayleigh with $\mathcal{CN}(0,1)$

the diagonal elements of (3.44) and (3.46) respectively.

As depicted by Figure 4.5 the sum-rate of the hybrid-BIA is higher than that of h-BIA and the improvement is significant for user distributions leading to a network throughput between 10-15 bits/sec/Hz. The difference in network throughput is due to the fact that h-BIA would require more time slots than the proposed hybrid-BIA scheme (this is so since hybrid-BIA only considers user-groups formed by top-BIA). Even though the curves for sync-BIA, ext-BIA and top-BIA appears to have a higher network throughput then h-BIA and hybrid-BIA a quick look at Table 4.1 points out these three methods require long supersymbol length and in most practical scenarios where coherence-time is limited they can not be implemented.

For the simulation of hybrid-BIA the user-groups can be formed by applying the top-BIA which will reduce the number of actual users from K_T to $|\Lambda|$. As mentioned before the number of user-groups generated by the top-BIA depends on the distribution of the users in the network and would vary in the range $K \leq |\Lambda| \leq FK$. Once the user-groups are formed, the hybrid-BIA scheme will apply the h-BIA on the set of user-groups $\lambda_i, \forall i \in |\Lambda|$. We note that for h-BIA to be applicable to groups formed by top-BIA, minimum preset mode of each user-group and the number of user-groups should be

$M_{\lambda_i} \geq 4$ & $|\Lambda| \geq 4$ (minimum group size and preset modes for applying h-BIA).

One final simulation was carried out to examine the performance of the proposed hybrid-BIA scheme under different number of user-groups. The number of user-groups generated by the proposed hybrid-BIA depends on the number of shared users in each cluster. As more users enter the shared region(s) between cells, number of shared users are increased which would lead to an increase in the number of user-groups.

Figure 4.6 shows the achievable DoF versus supersymbol length of the hybrid-BIA on the given toy example of Figure 4.1 by assuming different number of user-groups. Starting with one shared user, the hybrid-BIA could be applied on $|\Lambda| = 4$ user-groups as depicted in Figure 4.2. When the number of shared users are 2 and 3 then the number of user-groups would be $|\Lambda| = 5$ and $|\Lambda| = 6$ respectively. Note that, smaller number of user-groups can achieve the theoretical maximum DoF at a fewer symbol extensions. Finally, we would like to point out that the graph for $|\Lambda| = 6$ (each user-group with one member) matches the DoF for h-BIA depicted in Table. 4.1. This shows that h-BIA is a subset of the proposed hybrid-BIA scheme.

Note that, the staircase like behavior in the DoF versus symbol length curves is due to the optimization introduced in equation (4.12) of the hierarchical BIA paper [45] for the two-layer dynamic supersymbol design (DSD) algorithm which has also described in Section 3.6.5.
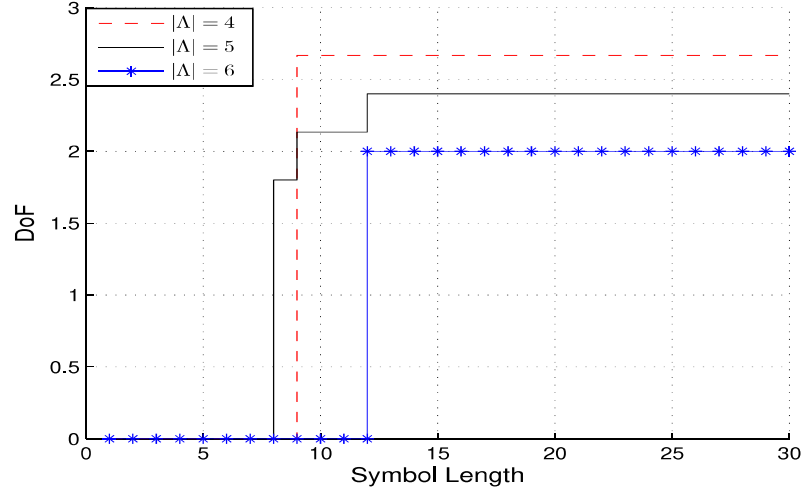
Figure 4.6: Effect of number of user-groups on performance of hybrid-BIA for the toy example in Figure 4.1.

4.5 DoF Gain and Supersymbol Length Ratio Evaluation

In this subsection the achievable DoF and supersymbol lengths for h-BIA and the proposed hybrid-BIA schemes would be compared under a symmetric cellular network with F small-cells. Each cell is assumed to have $[K, M]$ configuration and the network has total of $K_T = FK$ users. For h-BIA, it was assumed that number of user-groups was $K_G = \sqrt{K_T}$ and under perfect-grouping preset modes of groups and also of users in each group were respectively $M_{G_i} = \sqrt{M}$, $M_{E_k} = \sqrt{M}$ for $i \in [1 : K_G]$, $k \in [1 : K_E]$. For the proposed hybrid-BIA scheme, user-groups were determined via top-BIA and depending on the distribution of users in the network it could vary in the range

$$K \leq |\Lambda| \leq FK. \tag{4.7}$$

Afterwards, hybrid-BIA would apply h-BIA on the new user-groups where $K_G = \sqrt{|\Lambda|}$, $M_{G_i} = \sqrt{M}$ and $M_{E_\lambda} = \sqrt{M}$ for $i \in [1 : K_G]$, $\lambda \in [1 : K_E]$.

Note from (4.8)-(4.11) that, under complete grouping the hybrid-BIA can significantly reduce the supersymbol length and improve the sum-DoF. Equations (4.12) and (4.13)

93

represent the ratio of supersymbol length between h-BIA and hybrid-BIA and sum-DoF gain of hybrid-BIA over h-BIA.

$$\text{SL}_\text{h-BIA} = \left\lceil \left[\left(\sqrt{M} - 1 \right)^{\sqrt{K_T}-1} \left(\sqrt{M} - 1 + \sqrt{K_T} \right) \right]^2 \right\rceil \tag{4.8}$$

$$\text{SL}_\text{hybrid-BIA} = \left\lceil \left[\left(\sqrt{M} - 1 \right)^{\sqrt{|\Lambda|}-1} \left(\sqrt{M} - 1 + \sqrt{|\Lambda|} \right) \right]^2 \right\rceil \tag{4.9}$$

$$\text{sum-DoF}_\text{h-BIA} = K_T M \Big/ \left(\sqrt{K_T} + \sqrt{M} - 1 \right)^2, \, Q_{k_E} = Q_{k_G} = \left(\sqrt{M} - 1 \right)^{\sqrt{K_T}-1}, \tag{4.10}$$

$$\text{sum-DoF}_\text{hybrid-BIA} = K_T M \Big/ \left(\sqrt{|\Lambda|} + \sqrt{M} - 1 \right)^2, \, Q_{k_E} = Q_{k_G} = \left(\sqrt{M} - 1 \right)^{\sqrt{|\Lambda|}-1}, \tag{4.11}$$

$$1 \leq \underbrace{\frac{\text{SL}_\text{h-BIA}}{\text{SL}_\text{hybrid-BIA}}}_{\text{Supersymbol length ratio}} \leq \left(\sqrt{M} - 1 \right)^{2\sqrt{F}\left(\sqrt{K}-1 \right)} \left(\frac{\sqrt{F}\sqrt{K} + \left(\sqrt{M} - 1 \right)}{\sqrt{F} + \left(\sqrt{M} - 1 \right)} \right)^2. \tag{4.12}$$

$$1 \leq \frac{\text{sum-DoF}_\text{hybrid BIA}}{\text{sum-DoF}_\text{h-BIA}} \leq 1 + \underbrace{\frac{(K-1)F + \sqrt{K}(\sqrt{M} - 1)}{\left(\sqrt{M} + \sqrt{F} - 1 \right)^2}}_{\text{sum-DoF gain}}. \tag{4.13}$$

The lower and upper bounds for the ratio of the supersymbol lengths of h-BIA to hybrid-BIA are depicted in (4.12). The lower bound would be achieved when $|\Lambda| = K_T$. Similarly, when $|\Lambda| = K$ the upper bound will be attained. As can be seen from (4.13), the hybrid-BIA will achieve a higher DoF as long as top-BIA can group the users (that is $|\Lambda| < K_T$). For $|\Lambda| = K_T$ the hybrid-BIA performance will be identical with that of h-BIA. In essence this points out that h-BIA is a special case of hybrid-BIA.

To demonstrate the potential of the proposed hybrid-BIA scheme three more simulations were carried out. In the first simulation a two-cell scenario was assumed and the effect of user-groups on the supersymbol length ratio (between h-BIA and hybrid-BIA) and the DoF gain of hybrid-BIA over h-BIA was studied assuming $K = 4, M = 9$, and $F = 2$. Figure 4.7(a) clearly shows that the DoF gain will be

94

higher for small number of user-groups (i.e. $|\Lambda| = 4$), and the gain reduces down to unity as $|\Lambda|$ approaches its upper bound FK. The same observation is also true for the supersymbol length ratio between h-BIA and hybrid-BIA. In the second simulation, number of transmit antennas (preset mode of each user) was varied from 4 to 80 when both $|\Lambda|$ and K were set as 4. Figure 4.7(b) shows that the highest DoF gain would be achieved when $M = 4$ and as the number of transmit antennas is increased the DoF gain gradually will reduce.

(a)   (b)
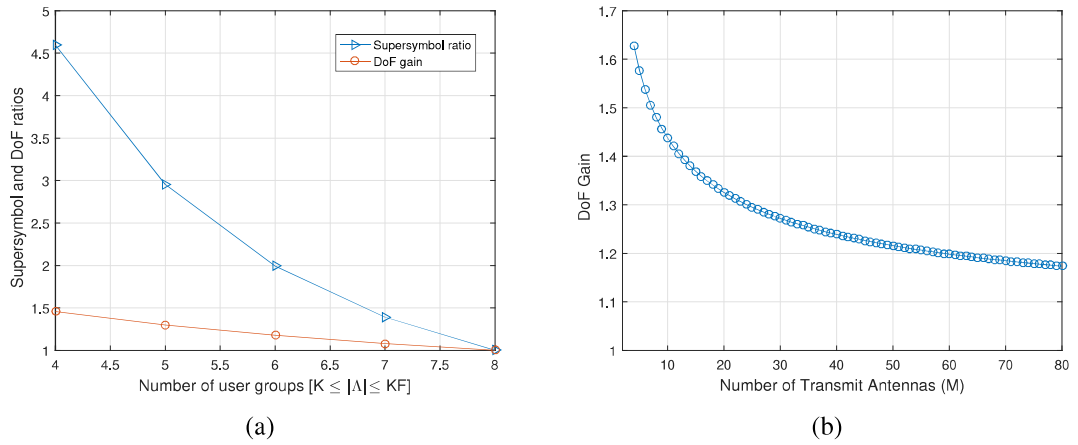
Figure 4.7: Supersymbol length and achievable DoF comparison between h-BIA and hybrid-BIA under two-cell ($F = 2$) scenario: (a) Effect of number of user-groups on DoF gain and supersymbol length ratio $4 \leq |\Lambda| \leq 8$, $M = 9$, $K = 4$, (b) Effect of number of transmit antennas (M) on the DoF gain $|\Lambda| = 4$, $K = 4$, $F = 2$.

Finally, in a third simulation, DoF gain and supersymbol length ratio between h-BIA and hybrid-BIA was studied for different number of small-cells. This last simulation also considered the effect of $|\Lambda|$ on the DoF gain as the network size is varied. Figures 4.8(a) and 4.8(b) depict the DoF gain of hybrid-BIA over h-BIA and the supersymbol length ratio between h-BIA and hybrid-BIA respectively. Clearly, both the DoF-gain and the supersymbol length ratio would scale up with the number of small-cells. Note that, for a five fold increase on the total number of users in the network (initial $K_T = FK = 2 \cdot 4$ and final $K_T = FK = 10 \cdot 4$) approximately a three fold increase in the DoF

gain would be obtained.

(a)   (b)
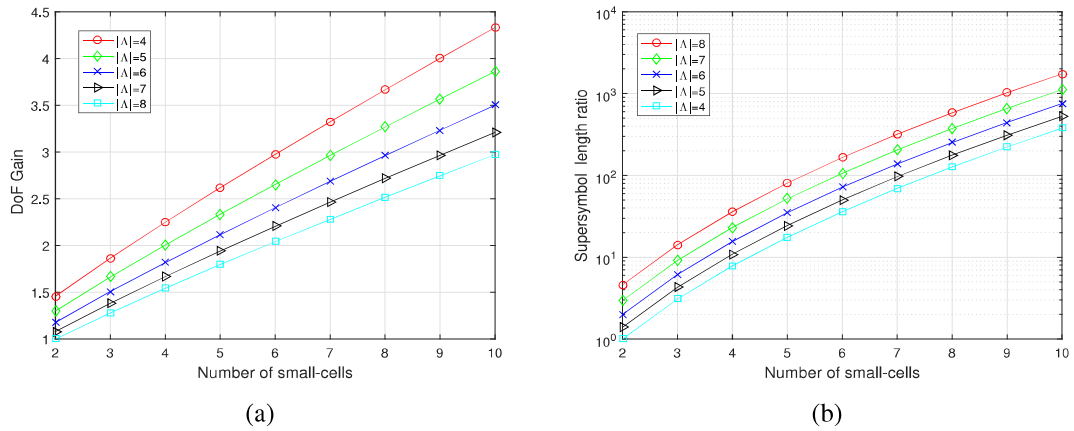
Figure 4.8: Effect of number of small-cells (F) on DoF-gain and supersymbol length ratio for $K = 4$,$M = 9$ and $4 \leq |\Lambda| \leq 8$: (a) DoF gain of hybrid-BIA over h-BIA, (b) supersymbol length ratio between h-BIA and hybrid-BIA.

In the second simulation, number of transmit antennas (preset mode of each user) was varied from 4 to 80 when both $|\Lambda|$ and K were set as 4. Figure 4.7(b) shows that the highest DoF gain would be achieved when $M = 4$ and as the number of transmit antennas is increased the DoF gain gradually will reduce.

Chapter 5

INTERFERENCE MANAGEMENT IN TWO-TIER HETEROGENEOUS NETWORKS USING BLIND INTERFERENCE ALIGNMENT

5.1 Introduction

The demand for better coverage and higher data rates has led to the deployment of femtocells under macrocell coverage in 3GPP LTE-Advanced systems [31]. This change was inevitable since the existing wireless communication systems were already pushed to the limits and were not in a position to meet the ever growing demands of indoor users on multimedia services. Femtocells which are also referred to as the home evolved NodeBs (HeNBs) are small coverage (10-50m) wireless data access points (APs) with transmit powers in the range 1-100 mW. Femtocells usually operate in the license spectrum of a service provider and are connected to the core network via an IP based backhaul.

Two-tier heterogenous networks can in principle provide cost-effective data delivery but there are interference issues that need to be addressed. Two types of interference exist at femtocell users (FUs), the interference from neighboring femtocells and the interference from the macrocell base station (MBS). Moreover, when a macrocell user (MU) is close to the edge of a femtocell, MU can receive interference from the nearby femtocell base station (FBS). In general, MBS transmit power is much higher than the transmit power of the FBS, thus in this chapter it is assumed that MU does not
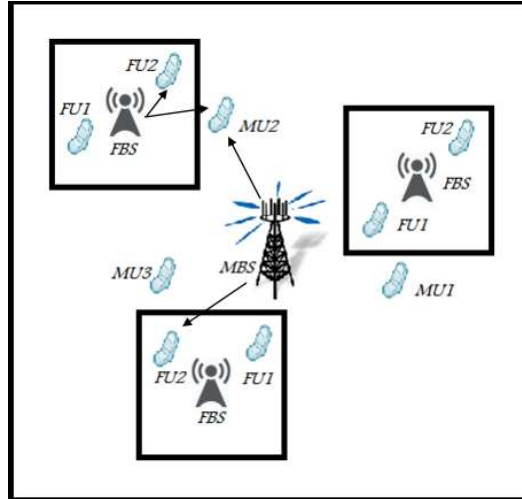
Figure 5.1: System model for a heterogeneous network with one MBS and multiple FBSs.

experience interference from the FBS. Under this mild assumption, a novel scheme is proposed that aligns MBS interference on the predetermined interference spaces of FUs. Basically each MU is paired with a femtocell, and the pairs are orthogonal among each other. While the orthogonalization eliminates the interference between femtocells, the alignment technique eliminates the MBS interference on the paired FUs. In each femtocell, standard blind interference alignment method (s-BIA) which does not require channel state information at the transmitter (CSIT) [24] is used. The predetermined interference dimensions of the FUs set by s-BIA are used by the MBS to align its interference on the paired FUs.

The feasibility of BIA in heterogeneous networks was first demonstrated in [85] which was later extended to a general scenario in [23]. In this chapter, the downlink of a two-tier heterogenous network with multiple femtocells under macrocell coverage with multiple MUs is studied. Particularly, a novel scheme is proposed under which each FBS adapts s-BIA with staggered antenna switching technique [24] and the interference from MBS is aligned on the predetermined interference

98

dimensions of FUs set by s-BIA.

The rest of the chapter is organized as follows: The system and the path loss models are detailed under Section 5.3. Sections 5.4 and 5.5 respectively state the proposed and baseline schemes. The simulation results are presented in Section 5.6 and results obtained for the proposed method are compared with the baseline scheme.

5.2 Blind Interference Alignment

The BIA scheme relies on a mild assumption on the coherence interval of the system while the transmitters have no CSI whatsoever including quantized or delayed. As presented in [24], the key for achieving interference alignment in a K-user ($M \times 1$) MISO BC is that over the duration of M symbols, the channel of desired user changes in each symbol duration while the channels of all undesired users remain fixed. This condition secures M streams of the desired user be distinguishable while they align into one dimension at all other users providing a total of $\frac{MK}{M+K-1}$ degrees of freedom (DoF). In this method each receiver is equipped with reconfigurable antennas. By the use of reconfigurable antennas, each receiver artificially generates a channel pattern to provide the aforementioned key condition for each user over a series of channel uses called alignment blocks. In Figure 5.2, the supersymbol structure and the beamforming matrices for achieving BIA in 2-user, 2×1 MISO BC are shown [24].
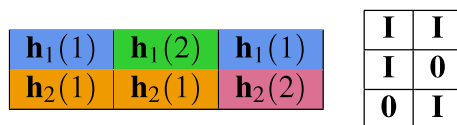
Figure 5.2: Supersymbol structure and beamforming matrices used in BIA for 2-user, 2×1 MISO BC.

Here $\mathbf{I}$ and $\mathbf{0}$ respectively represent the $M \times M$ identity and zero matrices. $\mathbf{h}_k(m)$ is a 1×2 channel vector corresponding to the mth mode of the kth user. The zero-forcing

receive filters for the two users are given as

$$\mathbf{U}_1 = \begin{bmatrix} \frac{1}{\sqrt{2}} & 0 \\ 0 & 1 \\ -\frac{1}{\sqrt{2}} & 0 \end{bmatrix} \text{ and } \mathbf{U}_2 = \begin{bmatrix} \frac{1}{\sqrt{2}} & 0 \\ -\frac{1}{\sqrt{2}} & 0 \\ 0 & 1 \end{bmatrix}. \tag{5.1}$$

The sum-rate for a 2-user, 2×1 MISO BC system with equal power allocation among streams is given as [24]

$$R = \sum_{k=1}^{2} \frac{1}{3} \; \mathbb{E}\Big\{ \log \; |\mathbf{I} + \frac{3P}{8}\mathbf{H}_k\mathbf{H}_k^{\dagger}| \Big\}, \tag{5.2}$$

where $\mathbf{H}_k = \begin{bmatrix} \frac{1}{\sqrt{2}}\mathbf{h}_k(1) \\ \mathbf{h}_k(2) \end{bmatrix}$. $\mathbb{E}\{\cdot\}$, $|\cdot|$, and † represent the expected value, determinant, and Hermitian operators, respectively.

5.3 System and Path Loss Models

This section outlines the system model and states the path loss models assumed for managing interference while using the proposed BIA scheme under a two-tier heterogeneous network.

5.3.1 System Model

As mentioned earlier, in the proposed scheme, the interference at FUs from other femtocells are eliminated by orthogonalization. Once again, each femtocell (FC-i, $i = 1,\dots,F$) is paired with a MU (MU-i, $i = 1,\dots,F$). The pairs operate orthogonal in time or frequency, i.e., [MU-i FC-i] $\perp$ [MU-j FC-j], $i \neq j$. Therefore at a FU, only the interference from the other FUs in the same femtocell and the paired MU interference are observed, thus the received signal in the tth channel use for the kth

user of femtocell f can be written as

$$y^{[kf]}(t) = \sqrt{\frac{P_f}{d_f}} \mathbf{h}^{[kf]}(m_k(t)) \mathbf{x}^{[kf]}(t)$$

$$+ \sum_{j=1, j \neq i}^{F} \sqrt{\frac{P_f}{d_f}} \mathbf{h}^{[kf]}(m_k(t)) \mathbf{x}^{[jf]}(t) + \sqrt{\frac{P_o}{d_o}} \mathbf{h}_o^{[kf]}(t) \mathbf{x}_o(t) + n_k,$$

$$\forall k \in \mathcal{K}, \forall f \in \mathcal{F}, \forall m_k(t) \in \mathcal{M}, \text{ and } \forall t \in \mathcal{T}$$

where $\mathcal{K} = \{1, \ldots, K\}$, $\mathcal{T} = \{1, \ldots, T\}$, $\mathcal{M} = \{1, \ldots, M\}$, $\mathcal{F} = \{1, \ldots, F\}$, $\mathbf{x}^{[kf]}(t) = \mathbf{V}^{[kf]}(t) \mathbf{s}^{[kf]}(t)$ and $\mathbf{x}_o(t) = \mathbf{V}_o(t) \mathbf{s}_o(t)$, K is the number of users in each femtocell, F is the number of femtocells, and T is the number of channel uses to achieve s-BIA. $\mathbf{h}^{[kf]}(m_k(t))$ and $\mathbf{h}_o^{[kf]}(t)$ is the $1 \times M$ and $1 \times N$ and channel matrix from the fth FBS and MBS to the kth user of the fth femtocell, respectively, $\mathbf{x}^{[kf]}(t)$, $\mathbf{V}^{[kf]}(t)$, and $\mathbf{s}^{[kf]}(t)$ are the $M \times 1$ transmitted signal, $M \times d_f$ beamforming matrix, and $d_f \times 1$ data streams by the fth FBS for the kth FU. Similarly, $\mathbf{x}_o(t)$, $\mathbf{V}_o(t)$, and $\mathbf{s}_o(t)$ are the $N \times 1$ transmitted signal, $N \times d_o$ beamforming matrix, and $d_o \times 1$ data streams by the MBS. Here $m_k(t)$ denotes the antenna switching pattern of kth FU, this parameter is pre-determined by design and known to everyone [24]. Once again it is assumed that MUs do not experience from the FBSs. P_f and P_o are the fth FBS and MBS transmit powers. n_k is the additive white Gaussian noise vector at the user k. As noted in [24] and Chapter3 the required coherence time in femtocell with $[K, M]$ configuration when the s-BIA is applied is $SL_{s-BIA} = (M-1)^K + K(M-1)^{K-1}$ symbols. In macrocell and also between macrocell and FUs, we assume the coherence time is a single symbol duration. In a dense urban environment, femtocells with long coherence intervals, macrocells and channels between MBS and FUs with short coherence intervals are reasonable assumptions.

5.3.2 Path Loss Models

Channels between the MBS and all users have been modeled using equation. (5.3) from the COST 231 channel model [102].

$$PL_{MC}(dB) = 46.3 + 33.9 \log_{10}(f_c) - 13.82 \log_{10}(h_t)$$

$$-a(h_r) + (44.9 - 6.55 \log_{10}(h_t)) \log_{10}(z) + C_M \tag{5.3}$$

where,

$$a(h_r) = 3.2(\log_{10}(11.75 h_r)) - 4.97.$$

In (5.3), f_c is the carrier frequency in MHz, z is the distance between MBS and users in km, and h_t is the MBS antenna height above ground level in meters. $a(h_r)$ denotes a correction factor for urban environment where h_r is the antenna height of the receiver in meters. The constant C_M is 3 dB for urban environment.

The channel between FBS and FUs has been modeled using the non-line-of-sight (NLoS) Indoor Hotspot (InH) channel model as follow:

$$PL_{FC}(dB) = 43.3 \log_{10}(z) + 25.5 + 20 \log_{10}(f_c/5). \tag{5.4}$$

Equation (5.4) shows the formula for computing the path loss between the FBS and FUs.

5.4 Proposed HetNet Scheme 1

This chapter proposes a novel scheme for a two-tier heterogeneous network where femtocells are located in a macrocell. We assume that each FBS is paired with a MU and all pairs are operating in different frequency bands or time slots. For simplicity, it is assumed that the number of MUs is equal to the number of femtocells, F. The proposed scheme can be extended to the general scenario via judicious selection algorithms [32]. It is assumed that the MBS causes interference on FUs, while FBSs

do not cause interference on MUs. Our scheme proposes to adopt the state of the art s-BIA within each femtocell. The scheme uses the knowledge of predetermined interference dimensions of the FUs set by s-BIA and CSIT at the MBS to align the MBS interference on the interference dimensions of FUs, hence MBS and FBS can coexist in the same frequency band or time slot.

The alignment condition of the MBS interference into the interference space of the kth FU is given as

$$\mathbf{h}_o^{[k,f]}(t)\mathbf{V}_o(t) \succ \delta^{[k,f]}(t), \ \forall k \in \mathcal{K} \text{ and } \forall t \in \mathcal{T} \tag{5.5}$$

where $\delta^{[k,f]}(t)$ is a $1 \times (K-1)(M-1)^{(K-1)}$ vector containing the interference dimensions for the kth user of femtocell f in the tth channel use, and $\mathbf{X} \succ \mathbf{Y}$ denotes that the column space of $\mathbf{X}$ spans that of $\mathbf{Y}$. Let $\Delta^{[k,f]}$ represent the interference dimensions of kth user over series of channel uses. Figure 5.3 depicts the interference dimension(s) for the 2-user 2×1 and 2-user 3×1 scenarios under s-BIA scheme based on their precoder matrices given in equations (3.2) and (3.11), respectively.
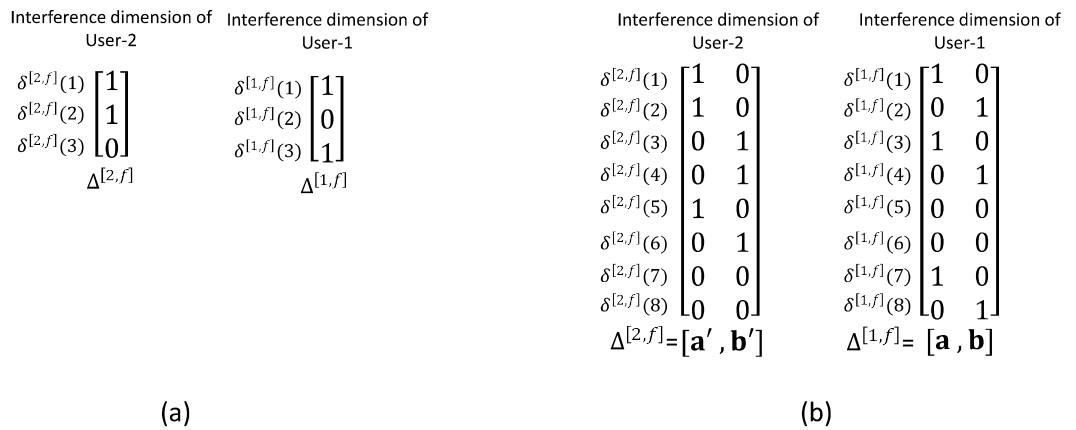

Figure 5.3: Interference dimension(s) of two examples under s-BIA MISO BC. a) demonstrates the interference dimension and dimensions of 2-user 2×1 and similarly b) for 2-user 3×1 example.

As depicted by Figure 5.3, for 2-user 2×1 $\Delta^{[1,f]} = \begin{bmatrix} 1 & 0 & 1 \end{bmatrix}^T$ and $\Delta^{[2,f]} = \begin{bmatrix} 1 & 1 & 0 \end{bmatrix}^T$. Similarly, for a 2-user 3×1 under s-BIA scheme, $\Delta^{[1,f]} = [\mathbf{ab}]$, where $\mathbf{a} = \begin{bmatrix} 1 & 0 & 1 & 0 & 0 & 0 & 1 & 0 \end{bmatrix}^T$ and $\mathbf{b} = \begin{bmatrix} 0 & 1 & 0 & 1 & 0 & 0 & 0 & 1 \end{bmatrix}^T$. For instance $\delta^{[1,f]}(1) = \begin{bmatrix} 1 & 0 \end{bmatrix}$, $\delta^{[1,f]}(3) = \begin{bmatrix} 1 & 0 \end{bmatrix}$, $\delta^{[1,f]}(5) = \begin{bmatrix} 0 & 0 \end{bmatrix}$ and $\delta^{[2,f]}(1) = \begin{bmatrix} 1 & 0 \end{bmatrix}, \delta^{[2,f]}(5) = \begin{bmatrix} 1 & 0 \end{bmatrix}$.

Under the s-BIA scheme, the receive filters $\mathbf{U}_k$ given in (5.1) eliminate interference at the kth user received along the dimension $\Delta^{[k,f]}$ from other FUs. This implies that by aligning the MBS interference at user k along the dimension $\Delta^{[k,f]}$, the MBS interference will be eliminated simultaneously with the interference from other FUs.

As the MBS interference is aligned on the interference dimensions of each FU, adapting our proposed scheme in case of 2-user, 2×1 MISO BC allows femtocell to achieve its optimum 4/3 DoF while macrocell achieves 1 DoF which leads to a total of 7/3 DoF for the whole heterogenous system. The DoF is fixed and does not scale with the number of femtocells.

5.5 Baseline Scheme

For the baseline scheme, we assume that all femtocells operate at the same time while the macrocell operates at a different time. This implies that FBSs and MBS are orthogonal. In each femtocell, the conventional s-BIA scheme is applied. The location of the MUs are uniformly selected in the coverage area of the MBS. The relative distance of each MU to the MBS leads to different channel gains and thus different SNR levels at each MU. To maximize the network sum-rate, zero-forcing precoder with the water filling power allocation strategy [17] is adopted at the MBS. As stated in [17], the sum-rate of the macrocell can be maximized through the

following optimization problem

$$\max_{\hat{\mathbf{w}}_1,\ldots,\hat{\mathbf{w}}_F} \sum_{i=1}^{F} \log \left(1 + \frac{\rho_i |\mathbf{h}_i \hat{\mathbf{w}}_i|^2}{\sum_{\substack{j=1 \\ j \neq i}}^{F} \rho_i |\mathbf{h}_i \hat{\mathbf{w}}_j|^2 + 1} \right) \tag{5.6}$$

$$\text{subject to } \sum_{i=1}^{F} \|\hat{\mathbf{w}}_i\|^2 \leq P_o,$$

where ρ_i is the average SNR of MU i, $\mathbf{h}_i$ is the $1 \times N$ channel from MBS to the ith MU, and $\hat{\mathbf{w}}_i$ is the $N \times 1$ beamforming vector of MU-i, which is the scaled form of the unnormalized beamforming vector $\mathbf{w}_i$, i.e., $\hat{\mathbf{w}}_i = \sqrt{p_i}\mathbf{w}_i$. Here p_i is the allocated power for MU i. Zero-forcing precoding vectors $\hat{\mathbf{w}}_{\mathbf{i}}$ are designed to eliminate the intra-cell interference, i.e., $\mathbf{h}_i \hat{\mathbf{w}}_j = 0$ for $j \neq i$. The unnormalized zero-forcing precoder matrix $\mathbf{W}_{\text{ZF}} = \begin{bmatrix} \mathbf{w}_1, \cdots, \mathbf{w}_F \end{bmatrix}$ is given as

$$\mathbf{W}_{\text{ZF}} = \mathbf{H} \left(\mathbf{H}^\dagger \mathbf{H} \right)^{-1}, \tag{5.7}$$

where $\mathbf{H} = \begin{bmatrix} \mathbf{h}_1^\dagger, \cdots, \mathbf{h}_F^\dagger \end{bmatrix}$. Under the optimal power allocation strategy, p_i can be obtained through the water filling algorithm

$$p_i = \left[\frac{\mu}{\gamma_i} - \frac{1}{\rho_i} \right]^+, \forall i \in \mathcal{F} \tag{5.8}$$

where μ is the water level, $\gamma_i = \left[\left(\mathbf{H}^\dagger \mathbf{H} \right)^{-1} \right]_{i,i}$ and $[x]^+ = \max(0, x)$. Here $[\mathbf{X}]_{u,p}$ denotes entry (u, p) of the matrix $\mathbf{X}$.

5.6 Simulation Results

In this section, the simulation results of the proposed and the baseline schemes based on the path loss models given under Section 5.3.2. The simulation parameters assumed are summarized in Table 5.1.

Simulations were carried out assuming single macrocell and the MBS was assumed within a square cell with 1 km sides. FBSs and MUs were uniformly and randomly

Table 5.1: Simulation parameters for heterogeneous cellular networks.

Parameter	Setting
Operating Frequency	2360 MHz
Transmitter Antenna Height	30 m
Receiver Antenna Height	2 m
MBS Transmitter Power	15 dBW [33]
FBS Transmitter Power	-10 dBW [34]
MBS Antenna Gain	15 dBi
UE Antenna Gain	0 dBi
Path loss Model for Macrocell	COST 231
Path loss Model for Femtocell	InH NLOS
Total Noise Power at UE	-110 dBW
Number of Monte Carlo simulations	500

distributed in the macrocell area. Each FBS was assumed at the center of a square cell with a 100 m sides and FUs were deployed randomly in the coverage area of each FBS. As crystalized in Section 5.4, adapting the proposed scheme for the case of 2-user, 2×1 in each femtocell, each femtocell can achieve 4/3 DoF and while the macrocell can achieve 1 DoF leading to a total of 7/3 DoF. On the other hand in the baseline scheme as described in Section 5.5 where FBSs operate at the same time and are orthogonal to the MBS using zero-forcing precoder with water filling power allocation strategy, the best achievable DoF is 1.

In Figures 5.4 and 5.5, the achievable sum-rates of the proposed scheme versus varying FBS and MBS transmit powers are plotted, respectively. In Figure 5.4, the MBS transmit power is fixed at 15 dBw and FBS transmit power varies from -20 to 0 dBw. In Figure 5.5, the FBS transmit power is fixed at -10 dBw while MBS transmit power varies from 4 to 20 dBw. In Figure 5.4 and 5.5, it is assumed there are only 1 femtocell and 1 MU in the network.
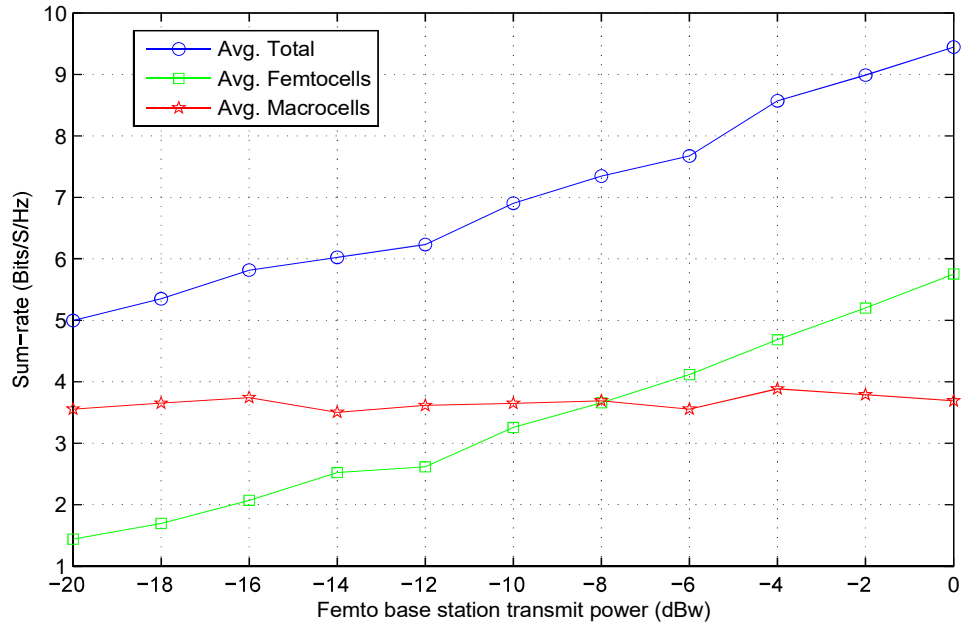
Figure 5.4: The sum-rate of the proposed scheme for the case of 2-user, 2×1 in each femtocell with varying FBS transmit power.
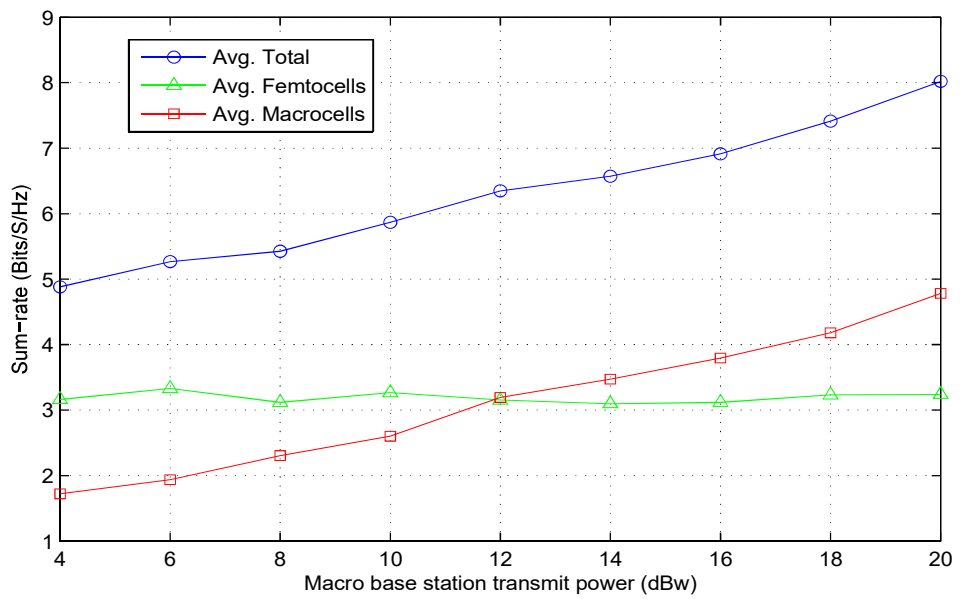

Figure 5.5: The sum-rate of the proposed scheme for the case of 2-user, 2×1 in each femtocell with varying MBS transmit power.

The sum-rate advantage of the proposed scheme over the baseline can be clearly seen when there are multiple femtocells, thus multiple MUs in the network as shown in Figure 5.6. This figure presents the aggregate sum-rate of the whole heterogeneous network (in other words the total sum-rate of femtocell and macrocell networks). FBS transmit power is fixed to -10dBw and the MBS transmit power is varied. It is easily seen that the proposed scheme achieves a higher sum-rate than the baseline scheme at all transmit power levels.
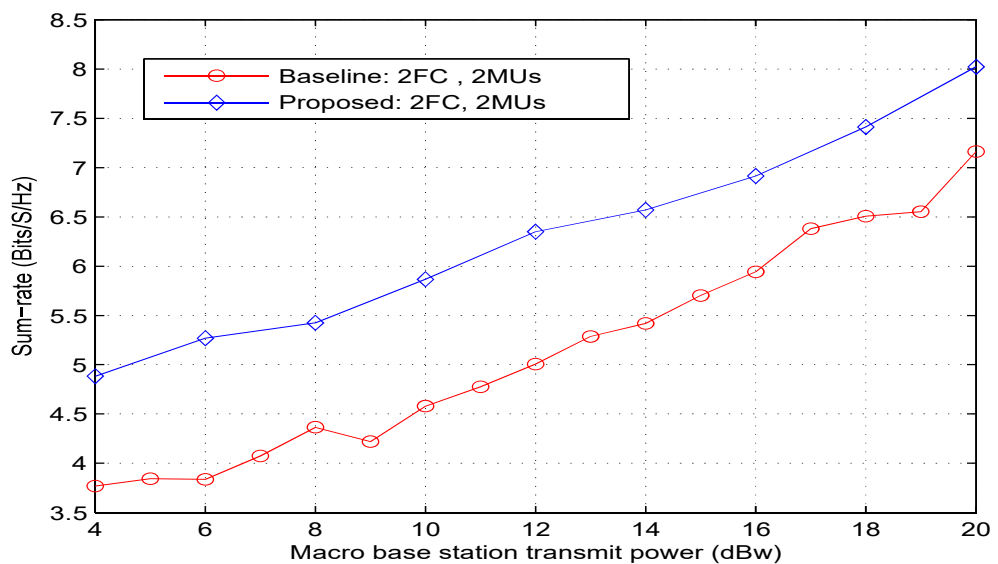

Figure 5.6: The total sum-rates of the proposed and baseline schemes for the case of 2-user 2×1 in each FC with varying MBS transmit power. It is assumed that there are 2 FCs and 2 MUs.

Chapter 6

COHERENCE-TIME BASED FEMTOCELL CONFIGURATIONS AND PARETO OPTIMIZATION TO ACHIEVE MAXIMUM DoF IN HETEROGENEOUS NETWORKS USING BIA

6.1 Introduction

Interference alignment (IA) technique known as blind interference alignment (BIA) [24] assumes that a transmitter is equipped with M antennas and there are K receivers, each equipped with a reconfigurable antenna capable of switching among M preset modes. BIA with K-user $M \times 1$ MISO BC, $[K, M]$ configuration, can achieve $\frac{KM}{(K+M-1)}$ degrees of freedom (DoF). BIA uses different antenna switching patterns for each of the K users in a network and requires that the channel does not change during one super-symbol. Therefore, coherence time is important to determine whether BIA can be used. In the literature one can find many BIA schemes that are applied in homogeneous [79, 89] and heterogeneous [35, 85, 103] cellular networks.

This chapter proposes a novel IA scheme for managing the cross-tier interference in a heterogeneous network with G macrocells (MCs) where each MC serves a single macro user (MU) and F femtocells (FCs) each of which applies $[K, M]$ s-BIA scheme as shown in Figure 6.1. Unlike in the proposed method of Chapter 5 for which DoF would not scale up with number of femtocells, in the newly proposed IA scheme DoFs would scale up based on the number of FCs and their respective configurations.

Furthermore, to maximize the achievable DoF of the proposed scheme the best possible FC configurations needs to be determined via Pareto optimization under limited coherence time. After the determination of FC configurations, the newly proposed IA scheme is applied that achieves more DoF in lesser coherence time than the existing schemes in the literature.
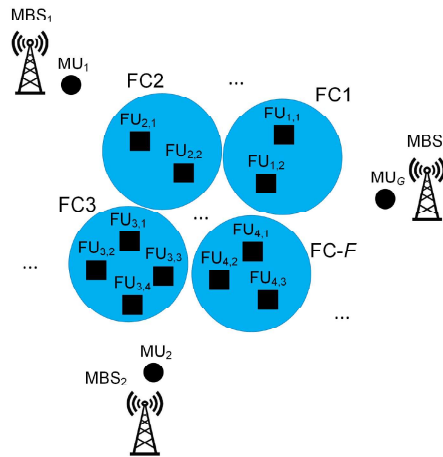
Figure 6.1: MBSs align the interference of MUs on FUs (assumes no interference between FCs).

6.2 System Model and IA Scheme

This section outlines the system model and provides details of the proposed interference alignment method. It is assumed that MBSs cause interference on FUs, while FBSs don't cause interference on MUs. The chapter also assumes that there is no interference between FCs.

6.2.1 System Model

Assuming that the interference from the FBSs is negligible in comparison to the interference caused by the MBSs, the received signal in the tth channel use for the kth

user of FC f can be written as

$$y_{[f,k]}(t) = \mathbf{h}_k^f(m_{[f,k]}(t))\mathbf{x}^f(t) + \sum_{g=1}^{G} \mathbf{h}_{[f,k]}^{[g]}(m_{[f,k]}(t))\mathbf{x}^g(t)$$

$$+ n_{[k,f]}, \ \forall f \in \mathcal{F} = \{1,...,F\}, \tag{6.1}$$

$$\forall k \in \mathcal{K} = \{1,...,K\}, \text{ and } \forall t \in \{1,...,T_{\max}\}.$$

$\mathbf{h}_k^f(m_{[f,k]}(t))$ denotes the $1 \times M$ channel corresponding to m^{th} mode between the fth FBS and k^{th} FU in the fth FC. $\mathbf{h}_{[f,k]}^{[g]}(m_{[f,k]}(t))$ denotes the $1 \times N$ channel between the gth MBS and the kth FU in the fth FC. Power of MBSs and FBSs are constraint to $E\left[||\mathbf{x}^g||^2\right] = P_G$ and $E\left[||\mathbf{x}^f||^2\right] = P_f$ respectively. $\mathbf{x}^g(t)$ and $\mathbf{x}^f(t)$ is the transmitted $N \times 1$ and $M \times 1$ vector from MBS and FBS, respectively. The transmitted vector from MBS is a product of transmit beamforming vector $\mathbf{v}^g(t) \in \mathbb{C}^{N \times 1}$ and a complex symbol $s^g(t)$. On the other hand, the transmitted vector from the fth FBS is the sum of products of s-BIA transmit beamforming vectors and symbols for each FU in the fth FC. $n_{[k,f]}$ denotes the Gaussian white noise vector at the kth user in the fth FC.

6.3 Proposed HetNet Scheme 2

The proposed interference alignment scheme relies on the same alignment principles presented in Chapter 5 and [35]. Since in [35] FCs are assumed to interfere with each other each MU is paired with a single FC, and all pairs in the network run on orthogonal dimensions in time or frequency. In this chapter the interference between FCs is assumed negligible and each MU is paired with a group of FCs. Later, the interference from MBS on FUs can be aligned in the same manner as in [35] wich has presented in Chapter 5. Moreover, the chapter also shows that extension to multiple MBSs where each MBS serves one MU with 1 DoF would also be possible.

The group of FCs is expected to serve a total of Z FUs. The knowledge of

predetermined interference dimensions of the FUs set by s-BIA and CSIT at the MBSs are used to align the MBSs' interference on a single dimension which is formed by all FUs at a single time slot. Then the beamforming vector of each MBS at each time slot can be solved by solving simple linear equations. As explained in [24] and Section 3.3, $(M-1)^K$ time slots constitute Block-1 of each user. Block-2 is partitioned into K subblocks each with length $(M-1)^{(K-1)}$ and the last symbols of alignment blocks of user k are placed in the kth subblock. In s-BIA scheme, while the last symbols of each user are transmitted, the other users remain silent thus interference free transmissions are achieved. Therefore at each time slot of the kth subblock of user k, the received interference from each MBS should equate to zero. On the other hand, during other time slots of Block-2 and at all time slots of Block-1, the received interference from each MBS should be zero.

$$\mathbf{h}_{[f,k]}^{[g]}(m_{[f,k]}(t))\mathbf{v}^g(t) = 0,$$

$$\forall f \in \mathcal{F}, \ \forall k \in \mathcal{K}, \ \forall g \in \{1,...,G\}, \text{and} \tag{6.2}$$

$$\forall t \in \{(M-1)^K + (k-1)(M-1)^{(K-1)} + 1, ..., (M-1)^K + k(M-1)^{(K-1)}\}.$$

At other time slots $\forall t' \notin t$, the right hand sight of the alignment condition (6.2) should equate to 1. The beamforming vector of each MBS is solved independently from other MBSs' beamforming vectors at each time slot. For each MBS there are Z equations to be solved thus the number of antennas at each MBS N should equal to Z, $(N = Z)$.

Therefore for the proposed IA scheme, the overall DoF of the network is $G + D_{\text{tot}}(T_{\text{max}})$, where $D_{\text{tot}}(T_{\text{max}})$ is the overall DoF of FCs at maximum possible number of symbol extensions (T_{max}) . Note that the proposed scheme can achieve more DoF in lesser time slots than the existing schemes [89]. Resembling the terminology used in [89], each MU can be considered as the private user of an MBS

while FUs can be considered as shared users but at where MBSs are causing interference in this scenario. Along with the proposed IA scheme, clearly posing FCs that apply s-BIA in the network help achieving higher DoF in lesser amount of symbol extensions.

6.4 Optimization Under Limited Coherence Time

In general, the overall DoF of FCs and the number of subtractions can be formulated as

$$D_{\text{tot}}(T_{\max}) = \sum_{k,m} A_{[k,m]} D_{[k,m]}(T_{\max}) \tag{6.3}$$

and

$$E_{\text{tot}}(T_{\max}) = \sum_{k,m} A_{[k,m]} k E_{[k,m]} \tag{6.4}$$

respectively where $A_{[K,M]}$ represents the number of FCs using $[K,M]$ configurations. Recall that, $E_{[k,m]}$ and $D_{[k,m]}(T_{\max})$ represent the number of subtraction and the achievable DoF of a FC using s-BIA with $[K,M]$ configuration under a given $T_{\max}$ which have been defined in equations (3.37) and (3.38) respectively.

Next, we draw a framework on how to maximize the DoF while supporting Z number of FUs in the network. While maximizing DoF the optimizer also tries to minimize the number of subtractions required at FUs assuming limited coherence time. This

problem can be formulated as

$$\text{max} \qquad D_{\text{tot}}(T_{\max}, Z) = \sum_{k,m} A_{[k,m]} D_{[k,m]}(T_{\max}) \qquad (6.5)$$

$$\text{min} \qquad E_{\text{tot}}(T_{\max}, Z) = \sum_{k,m} A_{[k,m]} k E_{[k,m]} \qquad (6.6)$$

$$\text{s.t.} \qquad \sum_{k,m} A_{[k,m]} k = Z \qquad (6.7)$$

$$SL_{[k,m]} \leq T_{\max} \qquad (6.8)$$

$$D_{[k,m]}(T_{\max}) > 1 \qquad (6.9)$$

$$A_{[k,m]} \in \mathbb{N}_0 \qquad (6.10)$$

To achieve this Pareto optimization two objective functions (Obj1 and Obj2) as defined by (6.5) and (6.6) have been used. The optimization is subject to the constraints (6.7)-(6.10) and the aim is to find the best possible structure $A_{[K,M]}^*$ for each FC.

Equation (6.7) forms the first constraint of the optimization problem that use the two objective functions as defined by (6.5) and (6.6). If Z FUs are available in the network, these users would be assigned to a set of FCs where each FC has its own $[K,M]$ configuration. The total number of FUs can be expressed as a function of number of FUs K in each FC and the number of FCs with $[K,M]$ configuration $A_{[K,M]}$ as stated by (6.7). Constraint (6.8) defines the limited coherence time. Since the main goal of IA is to transmit more interference free symbols per channel use than conventional schemes such as TDMA or FDMA, FCs using BIA with $[K,M]$ configurations must satisfy the constraint (6.9) to achieve DoF larger than unity.

[104] explains how to solve such bi-objective optimization problems (BOP) using an epsilon-constraint framework (ECF). ECF will iteratively solve each single-objective

version of the optimization problem to enumerate all Pareto-optimal solutions. Generally with two objective functions f_1 and f_2 the value of the constant ε is assumed small in comparison to the differences between values of f_1 and f_2. In this study, f_1 is the total DoF $D_{\text{tot}}(T_{\text{max}}, Z)$ and f_2 is total number of subtractions E_{tot}. Since the number of subtractions has an integer value equal to E_{tot} the optimization constant ε is chosen as 1. In this chapter each Pareto optimal solution **x** is a vector that contains the best possible configurations $A^*_{[k,m]}$ for all FCs to achieve maximum DoF with the minimum number of subtractions for serving Z FUs in T_{max} symbol extensions. After the best configurations of FCs are determined by the optimization, the proposed IA scheme in Section 6.2 can be applied.

6.5 Results of Optimization

Optimization results depend on maximum possible symbol extensions and the number of FUs that must be served. To demonstrate the effect of each parameter on the achievable DoF and number of antennas required, the above optimization problem has been solved for two cases: (i) when Z is fixed and T_{max} is varied and (ii) when Z is varied and T_{max} is fixed.

For case (i), $Z = 7$ FUs was assumed and T_{max} values of 7 and 15 were alternatively used. In the first step of the optimization, the optimizer would choose the set of $\{[K,M]\}$ configurations that satisfy condition (6.8) and in step-2, configurations in the set found would be used to select those FCs which satisfy $D_{[K,M]}(T_{\text{max}}) > 1$ condition. Results for (i) have been shown by Figures 6.2 and 6.3 respectively and summarized in Table 6.1.

Figure 6.2 depicts the result of optimization when $Z = 7$ and $T_{\text{max}} = 7$. In this particular example, only one Pareto optimal solution vector (best possible structure) exists which,
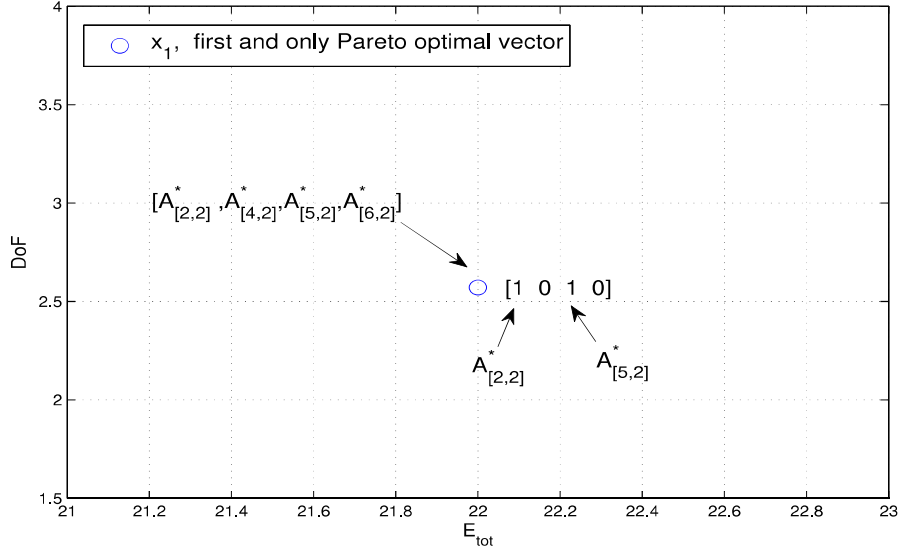
Figure 6.2: Pareto optimal solution vector when $Z = 7$ and $T_{max} = 7$.

satisfies the maximum DoF and minimum number of subtractions. This implies that to achieve maximum DoF with 7 users and $T_{\max} = 7$ the system must have two FCs one with $[K,M] = [2,2]$ ($A^*_{[2,2]} = 1$) and the other with $[K,M] = [5,2]$ ($A^*_{[5,2]} = 1$). The Pareto optimal solution vector $[1, 0, 1, 0]$ can then be used in (6.5) to determine the maximum total DoF possible; $D_{\text{tot}}(7,7) = 2.57$. Similarly, minimum number of subtractions at each channel use ($\min E_{\text{tot}}(7,7) = 7$) can be obtained from (6.6).

As shown by Figure 6.3 and summarized in Table 6.1, for same number of users ($Z = 7$) and $T_{\max} = 15$, three Pareto optimal solution vectors were achieved $\{\mathbf{x}_1, \mathbf{x}_2, \mathbf{x}_3\}$. It can be noted that the proposed scheme can achieve $D_{\text{tot}}(\mathbf{x}_3) = 4.44$ as its highest DoF (for FCs only). For $T_{\max} = 15$ the number of subtractions is $E_{\text{tot}}(\mathbf{x}_3) = 42$. Moreover $D_{\text{tot}}(\mathbf{x}_1) = 3.86$ can be achieved as the lowest DoF by having $E_{\text{tot}}(\mathbf{x}_3) = 10$ number of subtractions. Clearly, $T_{\max}$ value can change the number of Pareto optimal solution vectors and set of allowable $\{[K,M]\}$ configurations of each pair. With multiple Pareto optimal solutions, the network planner can flexibly choose one of these Pareto optimal solutions.
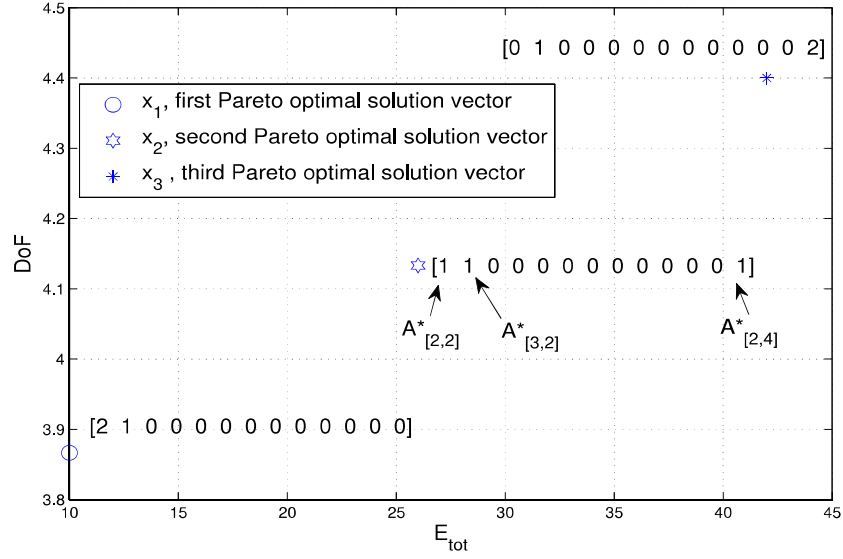
Figure 6.3: Pareto optimal solution vectors when $Z = 7$ and $T_{max} = 15$.

Table 6.1: Pareto optimal solutions when Z is fixed and $T_{\max}$ is varied.

	$Z = 7$ and $T_{\max} = 7$		
x	$\left[A^*_{[2,2]}, A^*_{[4,2]}, A^*_{[5,2]}, A^*_{[6,2]}\right]$	$D_{\text{tot}}(\mathbf{x})$	$E_{\text{tot}}(\mathbf{x})$
$\mathbf{x_1}$	$[1, 0, 1, 0]$	2.57	22
	$Z = 7$ and $T_{\max} = 15$		
x	$\left[A^*_{[2,2]}, A^*_{[3,2]}, A^*_{[4,2]}, A^*_{[5,2]}, A^*_{[6,2]}, A_{[8,2]}, A^*_{[9,2]}, A^*_{[10,2]}, A^*_{[11,2]}, A^*_{[12,2]}, A^*_{[13,2]}, A^*_{[14,2]}, A^*_{[2,4]}\right]$	$D_{\text{tot}}(\mathbf{x})$	$E_{\text{tot}}(\mathbf{x})$
$\mathbf{x_1}$	$[2, 1, 0, 0, 0, 0, 0, 0, 0, 0, 0, 0, 0]$	3.86	10
$\mathbf{x_2}$	$[1, 1, 0, 0, 0, 0, 0, 0, 0, 0, 0, 0, 1]$	4.13	26
$\mathbf{x_3}$	$[0, 1, 0, 0, 0, 0, 0, 0, 0, 0, 0, 0, 2]$	4.44	42

For case (ii), the BOP was solved for $T_{\max} = 15$, and $Z \in \{2, \cdots, 15\}$. As before the FC configurations that could satisfy the $SL_{[K,M]} \leq T_{\max}$ and $D_{[K,M]}(T_{\max}) > 1$ conditions were determined. Result of the Pareto optimization show that there would be more than one optimal solution for each different Z value. Hence for each Z value multiple DoFs and E_{tot} values would exist.

Figures 6.4 and 6.5 have been provided to show the upper and lower bounds for achievable DoFs and the number of subtractions. Since the Pareto optimal solution vectors of Figure 6.4 and 6.5 follow predictable patterns as Z changes the structure of the optimal solution vector,

117
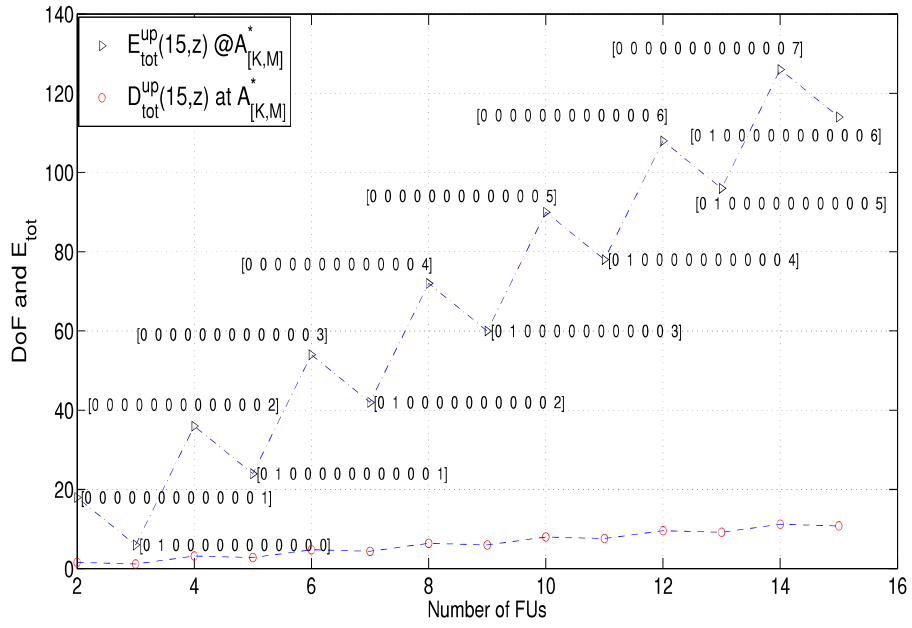
Figure 6.4: Upper bounds on DoF and E_{tot}.
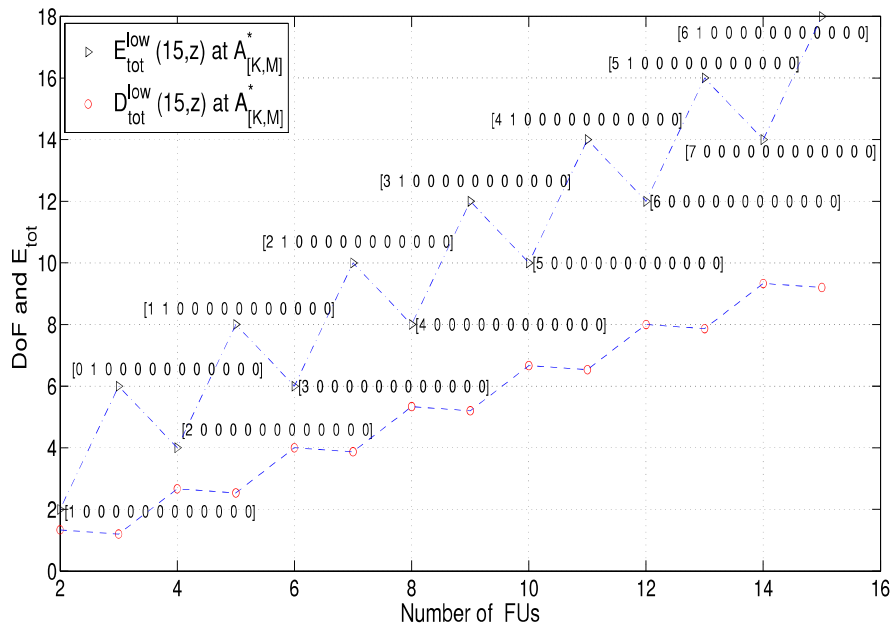
Figure 6.5: Lower bounds on DoF and E_{tot}.

$\left[A^*_{[K,M]} \right]$, can be formulated in both cases as:

$$x^{UB}(15,Z) = \left[A^*_{[2,2]}, A^*_{[3,2]}, A^*_{[4,2]}, A^*_{[5,2]}, A^*_{[6,2]}, A_{[8,2]}, A^*_{[9,2]}, A^*_{[10,2]}, A^*_{[11,2]}, A^*_{[12,2]}, A^*_{[13,2]}, A^*_{[14,2]}, A^*_{[2,4]} \right]$$

$$= \left[0, \left(\frac{Z - \sin^2\left(Z\frac{\pi}{2}\right)}{2} \right), 0,0,0,0,0,0,0,0,0,0, \sin^2(Z\frac{\pi}{2}) \right]$$

(6.11)

and

$$x^{LB}(15,Z) = \left[A^*_{[2,2]}, A^*_{[3,2]}, A^*_{[4,2]}, A^*_{[5,2]}, A^*_{[6,2]}, A^*_{[8,2]}, A^*_{[9,2]}, A^*_{[10,2]}, A^*_{[11,2]}, A^*_{[12,2]}, A^*_{[13,2]}, A^*_{[14,2]}, A^*_{[2,4]} \right]$$

$$= \left[\left(\frac{Z - 3\sin^2(Z\frac{\pi}{2})}{2} \right), \sin^2\left(Z\frac{\pi}{2}\right), 0,0,0,0,0,0,0,0,0,0 \right].$$

(6.12)

6.5.1 General Pareto Optimal Solutions Under Limited Coherence-time

This section describes the general method to solve the multi-objective optimization problem given in equations (6.5–6.10). This general method is known as weighted-sum method and could be used to determine the upper and lower bounds of $E_{\text{tot}}(T_{\max}, Z)$ and $D_{\text{tot}}(T_{\max}, Z)$ and any other possible optimal solution vectors in between.

To attain the optimization results, the weighted-sum method is applied to the problem defined in Section 6.4 as follows:

119

$$\underset{A_{[k,m]}}{\text{argmax}} \quad \Big(\alpha D_{\text{tot}}(T_{\text{max}}, Z) - \beta E_{\text{tot}}(T_{\text{max}}, Z)\Big)$$

$$\text{s.t.} \quad \sum_{k,m} kA_{[k,m]} = Z$$

$$SL_{[k,m]} \leq T_{\text{max}} \tag{6.13}$$

$$D_{[k,m]}(T_{\text{max}}) > 1$$

$$A_{[k,m]} \in \mathbb{N}_0$$

$$\text{and} \quad \alpha, \beta \geq 0, \ (\alpha + \beta) = 1$$

where, α and β are priority coefficients and represent the priority of each of the objective functions. In other words, to maximize $D_{\text{tot}}(T_{\text{max}}, Z)$ with no restriction (constraint) on total number of subtractions (upper bound), priority coefficients are set to $[\alpha, \beta] = [1, 0]$. Similarly to find the maximum achievable $D_{\text{tot}}(T_{\text{max}}, Z)$ using minimum possible number of subtractions (lower bound), the priority coefficients $[\alpha, \beta]$ would be set to $[0, 1]$.

Note that, for these two extreme cases the solution to the optimization problem in (6.13) are same as what has been provided in Figures 6.4 and 6.5 under case(ii) of Section 6.5 where $T_{\text{max}} = 15$, and $Z \in \{2, \cdots, 15\}$.

Moreover, as stated in Section 6.5 for certain value of T_{max} and number of FUs (Z), multiple Pareto optimal solution vectors may exist, and the network planner should be able to choose one of them to fulfill the requirement of the network. This can be done by converting the bi-objective optimization problem to a single-objective one where the number of subtractions is fixed by the network planner at a predefined value between the upper and lower bounds $\Big(E_{tot}^{UP}(T_{max}, Z) \text{ and } E_{tot}^{Low}(T_{max}, Z)\Big)$. Afterwards,

the corresponding maximum achievable DoF for desired number of subtraction can be found by solving the single-objective optimization problem. Herein, the desired number of subtractions has been denotes as $\left(E_{des}(T_{max}, Z)\right)$ and its value would determine the value of $D_{tot}(T_{max}, Z)$. The single–objective optimization problem that one has to solve can be defined as:

$$\max \quad D_{tot}(T_{max}, Z),$$

$$\text{s.t.} \quad E_{des}(T_{max}, Z) \leq E_{tot}^{UP}(T_{max}, Z) - \beta(E_{tot}^{UP}(T_{max}, Z) - E_{tot}^{Low}(T_{max}, Z)); 0 \leqslant \beta \leqslant 1$$

$$\sum_{k,m} kA_{[k,m]} = Z,$$

$$A_{[k,m]} \geq 0, \in \mathbb{N}.$$

$$(6.14)$$

The β value in (6.14) is selected such that the number of subtractions is in between the upper and lower bounds:

$$\begin{cases} \beta = 1, & E_{des}(T_{max}, Z) = E_{tot}^{UP}(T_{max}, Z) \\[2mm] \beta = 0, & E_{des}(T_{max}, Z) = E_{tot}^{Low}(T_{max}, Z) \\[2mm] 0 < \beta < 1 & E_{tot}^{Low}(T_{max}, Z) < E_{des}(T_{max}, Z) < E_{tot}^{UP}(T_{max}, Z) \end{cases}$$

Finally, based on predefined value $E_{des}(T_{max}, Z)$ and upper and lower bounds for the number of subtractions (found by solving extreme cases of (6.13)) a normalized value of β can be determined as follow:

$$\beta = \frac{E_{tot}^{UP}(T_{max}, Z) - E_{des}(T_{max}, Z)}{E_{tot}^{UP}(T_{max}, Z) - E_{tot}^{Low}(T_{max}, Z)}. \qquad (6.15)$$

The above equation can then be reformulated as

$$E_{des}(T_{max}, Z) \leq E_{tot}^{UP}(T_{max}, Z) - \beta(E_{tot}^{UP}(T_{max}, Z) - E_{tot}^{Low}(T_{max}, Z)) \qquad (6.16)$$

Note that, (6.16) is the condition that the single-objective obtimization function is

121
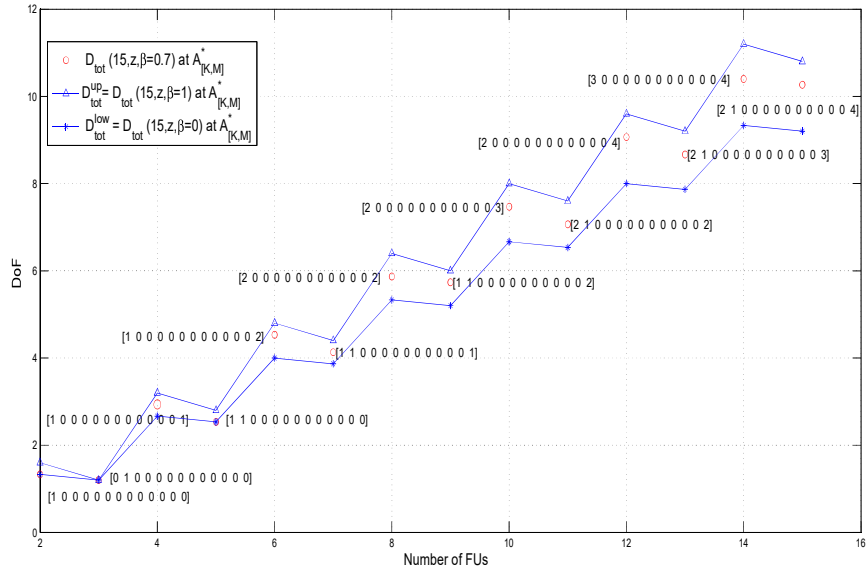
Figure 6.6: Maximum achievable D_{tot} when $T_{max} = 17$, $\beta = 0.7$ for different value of FUs.
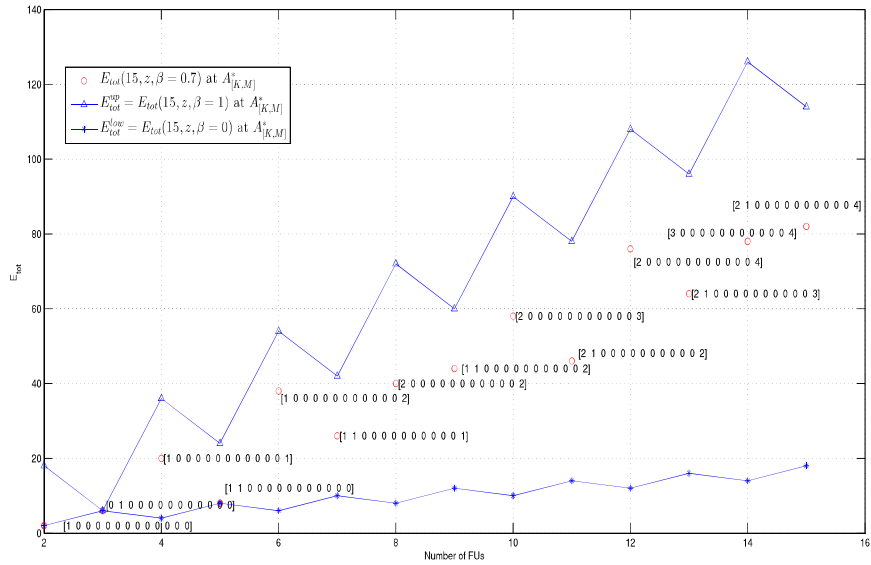

Figure 6.7: Maximum achievable E_{tot} when $T_{max} = 17$, $\beta = 0.7$ for different value of FUs.

subject to in (6.14). The optimizer would choose the closest possible integer value to $E_{des}(T_{max}, Z)$ and work out the corresponding maximum value of $D_{tot}(T_{max}, Z, \beta)$.

The above problem has been solved for case (ii), when $T_{\max} = 15$, and

$Z \in \{2, \cdots, 15\}$ and $E_{des}(T_{max}, Z)$ values corresponding to $\beta = 0$, 0.7 and 1. Results are demonstrated in Figures 6.6 and 6.7. Figure 6.6 demonstrates the value of $D_{tot}(T_{max}, Z, \beta)$ for different number of FUs. Results show that $D_{tot}(T_{max} = 15, Z, \beta = 0)$ and $E_{tot}(T_{max} = 15, Z, \beta = 1)$ are respectively same as $D_{tot}^{UP}(T_{max} = 15, Z)$ and $D_{tot}^{Low}(T_{max} = 15, Z)$ in previous section. Moreover, it can be noted that, $D_{tot}^{Low}(T_{max}, Z, \beta = 0) \leqslant D_{tot}(T_{max}, Z, \beta = 0.7) \leq D_{tot}^{UP}(T_{max}, Z, \beta = 1)$.

Figure 6.7 demonstrates the value of $E_{tot}(T_{max}, Z, \beta)$ under different number of FUs with $\beta \in \{1, 0, and 0.7\}$. Results indicate that $E_{tot}(T_{max}, Z, \beta = 0)$, $E_{tot}(T_{max}, Z, \beta = 1)$ are same as $E_{tot}^{UP}(T_{max}, Z)$ and $E_{tot}^{Low}(T_{max}, Z)$ as in previous section and $E_{tot}^{Low}(T_{max}, Z) \leqslant E_{tot}(T_{max}, Z, \beta = 0.7) \leq E_{tot}^{UP}(T_{max}, Z)$.

Chapter 7

CONCLUSIONS AND FUTURE WORK

7.1 Conclusions

This thesis focuses on managing interference under cellular networks where global CSIT is not available. It has proposed three new blind interference alignment schemes that could work under the limited coherence time assumption and would provide competitive DoF and sum-rate values both under homogeneous and heterogeneous cellular networks.

The journal paper entitled *"Hybrid Blind Interference Alignment in Cellular Networks with Limited Coherence Time"* [36], has proposed a new blind interference alignment scheme called hybrid-BIA to handle inter and intracell interference, to reduce the supersymbol length and to overcome the DoF loss of the state-of-the-art hierarchical BIA (h-BIA) over homogeneous cellular networks. Hybrid-BIA is inspired by the user grouping approach of semi-blind topological blind interference alignment (top-BIA) and the fact that the partially connected networks can help achieve better DoF and sum-rates. Hybrid-BIA requires no data sharing between BSs and users are assumed to only switch between their actual preset modes. The work in this thesis has showed that the hybrid-BIA can be applied under different scenarios such as: 1) dense clustered cellular network where the user association of each BS is known, 2) partially-connected network where the transmission of each BS does not cause intercell interference on private users of the neighboring cells.

- Hybrid-BIA has been compared against the five different BIA schemes introduced in Chapter 3 and through a series of simulations it was shown that the proposed scheme had the shortest supersymbol length among all.

- The sum-rate formula for hybrid-BIA was derived and its throughput was analyzed via simulations. In particular CDF versus throughput graphs were produced for the five different BIA schemes at the center cluster of a clustered cellular network where each cluster had F small-cells and each small-cell had $[K_f, M]$ configuration, $f \in [1 : F]$. The simulation results has shown that the throughput for hybrid-BIA was better than that of h-BIA which till recently had the shortest supersymbol length in the literature. hybrid-BIA had network throughput between 10-15 bits/sec/Hz and this was $20-25$ % higher than that of h-BIA. It was also demonstrated that the throughput would scale up as the number of small-cells is increased.

- Hybrid-BIA was simulated with different number of user-groups and results has shown that the case where each user-group had a single member would correspond to h-BIA. Hence the work has concluded that h-BIA constitutes a special case of hybrid-BIA.

- Ratio of supersymbol lengths for h-BIA and hybrid-BIA plus the sum-DoF gain of hybrid-BIA over its competitor h-BIA was evaluated under a symmetric cellular network with F small-cells. During simulations, it was assumed that each cell had $[K, M]$ configuration and the network had a total of $K_T = FK$ users. It was observed that the lowest values for the ratio of supersymbol lengths and DoF gain were achieved when $|\Lambda| = K_T$ while $|\Lambda| = K$ would lead

to the highest values.

- DoF gain and supersymbol length ratio between h-BIA and hybrid-BIA was studied for different number of small-cells. This study also considered the effect of $|\Lambda|$ on the DoF gain as the network size (number of small-cells) was varied.

  - Assuming $K = 4, M = 9$, and $F = 2$ it was shown that both the DoF-gain and the supersymbol length ratio would scale up with the number of small-cells. It was observed that, for a five fold increase on the total number of users in the network (initial $K_T = FK = 2 \cdot 4$ and final $K_T = FK = 10 \cdot 4$) approximately a three fold increase in the DoF gain would be obtained. Moreover it was demonstrated that the upper bound would be achieved when $|\Lambda| = K$.

- Effect of number of transmit antennas on DoF-gain and supersymbol length ratio was also evaluated. While the number of transmit antennas was varied from 4 to 80, $|\Lambda|$ and K were set to 4. It was shown that the highest DoF gain would be achieved when $M = 4$ and as the number of transmit antennas is increased the DoF gain would gradually reduce.

The two conference papers which were presented in SIU2015 [35] and SIU2016 [26] have proposed two novel BIA schemes to manage the cross and co-tier interference in two-tier HetNets comprised of macrocell and femtocells. These schemes have assumed that MCs and FCs were working at the same time or in the same frequency band where MCs had access to the global CSIT and s-BIA was employed by each FC to manage intracell interference.

The first conference paper titled *"Interference Management in Two-Tier*

Heterogeneous Networks Using Blind Interference Alignment" was proposed to align the cross-tier interference in heterogeneous cellular network. This paper has considered a scenario where multiple femtocells were deployed under the coverage area of a macrocell and each femto BS has paired with a MU and all pairs were operating in different time slots or frequency bands. The proposed scheme has assumed that femtocells did not interfere with each other and also they wouldnt shed interfere on MUs. On the other hand, MBSs interfered with FUs, but not with neighboring MUs. Within each femtocell, BIA with staggered antenna switching was used. The proposed scheme would use the knowledge of predetermined interference dimensions of the FUs set by BIA and CSIT at MBS to align the interference shed by MBS on the interference dimensions of FUs.

- By allowing MBSs and FBSs to coexist and operate in the same frequency band and/or time slot the proposed Hetnet scheme-#1 could achieve higher DoF and sum-rates and also at the same time it would lower the load of the macrocell (when MUs are close to FCs they are served by FCs).

- With a single MBS and multiple FBS it was shown that the proposed scheme could achieves 7/3 DoF where each femtocell had 2-user, 2×1 MISO BC configuration. This was more than the 1 DoF which the conventional orthogonal zero-forcing precoder using water-filling power allocation strategy (also known as baseline scheme) would deliver. Recall that, under the base line scheme where all FBSs operate at the same time but in an orthogonal manner with the MBS the best achievable DoF would be 1 DoF.

- Furthermore the proposed scheme can be extended to a generalized scenario where each femtocell would have K-user, $M \times 1$ MISO BC configuration.

– For example, given 2 MCs each with 2 MUs and 2 femtocells each having 2-user, 2×1 MISO BC configuration, 14/3 DoF could be achieved under the extended proposed scheme, while the basic proposed scheme could only deliver 7/3 DoF.

Finally, the sum-DoF of generalized proposed scheme can further be scaled up by increasing the number of femtocells.

• The sum-rate of the proposed Hetnet scheme-#1 was also compared with that of the baseline scheme by varying FBS and MBS transmit powers under a realistic channel model (COST 231 for macrocell and InH NLOS model for femtocells). It was showed that proposed scheme could achieve a higher sum-rate than the baseline scheme at all transmit power levels.For multiple femtocells (generalized proposed scheme) the sum-rate would further scale up.

The second conference paper titled " *Coherence-time Based Femtocell Configurations and Pareto Optimization to Achieve Maximum DoF in Heterogeneous Networks Using BIA*" [26], has extended the work presented in [35], by aligning the interference from MBS on predetermined interference dimensions of femtocell at each symbol extension where the predetermined dimensions are set by BIA.The paper focuses on the downlink of a two-tier partially connected heterogeneous network with multiple femtocells deployed under the dead zone between two adjacent macro cells. It is assumed that each MC is serving two MUs and each femtocell supports *K* users. [26] describes a framework in which maximum possible DoF can be determined by femtocell configurations and structure optimization. Due to the fact that only some femtocell configurations could satisfy the maximum symbol extension condition, the analysis was carried out assuming both fixed and unlimited coherence

times. The paper has adopted Pareto-optimization to determine maximum DoF for minimum number of subtractions at FCs and makes use of s-BIA.

- The proposed scheme assumes no interference between FCs and MUs' streams are aligned on a single dimension which is formed by all FUs at each channel use. Results indicate that, the DoF of proposed BIA scheme (HetNet scheme-#2) is scalable with the number of FCs and their configurations. Moreover higher DoF can be achieved in fewer symbol extensions than top-BIA and cognitive-BIA schemes.

- The study has also demonstrated that $T_{\max}$ value can change the number of Pareto optimal solution vectors and the set of allowable $\{[K,M]\}$ configurations of each pair. It was pointed out that with multiple Pareto optimal solutions, the network planner could flexibly choose one of these Pareto optimal solutions based on available resources.

- When maximum allowable coherence time $T_{\max}$ was fixed and number of FUs in the network (Z) was varied, it was observed that the Pareto optimal solutions vectors follow predictable patterns and thereafter the upper and lower bounds for the optimal solution vector was written.

7.2 Future Work

In [99], a cognitive-BIA (cog-BIA) scheme for heterogeneous networks has also been proposed for eliminating the intracell interference of each tier plus the inter-tier interference. Since hybrid-BIA does not require any data sharing between BSs, it would be possible to apply the hybrid-BIA scheme in heterogeneous network. Independent of their tiers users can be grouped together using top-BIA and be served by their respective BSs by applying h-BIA. hybrid-BIA can also be applied to

129

partially connected IC networks when condition in (3.16) holds.

In addition Hierarchical BIA suffers from some DoF-loss due to the following reasons 1) incomplete grouping problem and 2) indivisibility of users preset modes ($M_{[k,i]}$) by user-group preset modes (M_{G_i}) e.g. DoF of $< 5,5,5,5 >$ would be same as $< 4,4,4,4 >$. It would be interesting to investigate an approach to solve theses two issues.

Finally, the theoretical upper bound for DoF of K-user SISO IC using BIA has been evaluated in [75], however the achievability is still an open issue.

REFERENCES

[1] D. J. Goodman *et al.*, "Trends in cellular and cordless communications," *IEEE Communications Magazine*, vol. 29, no. 6, pp. 31–40, 1991.

[2] A. Furuskar, S. Mazur, F. Muller, and H. Olofsson, "EDGE: Enhanced data rates for GSM and TDMA/136 evolution," *IEEE personal communications*, vol. 6, no. 3, pp. 56–66, 1999.

[3] R. Kalavakunta and A. Kripalani, "Evolution of mobile broadband access technologies and services-considerations and solutions for smooth migration from 2G to 3G networks," in *International Conference on Personal Wireless Communications*. IEEE, 2005, pp. 144–149.

[4] D. Calin, P. Gardell, A. Mackay, T. B. Morawski, L. Pinzon, R. Sackett, and H. Zhang, "A new approach to capacity growth planning for CDMA networks," in *12th International Telecommunications Network Strategy and Planning Symposium*. IEEE, 2006, pp. 1–6.

[5] H. Sampath, S. Talwar, J. Tellado, V. Erceg, and A. Paulraj, "A fourth-generation MIMO-OFDM broadband wireless system: design, performance, and field trial results," *IEEE Communications Magazine*, vol. 40, no. 9, pp. 143–149, 2002.

[6] H. Bolcskei, "MIMO-OFDM wireless systems: basics, perspectives, and challenges," *IEEE wireless communications*, vol. 13, no. 4, pp. 31–37, 2006.

[7] P. Demestichas, A. Georgakopoulos, D. Karvounas, K. Tsagkaris, V. Stavroulaki, J. Lu, C. Xiong, and J. Yao, "5G on the horizon: Key challenges for the radio-access network," *IEEE Vehicular Technology Magazine*, vol. 8, no. 3, pp. 47–53, 2013.

[8] F. Boccardi, R. W. Heath, A. Lozano, T. L. Marzetta, and P. Popovski, "Five disruptive technology directions for 5G," *IEEE Communications Magazine*, vol. 52, no. 2, pp. 74–80, 2014.

[9] S. Chen and J. Zhao, "The requirements, challenges, and technologies for 5G of terrestrial mobile telecommunication," *IEEE Communications Magazine*, vol. 52, no. 5, pp. 36–43, 2014.

[10] Q. H. Spencer, A. L. Swindlehurst, and M. Haardt, "Zero-forcing methods for downlink spatial multiplexing in multiuser MIMO channels," *IEEE transactions on signal processing*, vol. 52, no. 2, pp. 461–471, 2004.

[11] T. Yoo and A. Goldsmith, "On the optimality of multi antenna broadcast scheduling using zero-forcing beamforming," *IEEE Journal on selected areas in communications*, vol. 24, no. 3, pp. 528–541, 2006.

[12] G. Caire and S. Shamai, "On the achievable throughput of a multi antenna gaussian broadcast channel," *IEEE Transactions on Information Theory*, vol. 49, no. 7, pp. 1691–1706, 2003.

[13] S. Shim, J. S. Kwak, R. W. Heath, and J. G. Andrews, "Block diagonalization for

multi-user MIMO with other-cell interference," *IEEE Transactions on Wireless Communications*, vol. 7, no. 7, 2008.

[14] N. Ravindran and N. Jindal, "Limited feedback-based block diagonalization for the MIMO broadcast channel," *IEEE Journal on Selected Areas in Communications*, vol. 26, no. 8, 2008.

[15] J. Zhang, R. Chen, J. G. Andrews, and R. W. Heath, "Coordinated multi-cell MIMO systems with cellular block diagonalization," in *41th Asilomar Conference on Signals, Systems and Computers ACSSC 2007.* IEEE, 2007, pp. 1669–1673.

[16] R. Zhang, "Cooperative multi-cell block diagonalization with per-base-station power constraints," *IEEE Journal on Selected Areas in Communications*, vol. 28, no. 9, pp. 1435–1445, 2010.

[17] D. H. Nguyen and T. Le-Ngoc, "MMSE precoding for multiuser MISO downlink transmission with non-homogeneous user SNR conditions," *EURASIP Journal on Advances in Signal Processing*, vol. 2014, no. 1, p. 85, 2014.

[18] M. A. Maddah-Ali, A. K. Khandani, and A. S. Motahari, *Communication over X channel: Signalling and multiplexing gain.* Citeseer, 2006.

[19] S. A. Jafar and S. Shamai, "Degrees of freedom region of the MIMO X channel," *IEEE Transactions on Information Theory*, vol. 54, no. 1, pp. 151–170, 2008.

[20] V. R. Cadambe and S. A. Jafar, "Interference alignment and degrees of freedom of the K-user interference channel," *IEEE Transactions on Information Theory*, vol. 54, no. 8, pp. 3425–3441, 2008.

[21] S. A. Jafar *et al.*, "Interference alignment—a new look at signal dimensions in a communication network," *Foundations and Trends® in Communications and Information Theory*, vol. 7, no. 1, pp. 1–134, 2011.

[22] G. Tiangao and S. Jafar, "Degrees of freedom of the K-user $M \times N$ MIMO interference channel," *IEEE Transactions on Information Theory*, vol. 56, no. 12, pp. 6040–6057, 2010.

[23] V. Kalokidou, O. Johnson, and R. Piechocki, "Blind interference alignment in general heterogeneous networks," in *25th Annual International Symposium on Personal, Indoor, and Mobile Radio Communication (PIMRC)*. IEEE, 2014, pp. 816–820.

[24] G. Tiango, C. Wang, and S. Jafar, "Aiming perfectly in the dark-blind interference alignment through staggered antenna switching," *IEEE Transactions on Signal Processing*, vol. 59, no. 6, pp. 2734–2744, June,2011.

[25] S. Jafar, "Blind interference alignment," *IEEE Journal of Selected Topics in Signal Processing*, vol. 6, no. 3, pp. 216–227, 2012.

[26] R. Bakhshi, E. A. Ince, and C. M. Yetiş, "DoF maximization in heterogeneous networks using BIA under limited coherence time," in *24th Signal Processing*

and Communication Application Conference (SIU). IEEE, 2016, pp. 1721–1724.

[27] H. Sun, C. Geng, and S. A. Jafar, "Topological interference management with alternating connectivity," in *International Symposium on Information Theory Proceedings (ISIT)*. IEEE, 2013, pp. 399–403.

[28] C. Geng, H. Sun, and S. A. Jafar, "Multilevel topological interference management," in *Information Theory Workshop (ITW)*. IEEE, 2013, pp. 1–5.

[29] J. Chen, P. Elia, and S. A. Jafar, "On the vector broadcast channel with alternating CSIT: A topological perspective," in *International Symposium on Information Theory (ISIT)*. IEEE, 2014, pp. 2579–2583.

[30] M. Morales-Céspedes, J. Plata-Chaves, D. Toumpakaris, S. A. Jafar, and G. Armada, "Blind interference alignment for cellular networks," *IEEE Transactions on Signal Processing*, vol. 63, no. 1, pp. 41–56, October, 2015.

[31] I. Shgluof, M. Ismail, and R. Nordin, "Efficient femtocell deployment under macrocell coverage in LTE-Advanced system," in *International Conference on Computing, Management and Telecommunications (ComManTel)*. IEEE, 2013, pp. 60–65.

[32] B. Guler and A. Yener, "Selective interference alignment for MIMO cognitive femtocell networks," *IEEE Journal on Selected Areas in Communications*,

vol. 32, no. 3, pp. 439–450, 2014.

[33] U. Equipment, "Evolved universal terrestrial radio access (e-utra); radio frequency (rf) system scenarios, 3rd generation partnership project (3GPP)," Technical report, TR 36.942, Tech. Rep., 2010.

[34] D. N. Knisely, T. Yoshizawa, and F. Favichia, "Standardization of femtocells in 3GPP," *IEEE Communications Magazine*, vol. 47, no. 9, 2009.

[35] K. Bahmani, R. Bakhshi, E. A. Ince, and C. M. Yetis, "Interference management in two-tier heterogeneous networks using blind interference alignment," in *23rd Signal Processing and Communications Applications Conference (SIU)*. IEEE, 2015, pp. 1737–1740.

[36] R. Bakhshi and E. A. Ince, "Hybrid blind interference alignment in homogeneous cellular networks with limited coherence time," *International Journal of Communication Systems*, vol. 10.1002/dac.3836, March, 2018.

[37] B. Vucetic and J. Yuan, "Performance limits of multiple-input multiple-output wireless communication systems," *Space-Time Coding*, pp. 1–47, 2003.

[38] Y. S. Cho, J. Kim, W. Y. Yang, and C. G. Kang, *MIMO-OFDM wireless communications with MATLAB*. John Wiley & Sons, 2010.

[39] P. Viswanath and D. Tse, "Fundamentals of wireless communications," *class notes for ECE*, vol. 459, 2005.

[40] Y. Lu and W. Zhang, "Downlink blind interference alignment for cellular networks," in *Global Communications Conference*. Austin, USA: IEEE, 2014, pp. 3337–3342.

[41] C. Suh, M. Ho, and D. N. Tse, "Downlink interference alignment," *IEEE Transactions on Communications*, vol. 59, no. 9, pp. 2616–2626, 2011.

[42] W. Shin, N. Lee, J.-B. Lim, C. Shin, and K. Jang, "On the design of interference alignment scheme for two-cell MIMO interfering broadcast channels," *IEEE Transactions on Wireless Communications*, vol. 10, no. 2, pp. 437–442, 2011.

[43] D. Aziz, M. Mazhar, and A. Weber, "Multi user inter cell interference alignment in heterogeneous cellular networks," in *79th Vehicular Technology Conference (VTC Spring)*. IEEE, 2014, pp. 1–5.

[44] V. Ntranos, M. A. Maddah-Ali, and G. Caire, "Cellular interference alignment," *IEEE Transactions on Information Theory*, vol. 61, no. 3, pp. 1194–1217, 2015.

[45] H. Yang, W. Shin, and J. Lee, "Hierarchical blind interference alignment over interference networks with finite coherence time," *IEEE Trans. Signal Processing*, vol. 64, no. 5, pp. 1289–1304, March, 2016.

[46] W. Yu and J. M. Cioffi, "Sum capacity of gaussian vector broadcast channels," *IEEE Transactions on information theory*, vol. 50, no. 9, pp. 1875–1892, 2004.

[47] P. Viswanath and D. N. C. Tse, "Sum capacity of the vector Gaussian broadcast

channel and uplink-downlink duality," *IEEE Transactions on Information Theory*, vol. 49, no. 8, pp. 1912–1921, 2003.

[48] S. Vishwanath, N. Jindal, and A. Goldsmith, "Duality, achievable rates, and sum-rate capacity of Gaussian MIMO broadcast channels," *IEEE Transactions on Information Theory*, vol. 49, no. 10, pp. 2658–2668, 2003.

[49] D. N. C. Tse, P. Viswanath, and L. Zheng, "Diversity-multiplexing tradeoff in multiple-access channels," *IEEE Transactions on Information Theory*, vol. 50, no. 9, pp. 1859–1874, 2004.

[50] C. Huang, S. A. Jafar, S. Shamai, and S. Vishwanath, "On degrees of freedom region of MIMO networks without CSIT," *arXiv preprint arXiv:0909.4017*, 2009.

[51] C. S. Vaze and M. K. Varanasi, "The degree-of-freedom regions of MIMO broadcast, interference, and cognitive radio channels with no CSIT," *IEEE Transactions on Information Theory*, vol. 58, no. 8, pp. 5354–5374, 2012.

[52] D. J. Love, R. W. Heath, and T. Strohmer, "Grassmannian beamforming for multiple-input multiple-output wireless systems," *IEEE transactions on information theory*, vol. 49, no. 10, pp. 2735–2747, 2003.

[53] M. A. Maddah-Ali and D. Tse, "Completely stale transmitter channel state information is still very useful," *IEEE Transactions on Information Theory*, vol. 58, no. 7, pp. 4418–4431, 2012.

[54] T. Gou and S. A. Jafar, "Optimal use of current and outdated channel state information: Degrees of freedom of the MISO BC with mixed CSIT," *IEEE Communications Letters*, vol. 16, no. 7, pp. 1084–1087, 2012.

[55] C. S. Vaze and M. K. Varanasi, "The degrees of freedom region and interference alignment for the MIMO interference channel with delayed CSIT," *IEEE Transactions on Information Theory*, vol. 58, no. 7, pp. 4396–4417, 2012.

[56] S. Yang, M. Kobayashi, D. Gesbert, and X. Yi, "Degrees of freedom of time correlated MISO broadcast channel with delayed CSIT," *IEEE Transactions on Information Theory*, vol. 59, no. 1, pp. 315–328, 2013.

[57] R. Tandon, S. A. Jafar, S. Shamai, and H. V. Poor, "On the synergistic benefits of alternating CSIT for the MISO broadcast channel," *IEEE Transactions on Information Theory*, vol. 59, no. 7, pp. 4106–4128, 2013.

[58] M. Kobayashi, Y. Liang, S. Shamai, and M. Debbah, "On the compound MIMO broadcast channels with confidential messages," in *International Symposium on Information Theory ISIT*. IEEE, 2009, pp. 1283–1287.

[59] H. Weingarten, S. Shamai, and G. Kramer, "On the compound MIMO broadcast channel," in *Proceedings of Annual Information Theory and Applications Workshop UCSD*. Citeseer, 2007.

[60] T. Gou, S. A. Jafar, and C. Wang, "On the degrees of freedom of finite state compound wireless networks," *IEEE Transactions on Information Theory*,

vol. 57, no. 6, pp. 3286–3308, 2011.

[61] C. M. Yetis, T. Gou, S. A. Jafar, and A. H. Kayran, "On feasibility of interference alignment in MIMO interference networks," *IEEE Transactions on Signal Processing*, vol. 58, no. 9, pp. 4771–4782, 2010.

[62] Ó. González, C. Beltrán, and I. Santamaría, "A feasibility test for linear interference alignment in MIMO channels with constant coefficients," *IEEE Transactions on Information Theory*, vol. 60, no. 3, pp. 1840–1856, 2014.

[63] M. A. Maddah-Ali, A. S. Motahari, and A. K. Khandani, "Communication over MIMO X channels: Interference alignment, decomposition, and performance analysis," *IEEE Transactions on Information Theory*, vol. 54, no. 8, pp. 3457–3470, 2008.

[64] K. Gomadam, V. R. Cadambe, and S. A. Jafar, "Approaching the capacity of wireless networks through distributed interference alignment," *Global Telecommunications Conference, 2008, IEEE GLOBECOM 2008, IEEE*, pp. 1–6, 2008.

[65] N. Zhao, F. Yu, J. M., Q. Yan, and V. Leung, "Interference alignment and its applications: A survey, research issues, and challenges," *IEEE Communications Survey and Tutorials*, vol. 18, no. 3, pp. 1779–1803, March, 2016.

[66] H. Huang, V. Lau, and L. S., "Robust lattice alignment for K-user MIMO interference channels with imperfect channel knowledge," *IEEE Transactions*

on Signal Processing, vol. 59, no. 7, pp. 3315–3325, July, 2011.

[67] B. A. Cetiner, H. Jafarkhani, J.-Y. Qian, H. J. Yoo, A. Grau, and F. De Flaviis, "Multifunctional reconfigurable MEMS integrated antennas for adaptive MIMO systems," *IEEE Communications Magazine*, vol. 42, no. 12, pp. 62–70, 2004.

[68] A. Grau, H. Jafarkhani, and F. De Flaviis, "A reconfigurable multiple-input multiple-output communication system," *IEEE Transactions on Wireless Communications*, vol. 7, no. 5, 2008.

[69] D.-C. Chang, "Reconfigurable antennas for digital data communication systems," in *International Workshop on Electromagnetics (IWEM)*. IEEE, 2014, pp. 1–1.

[70] J. Costantine, Y. Tawk, S. E. Barbin, and C. G. Christodoulou, "Reconfigurable antennas: Design and applications," *Proceedings of the IEEE*, vol. 103, no. 3, pp. 424–437, 2015.

[71] M. Yang, S.-W. Jeon, and D. K. Kim, "Linear degrees of freedom of MIMO broadcast channels with reconfigurable antennas in the absence of CSIT," *IEEE Transactions on Information Theory*, vol. 63, no. 1, pp. 320–335, 2017.

[72] C. Wang, "Degrees of freedom characterization: The 3-user SISO interference channel with blind interference alignment," *IEEE Communications letters*, vol. 18, no. 5, pp. 757–760, 2014.

[73] A. M. Alaa and M. H. Ismail, "Degrees-of-freedom of the K-user SISO interference channel with blind interference alignment using staggered antenna switching," *arXiv preprint arXiv*, vol. 1408, 2014.

[74] K. Zhong, K. Anand, N. T. Hieu, E. Gunawan, and Y. L. Guan, "A blind and partial interference alignment scheme based on pulse shaping for 3-user SISO interference channel," in *10th International Conference on Information, Communications and Signal Processing (ICICS)*. IEEE, 2015, pp. 1–5.

[75] H. Yang, W. Shin, and J. Lee, "Degrees of freedom for K-user SISO interference channels with blind interference alignment," in *49th Asilomar Conference on Signals, Systems and Computers*. IEEE, 2015, pp. 1097–1101.

[76] M. Johnny and M. R. Aref, "Sum degrees of freedom for the K-user interference channel using antenna switching," in *21th International ITG Workshop on Smart Antenna*. VDE, WSA 2017, pp. 1–6.

[77] Y. Lu, W. Zhang, and K. B. Letaief, "Blind interference alignment with diversity in K-user interference channels," *IEEE Transactions on Communications*, vol. 62, no. 8, pp. 2850–2859, 2014.

[78] C. Wang, H. C. Papadopoulos, S. A. Ramprashad, and G. Caire, "Design and operation of blind interference alignment in cellular and cluster-based systems," in *Information Theory and Applications Workshop (ITA)*. IEEE, 2011, pp. 1–10.

[79] F. C. Kavasoglu, Y. Huang, and B. D. Rao, "Semi-blind interference alignment techniques for small cell networks," *IEEE Transactions on Signal Processing*, vol. 62, no. 23, pp. 6335–6348, 2014.

[80] S. Akoum, C. S. Chen, M. Debbah, and R. W. Heath, "Data sharing coordination and blind interference alignment for cellular networks," in *Global Communications Conference*. California, USA: IEEE, 2012, pp. 4273–4277.

[81] C. Wang, H. C. Papadopoulos, S. A. Ramprashad, and G. Caire, "Improved blind interference alignment in a cellular environment using power allocation and cell-based clusters," in *International Conference on Communications (ICC)*. IEEE, 2011, pp. 1–6.

[82] C. Geng, N. Naderializadeh, A. S. Avestimehr, and S. A. Jafar, "On the optimality of treating interference as noise," *IEEE Transactions on Information Theory*, vol. 61, no. 4, pp. 1753–1767, 2015.

[83] H. Yang, N. Naderializadeh, A. S. Avestimehr, and J. Lee, "Topological interference management with reconfigurable antennas," *IEEE Transactions on Communications*, vol. 65, no. 11, pp. 4926–4939, 2017.

[84] S. A. Jafar, "Elements of cellular blind interference alignment—aligned frequency reuse, wireless index coding and interference diversity," *arXiv preprint arXiv:1203.2384*, 2012.

[85] S. A. Jafar., "Topological interference management through index coding,"

IEEE Transactions on Information Theory, vol. 60, no. 1, pp. 529–568, 2014.

[86] Z. Bar-Yossef, Y. Birk, T. Jayman, and T. Kol, "Index coding with side information," *IEEE Transactions on Information Theory*, vol. 57, no. 3, pp. 1479–1494, March, 2011.

[87] H. Maleki, V. Cadambe, and S. Jafar, "Index coding – an interference alignment perspective," *IEEE Transactions on Information Theory*, vol. 60, no. 9, pp. 5402–5432, September, 2014.

[88] Q. Yang, T. Jiang, C. Jiang, Z. Han, and Z. Zhou, "Joint optimization of user grouping and transmitter connection on multi-cell SNR blind interference alignment," *IEEE Access*, vol. 4, pp. 4974–4988, 2016.

[89] M. M. Céspedes, J. Plata-Chaves, D. Toumpakaris, and A. G. Armada, "On the choice of blind interference alignment strategy for cellular systems with data sharing," in *International Conference o Communications (ICC) n.* IEEE, 2014, pp. 5735–5740.

[90] P. Xia, H.-S. Jo, and J. G. Andrews, "Fundamentals of inter-cell overhead signaling in heterogeneous cellular networks," *IEEE Journal of Selected Topics in Signal Processing*, vol. 6, no. 3, pp. 257–269, 2012.

[91] H.-H. Lee and Y.-C. Ko, "Linear transceiver design based on interference alignment for MIMO heterogeneous networks," in *23rd International Symposium on Personal Indoor and Mobile Radio Communications (PIMRC).*

IEEE, 2012, pp. 1645–1650.

[92] M. M. Céspedes and A. S. Rodríguez, "Statistical characterization of zero-forcing coordinated base station transmission for femtocell environments," in *16th Mediterranean Electrotechnical Conference (MELECON).* IEEE, 2012, pp. 920–925.

[93] F. Pantisano, M. Bennis, W. Saad, M. Debbah, and M. Latva-Aho, "Interference alignment for cooperative femtocell networks: A game-theoretic approach," *IEEE Transactions on Mobile Computing*, vol. 12, no. 11, pp. 2233–2246, 2013.

[94] G. Gur, S. Bayhan, and F. Alagoz, "Cognitive femtocell networks: an overlay architecture for localized dynamic spectrum access [dynamic spectrum management]," *IEEE Wireless Communications*, vol. 17, no. 4, 2010.

[95] S.-M. Cheng, S.-Y. Lien, F.-S. Chu, and K.-C. Chen, "On exploiting cognitive radio to mitigate interference in macro/femto heterogeneous networks," *IEEE Wireless Communications*, vol. 18, no. 3, 2011.

[96] M. Bennis and S. M. Perlaza, "Decentralized cross-tier interference mitigation in cognitive femtocell networks," in *Communications (ICC), 2011 IEEE International Conference on.* IEEE, 2011, pp. 1–5.

[97] Y. S. Soh, T. Q. Quek, M. Kountouris, and G. Caire, "Cognitive hybrid division duplex for two-tier femtocell networks," *IEEE Transactions on Wireless Communications*, vol. 12, no. 10, pp. 4852–4865, 2013.

[98] M. M. CESPEDES, "Blind interference alignment for cellular networks," Ph.D. dissertation, Departamento de Teoria de la Senaly Comunicaciones, Universidad Carlor III de Madrid, November 2015.

[99] M. M. Céspedes, J. Plata-Chaves, D. Toumpakaris, S. A. Jafar, and A. G. Armada, "Cognitive blind interference alignment for macro-femto networks," *IEEE Transactions on Signal Processing*, vol. 65, no. 19, pp. 5121–5136, 2017.

[100] Y. Lu and W. Zhang, "Blind interference alignment in the K-user MISO interference channel," in *Global Communications Conference (GLOBECOM), 2013 IEEE*. IEEE, 2013, pp. 3464–3469.

[101] D. N. Knisely and F. Favichia, "Standardization of femtocells in 3GPP2," *IEEE Communications Magazine*, vol. 47, no. 9, 2009.

[102] R. Mardeni and T. Priya, "Optimised COST-231 HATA models for WiMAX path loss prediction in suburban and open urban environments," *IEEE-J-MAS*, vol. 4, no. 9, p. 75–89, September 2010.

[103] V. Kalokidou, O. Johnson, and R. Piechocki, "Interference management in heterogeneous networks with blind transmitters," January 2016, ArXiv pre-print cs.IT/1601.08132v1. http://arxiv.org/abs/1601.08132v1.

[104] M. Caramia and P. Dell'Olmo, *Multi-objective management in freight logistics: Increasing capacity, service level and safety with optimization algorithms*. Springer Science & Business Media, 2008.